(2)

September 25, 1989

Final Scientific Report

AFOSR-86-0205

Covering the Period from 1 August 1986 to 31 July 1989

ELECTRON PRODUCTION, ELECTRON ATTACHMENT, AND CHARGE RECOMBINATION PROCESS IN HIGH PRESSURE GAS DISCHARGES

Long C. Lee

Department of Electrical & Computer Engineering
San Diego State University
San Diego, California 92182-0190

Submitted to:

U. S. Air Force Office of Scientific Research
Physical and Geophysical Sciences
Bolling Air Force Base
Washington, DC 20332-6448

UNCLASSIFIED

SECURITY CLASSIFICATION OF THIS PAGE

REPORT DOCUMENTATION PAGE

Form Approved OMB No. 0704-0188

1a. REPORT SECURITY CLASSIFICATION Unclassified	1b. RESTRICTIVE MARKINGS
2a. SECURITY CLASSIFICATION AUTHORITY	3. DISTRIBUTION/AVAILABILITY OF REPORT Approved for public release; distribution is unlimited.
2b. DECLASSIFICATION/DOWNGRADING SCHEDULE	
4. PERFORMING ORGANIZATION REPORT NUMBER(S)	5. MONITORING ORGANIZATION REPORT NUMBER(S) AFOSR-TR- 89-1694
6a. NAME OF PERFORMING ORGANIZATION San Diego State University 6b. OFFICE SYMBOL (If applicable)	7a. NAME OF MONITORING ORGANIZATION Air Force Office of Scientific Research
6c. ADDRESS (City, State, and ZIP Code) Dept. Electrical & Computer Engineering San Diego, CA 92182	7b. ADDRESS (City, State, and ZIP Code) Bolling Air Force Base Washington, DC 20332-6448
8a. NAME OF FUNDING/SPONSORING ORGANIZATION Air Force Office of Scientific Research 8b. OFFICE SYMBOL (If applicable) AFOSR/NP	9. PROCUREMENT INSTRUMENT IDENTIFICATION NUMBER AFOSR-86-0245
8c. ADDRESS (City, State, and ZIP Code) Bolling Air Force Base Washington, DC 20332-6448	10. SOURCE OF FUNDING NUMBERS PROGRAM ELEMENT NO. 61102F; PROJECT NO. 2301; TASK NO A7; WORK UNIT ACCESSION NO.

11. TITLE (Include Security Classification)
Electron Production, Electron Attachment, and Charge Recombination Process in High Pressure Gas Discharges (U)

12. PERSONAL AUTHOR(S)
Long C. Lee

13a. TYPE OF REPORT	13b. TIME COVERED	14. DATE OF REPORT (Year, Month, Day)	15. PAGE COUNT
Final	FROM 86-8-1 TO 89-7-31	1989 September 25	68

16. SUPPLEMENTARY NOTATION

17. COSATI CODES			18. SUBJECT TERMS (Continue on reverse if necessary and identify by block number)
FIELD	GROUP	SUB-GROUP	Electron production, electron attachment rate constants, electronegative gases, negative ions, electron transport parameters, gaseous discharges, laser-induced current

19. ABSTRACT (Continue on reverse if necessary and identify by block number)

Electron transport parameters in gaseous discharges are investigated for the development of discharge switches. Electron attachment rate constants of several halogen compounds are measured, and the attachment rate constants are converted to cross sections using the electron energy distribution function of buffer gases. The electron drift velocities for the gas mixtures of trace halogen compounds in buffer gases are measured. Current switching induced by laser detachment of electrons from negative ions in discharge media is observed. The photodetachment cross sections of negative ions in discharge media are derived from the current switching. An apparatus that consists of double differential pump system and a mass spectrometer has been constructed to analyze the negative ions in discharge media. The measured electron transport parameters are used to assess the characteristics of discharge switches.

20. DISTRIBUTION/AVAILABILITY OF ABSTRACT	21. ABSTRACT SECURITY CLASSIFICATION
☒ UNCLASSIFIED/UNLIMITED ☐ SAME AS RPT. ☐ DTIC USERS	UNCLASSIFIED
22a. NAME OF RESPONSIBLE INDIVIDUAL Col. Jerry Perrizo	22b. TELEPHONE (Include Area Code) (202) 767-4904 22c. OFFICE SYMBOL AFOSR/NP

DD Form 1473, JUN 86 Previous editions are obsolete. SECURITY CLASSIFICATION OF THIS PAGE

UNCLASSIFIED

89 12 20 028

I. INTRODUCTION

Electron transport parameters for gaseous mixtures containing electronegative gases in buffer gases were investigated in this research program. Absolute electron attachment rate constants and cross sections of halogen compounds were measured. Photodetachment cross sections of halogen negative ions in discharge media were determined. Discharge current switching induced by laser irradiation of discharge media was observed. These basic data are obtained for the development of various gaseous discharge switches and for the study of basic discharge phenomena as well. High repetition-rate discharge switches, opening switches, and radiation or e-beam controlled switches are needed for the development of high power lasers, fusion experiments, magnetic energy storage systems, and particle beam experiments. High pressure gaseous discharges could be used for the development of these switches. The measured electron transport parameters are needed for determining the rise and decay times of discharge pulses, discharge stability, discharge uniformity, and current density.

II. RESEARCH ACCOMPLISHED

A. Laser-Induced Switching of Discharge Current

Current switching induced by laser irradiation was observed in the discharge media that contain halogen compounds (F_2, HF, HCl, Cl_2, HBr, CH_3Br, CH_3I, CH_2I_2, CH_3Cl, CF_2Cl_2) in the N_2 buffer gas. It was observed that discharge current increased following the irradiation of a discharge medium by ArF or KrF laser pulses. The increased conduction current recovered to the DC level after 1-2 μs duration. The current increase is caused by the release of electrons from photodetachment of halogen negative ions (F^-, Cl^-, Br^-, and I^-) in the discharge medium. The electron drift velocity is usually higher than the drift velocity of a negative ion by a

factor of 10^3-10^4; thus, the current switching induced by the release of electrons from negative ions could increase by the same factor. The observed current switching induced by laser irradiation of discharge medium could be applied for the design of high power discharge switches. The results for the observation of current switching in the discharge media of CF_2Cl_2-N_2 and CH_3Cl-N_2 are described in more detail in a paper attached as Appendix A, which has been published in the IEEE Transactions on Plasma Science.

B. Photodetachment Cross Sections of Negative Ions in Discharge Media

The photodetachment cross section is one of the key parameters that determines the magnitude of the laser-induced current switching. The photodetachment cross sections of F^-, Cl^-, Br^- and I^- were measured from the increase of transient current induced by laser irradiation of the discharge media. The measurements at the ArF (193 nm) and KrF (248 nm) excimer laser wavelengths are described in detail in the paper attached as Appendix B, which has been published in the Journal of Physics D: Applied Physics.

C. Electron Drift Velocity

The electron conduction current is proportional to the electron drift velocity; therefore, this parameter is important for determining the magnitude of current switching. The electron drift velocity can be affected by the composition of gas mixture. This effect was investigated by measuring the electron drift velocity as a function of the concentration of CH_3Br in Ar. The electron drift velocity increased dramatically when CH_3Br was added to Ar. The results are described in more detail in the paper attached as Appendix C, which has been published in the Journal of Applied Physics.

D. Electron Attachment Rate Constants

The electron attachment rate constant is one of the key parameter that determines the production rates of negative ions and the pulse duration of

A-1

current switching. The electron attachment rate constants of halogen compounds such as HCl, HBr, BCl_3, $SOCl_2$, CH_3Cl, CH_3Br, CF_2Cl_2, C_2H_3Cl, C_2H_5Cl, and C_2H_5Br were measured. The results were described in detail in the papers attached as Appendices A, C, D, E, F, and G.

E. Electron Attachment Cross Sections

The measured electron attachment rate constants were converted into electron attachment cross sections using the electron energy distribution functions of pure Ar and N_2. The unfolded electron attachment cross sections are reported in Appendix D for HCl and Appendix F for CH_3Cl, $SOCl_2$, CCl_2F_2, C_2H_3Cl, and C_2H_5Cl. The obtained data are consistent with the published data measured by electron beam experiments.

F. Application of the Observed Data to the Design of Discharge Switches

The current switching and the basic data obtained in this program are useful for the design of discharge switches. As an illustration for such application, the discharge medium of trace HBr and CH_3Br in Ar (or N_2) is taken as an example. Br^- could be totally photodetached by an ArF laser pulse energy of 0.1 J/cm^2 as calculated from the photodetachment cross section listed in Table 1 of Appendix B. At E/N = 1 Td (10^{-17} V cm^2), the drift velocity of a negative ion in Ar is about 10^3 cm/s, and the electron drift velocity is about 10^6 cm/s (see Appendix C). Thus, the transient current due to laser-detachment of Br^- could be 10^3 time more than the DC discharge current. The recovery time for the transient pulse could be less than 1 μs, if 0.3 torr of HBr is mixed in the discharge Medium. (The electron attachment rate constant reported in Appendix C was used for the calculation.) This example demonstrates that the gas mixture of trace HBr and CH_3Br in Ar or N_2 could be used for the switching of high electrical energy.

G. Analysis of Ion Species in Discharge Media

A mass spectrometer using a double differential pumping system was constructed in this program for the analysis of transient species (positive ions, negative ions, and radicals) in electrical discharge media. The schematic diagram of the apparatus is shown in Fig. 1 of Appendix G. This apparatus is being used to analyze the transient species in discharge media.

III. Publications and Presentations

1. "Electron Attachment Rate Constants of $SOCl_2$ in Ar, N_2 and CH_4," W. C. Wang and L. C. Lee, J. Chem. Phys. **85**, 6470 (1986).

2. "Switching of Conduction Current by Photodetachment and Photodissociation Processes Occurring in the $SOCl_2$-N_2 Gas Mixture, " W. C. Wang and L. C. Lee, presented at the 39th Gaseous Electr. Conf. Madison, Wisconsin, October 7-10, 1986.

3. "Switching of Electron Conduction Current by molecular Photoelectron Detachment and Photodissociation Processes," L. C. Lee and W. C. Wang, Invited Paper presented at the SPIE, Optoelectronics and Laser Applications in Science and Engineering, Los Angeles, California, January 11-16, 1987.

4. "Photodetachment Cross Sections of Negative Halogen Ions in Discharge Media," W. C. Wang and L. C. Lee, presented at the Annual Meeting of Atomic, Molecular and Optical Physics, Cambridge, Massachusetts, May 18-20, 1987.

5. "Laser-Induced Switching of Discharge Current," L. C. Lee and W. C. Wang, presented at the 6th IEEE Pulsed Power Conference, Arlington, Virginia, June 29 - July 1, 1987.

6. "Laser-Induced Current Switching Observed in the Discharge Media of CF_2Cl_2-N_2 and CH_3Cl-N_2," W. C. Wang and L. C. Lee, IEEE Trans. Plas. Sci. **PS-15**. 460 (1987).

7. "Electron Attachment Rate Constants of Bromine Compounds," W. C. Wang, D. P. Wang, and L. C. Lee, presented at the 40th Gaseous Electr. Conf. Atlanta, Georgia, October 13-16, 1987.

8. "Laser-Induced Current Switching in Gaseous Discharges," L. C. Lee. W. C. Wang, and D. P. Wang, presented at the Symposium On Innovative Science and Technology, Los Angeles, California, January 10-15, 1988.

9. "Photodetachment Cross Sections of Negative Halogen Ions in Discharge Media," W. C. Wang and L. C. Lee, J. Phys. D: Appl. Phys. **21**, 675 (1988).

10. "Electron Attachment Rate Constants of HBr, CH_3Br, and C_2H_5Br in N_2 and Ar," W. C. Wang and L. C. Lee, J. Appl. Phys. **63**, 4905 (1988).

11. "Attachment of Low Energy Electrons to HCl," Z. Lj. Petrovic, W. C. Wang, and L. C. Lee, J. Appl. Phys. **64**, 1625 (1988).

12. "Electron Kinetics and Optical Diagnostics for Plasma-Assisted Material Processing," L. C. Lee, presented at the NSF Workshop on New Directions in Plasma Engineering, University of California, Berkeley, June 9-10, 1988.

13. "Electron Kinetics and Spectroscopic Data of Molecules Important in Plasma Processing of Electronic Materials," L. C. Lee, W. C. Wang, and M. Suto, presented at the Gordon Research Conference on Plasma Chemistry, New Hampshire, August 15-19, 1988.

14. "Rates of Electron Attachment to Some Molecules Containing Chlorine," Z. Lj. Petrovic, W. C. Wang, and L. C. Lee, presented at the Summer School and International Symposium on the Physics of Ionized Gases, Sarajevo, Yugoslavia, August 15-19, 1988.

15. "Cross Sections for Electron Attachment to Some Chlorine Containing Molecules," Z. Lj. Petrovic, W. C. wang, and L. C. Lee, presented at the European Section of Conference on Atomic and Molecular Processes in Ionized Gases, August 30 - September 2, 1988.

16. "Dissociative Attachment of electrons to HCl at Moderate Values of E/N," Z. Lj. Petrovic, W. C. Wang, and L. C. Lee, presented at the International Conferences on Gas Discharges and Applications, September 19-23, 1988.

17. "Low Energy Electron attachment to BCl_3" Z. Lj. Petrovic, W. C. Wang, L. C. Lee, presented at the XIXth International Conference on Phenomena in Ionized Gases, Belgrade, Yugoslava, July 10-14, 1989.

18. "Negative Ion Kinetics in BCl_3 Discharges," Z. Lj. Petrovic, W. C Wang, J. C. Han, M. Suto, and L. C. Lee, presented at the Sixth International Swarm Seminar, Webb Institute, New York, August 3-5, 1989.

19. "Dissociative Electron Attachment to Some Chlorine-Containing Molecules," Z. Lj. Petrovic, W. C. Wang, and L. C. Lee, J. Chem. Phys. **90**, 3145 (1989).

20. "Low Energy Electron attachment to BCl_3," Z. Lj. Petrovic, W. C. Wang, M. Suto, J. C. Han, and L. C. Lee, submitted to J. Appl. Phys. (1989).

IV. Personnel Involved In This Research

1. **Principal Investigator:**

   Dr. Long C. Lee

   Professor of Electrical Engineering and Chemistry

2. **Co-Investigator:**

   Dr. Masako Suto

   Professor of Electrical and Computer Engineering

3. **Postdoctoral Research Associates:**

   Dr. Z. Lj. Petrovic

   Dr. Wen C. Wang

4. **Visiting Scholar:**

   Professor Jing C. Han

5. **Students:**

   Mr. Oscar Arias

   Ms. Lynn Dinh

   Mr. Zhiming Feng

   Mr. Allen Ho

   Mr. Shougin Huo

   Ms. Duyen P. Ly

   Mr. Salvador Plasencia

   Mr. John Spooner

   Ms. Kim Tran

T-PS/15/4//16395

Laser-Induced Current Switching Observed in the Discharge Media of CF_2Cl_2–N_2 and CH_3Cl–N_2

W. C. Wang and L. C. Lee

Reprinted from
IEEE TRANSACTIONS ON PLASMA SCIENCE
Vol. PS-15, No. 4, AUGUST 1987

Laser-Induced Current Switching Observed in the Discharge Media of CF_2Cl_2–N_2 and CH_3Cl–N_2

W. C. WANG AND L. C. LEE, MEMBER, IEEE

Abstract—**Switchings of discharge current induced by ArF and KrF laser pulses in the discharge media of CF_2Cl_2–N_2 and CH_3Cl–N_2 were investigated using a negative point-to-plane discharge apparatus. The electron attachment rate constants of CF_2Cl_2 in buffer gases of N_2 and Ar were measured by a parallel-plate drift-tube apparatus at various E/N, from which the dominant negative ions in the discharge media were inferred. The conductivity of the discharge medium is enhanced upon laser irradiation due to conduction electrons being produced from photoelectron-detachment of Cl^-. From the dependence of the enhanced current on laser power, the photodetachment cross sections of Cl^- in a given discharge condition were derived to be 2.5×10^{-17} cm^2 at 193 nm and 1.0×10^{-17} cm^2 at 248 nm. After the current enhancement, the current was greatly reduced as was observed in the discharge medium of CF_2Cl_2–N_2, but not in CH_3Cl–N_2. The mechanism for the optically induced reduction of discharge current is discussed.**

I. Introduction

RECENTLY, Schaefer *et al.* [1] demonstrated that photoelectron-detachment of O^- in the afterglow of a dc discharge in oxygen could be used as a control mechanism for diffuse discharge switching. This principle is useful for the design of opening switches which are needed for the development of an inductive energy storage system for which the intrinsic energy density is much higher than that of a capacitive storage system [2], [3]. In addition to O^-, photoelectron-detachment of F^- and Cl^-, which was observed [4], [5] in glow discharge containing NF_3 and Cl_2, respectively, could also be useful for the control of discharge current. The use of photoelectron-detachment of Cl^- as a switching control is reported in this paper.

Photoelectron-detachment of Cl^- in discharge medium of CF_2Cl_2–N_2 or CH_3Cl–N_2 by excimer laser photons was studied in this experiment. The study of the chlorine compound is of interest, because the dielectric strength for a chlorine compound containing gas mixture is usually high. In addition to practical applications, this experiment also provides fundamental data for the photoelectron-detachment cross section of Cl^- in a discharge condition. The cross section was derived from measurements of the laser-induced current as a function of laser power. This measurement method is subject to the effect of photoelectron on the local field. Nevertheless, the measured cross sections are comparable with published data in the 200-350-nm region as measured by a negative ion beam experiment [6].

In addition to the enhancement of conductivity, a reduction in conductivity was also observed in the CF_2Cl_2–N_2 discharge medium; however, this reduction was not observed in the CH_3Cl–N_2 discharge medium. This reduction of conductivity is likely due to the impedance change of gas medium caused by laser irradiation or by the increase of electron attachment to photodissociation products. Such optically induced current decrease is useful for controlling the opening time of a discharge current.

The electron attachment rate constants of CF_2Cl_2 in buffer gases of N_2 and Ar were also measured at various E/N (reduced electric field) in this experiment. The electron attachment rate constant of CF_2Cl_2 in the buffer gas of N_2 has been measured by McCorkle *et al.* [7], but the data in Ar are not yet known. Our results provide the electron attachment rate constant over a wide range of electron energy which is needed for understanding the electron attachment process. We use such information to elucidate the major negative ion in the discharge medium, which is essential for the interpretation of our experimental observation.

II. Experiment

The experimental setup for the measurement of electron attachment rate constant is shown in Fig. 1, where the gas cell was a 6-in-OD six-way black-anodized-aluminum cross. The electrodes were two parallel uncoated stainless steel plates 5 cm in diameter and 2.5 cm apart. The electron swarm was produced by irradiation of the cathode with an excimer laser beam (Lumonics Model 861S) with an incident angle of about 70°. The laser pulse duration was about 10 ns and the laser beam size was reduced to 3 mm in diameter by a diaphragm. A negative high voltage was applied to the cathode to maintain an electric field. The conduction current induced by the electron motion between the electrodes was measured as a transient voltage across a resistor (1-2 kΩ) connecting the anode to ground.

For the discharge experiment, the parallel-plate electrodes were replaced by a negative point-to-plane electrode set inside the gas cell. The cathode was a steel wire 0.5 mm in diameter, and the anode was a stainless steel plate 5 cm in diameter. They were positioned 1.5 cm apart. A negative high voltage was applied to the cathode through a 5.6-MΩ resistor. The discharge current was

Manuscript received February 9, 1987; revised April 13, 1987. This work was supported by the Air Force Office of Scientific Research under Grant AFOSR-86-0205.

The authors are with the Department of Electrical and Computer Engineering, San Diego State University, San Diego, CA 92182.

IEEE Log Number 8716395.

0093-3813/87/0800-0460$01.00 © 1987 IEEE

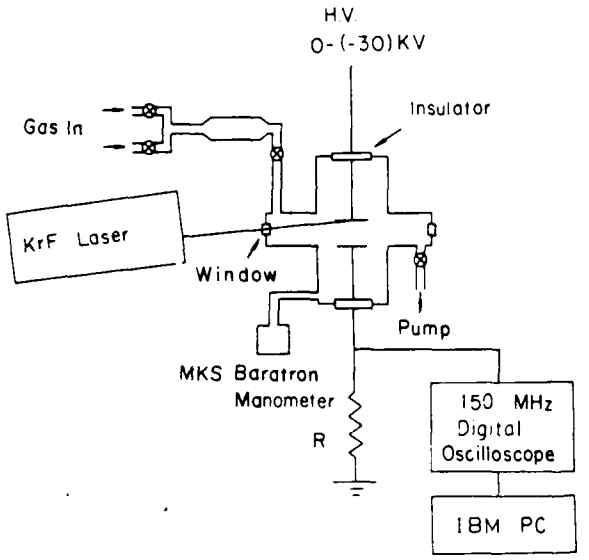

Fig. 1. Schematic diagram of experimental apparatus for electron attachment rate measurement.

measured by the voltage across a 1000-Ω resistor connecting the anode to ground. An ArF (or KrF) laser beam with a photon energy of 6.42 eV (or ~5 eV) was used to irradiate the discharge medium. The laser flux was monitored by an energy meter (Scientech Model 365). The transient waveforms were monitored by a 150-MHz digital storage oscilloscope (Tektronix 2430) and were subsequently stored and analyzed by an IBM-PC microcomputer.

Pressure of the flowing gas in the cell was monitored by a Baratron manometer (MKS Instrument). All measurements were performed at room temperature. Diluted mixtures of CF_2Cl_2 (<0.5 percent) in N_2 or Ar and diluted CH_3Cl mixtures (~2.7 percent) in N_2 were premixed before being introduced into the gas cell. The purities of N_2 and Ar (MG Scientific) were better than 99.998 percent, and the purities of CF_2Cl_2 and CH_3Cl (Matheson Gas Products) were 99.0 and 99.5 percent, respectively. These gases were used as delivered.

III. Results and Discussion

A. Electron Attachment to CF_2Cl_2

The electron attachment rate constants of CF_2Cl_2 in N_2 and Ar were measured at various E/N. These data are used to infer the nature of negative ions produced in the discharge medium. In these measurements, electrons were produced by irradiation of the cathode with KrF laser photons (see Fig. 1). The transient current induced by electron motion between the electrodes under an applied electric field was observed. When CF_2Cl_2 was added to the buffer gas, the electron conduction current was reduced due to electron attachment to CF_2Cl_2. The electron attachment rate ν_a at a fixed CF_2Cl_2 concentration was obtained from the decay slopes of $\ln(i/i_0)$ versus time, where i and i_0 are the current with and without CF_2Cl_2, respectively.

The electron attachment rate constant k_a is determined by $\nu_a/[CF_2Cl_2]$. Similar to the previous measurements [8], [9], the measured k_a values in Ar buffer gas decrease with increasing $[CF_2Cl_2]/[Ar]$. This may be caused by the effect of CF_2Cl_2 on the electron energy distribution in Ar. The electron attachment rate constant of CF_2Cl_2 is taken as the extrapolated value of $\nu_a/[CF_2Cl_2]$ at $[CF_2Cl_2] = 0$, for which the electron energy distribution is associated with pure Ar. The measured electron attachment rate is proportional to the partial pressure of added CF_2Cl_2 but independent of buffer gas pressure, indicating that the electron attachment is a two-body dissociative process. The k_a values of CF_2Cl_2 in the buffer gases of N_2 and Ar at various E/N are shown in Fig. 2, curves (*a*) and (*b*), respectively, where the buffer gas pressure was about 250 torr. The experimental uncertainty is estimated to be ±20 percent of the given value. The dotted line in Fig. 2 is the k_a value of CF_2Cl_2 in N_2 measured by McCorkle *et al.* [7]. The agreement between these two data is satisfactory.

The attachment rate constants of CF_2Cl_2 in N_2 and Ar are plotted in Fig. 3 as a function of the mean electron energy $\langle \epsilon \rangle$. The mean electron energies in N_2 and Ar at various E/N were reproduced from the calculation of Hunter and Christophorou [9]. Since the electron energy distributions in Ar and N_2 are similar [9], it is expected that the k_a values in both CF_2Cl_2–N_2 and CF_2Cl_2–Ar mixtures as a function of $\langle \epsilon \rangle$ will overlap as shown in Fig. 3. Our datum of about 1.7×10^{-9} cm^3/s at $\langle \epsilon \rangle \to 0$ lies among the reported values of $(0.4 - 3.2) \times 10^{-9}$ cm^3/s measured at thermal electron energy [10]–[12].

As shown in Fig. 3, the k_a values show peaks at ~0 (thermal energy) and ~0.7 eV and a broad band with a maximum around 3 eV. The k_a curve indicates the electron energies for the maxima of electron attachment cross sections, which show three peaks at 0, 0.6, and 3.5 eV as measured by Pejcev *et al.* [13]. These k_a values and the electron attachment cross sections can be used to infer the electron attachment process. The possible dissociative electron attachment processes of CF_2Cl_2 are

$$CF_2Cl_2 + e \to Cl^- + CF_2Cl \qquad \Delta H = -0.17 \text{ eV} \quad (1a)$$

$$\to Cl_2^- + CF_2 \qquad 0.86 \text{ eV} \quad (1b)$$

$$\to F^- + CCl_2F \qquad 1.50 \text{ eV} \quad (1c)$$

$$\to Cl^- + Cl + CF_2 \qquad 1.98 \text{ eV} \quad (1d)$$

$$\to CCl_2^- + F_2 \qquad 5.75 \text{ eV}. \quad (1e)$$

Here, the thermochemical energies were calculated from the dissociation energies [14] of 3.5, 2.479, and 1.56 eV

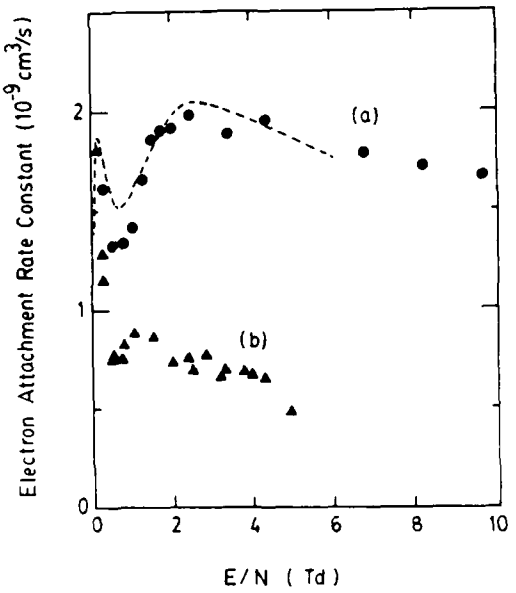

Fig. 2. Electron attachment rate constants as a function of E/N for CF_2Cl_2 in buffer gases of (*a*) N_2, and (*b*) Ar. The buffer gas pressures were ~250 torr. The dotted line represents the data of McCorkle *et al.* [7].

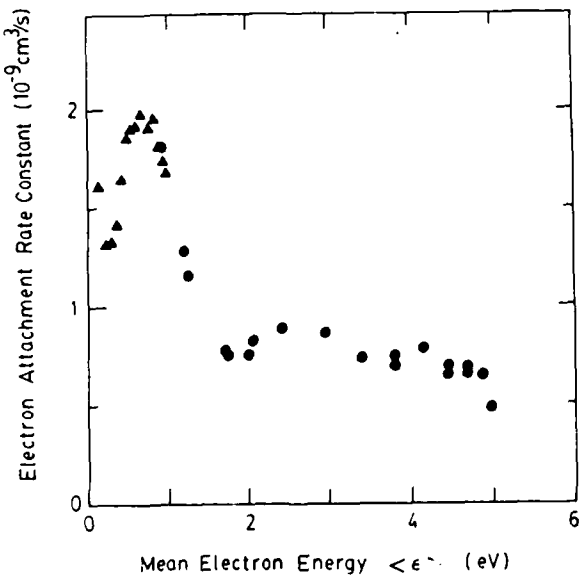

Fig. 3. Electron attachment rate constant of CF_2Cl_2-N_2 as a function of mean electron energy in N_2 (▲) and Ar (●).

for CF_2Cl-Cl, Cl-Cl, and F-F; the heats of formation [14], [15] of −116.5, −43.6, 18.36, −21, 28.587, and 56.7 kcal/mol for CF_2Cl_2, CF_2, F, CCl_2F, Cl, and CCl_2; and the electron affinities [16] of 3.67, 2.3, 3.44, and 1.8 eV for Cl, Cl_2, F, and CCl_2, respectively. The energy threshold for process (1a) is about 0.17 eV below the ground-state energy of CF_2Cl_2, indicating that this is the main attachment process at thermal energy. In fact, it was reported that Cl^- was the only observed negative ion at thermal energy [12], [17]. The second peak may correlate with process (1b), and the broad band in the 2–5-eV region may correlate with processes (1c) and (1d).

For electron energy less than 5 eV, the negative ions are dominated by Cl^-, Cl_2^-, and F^-. Since Cl_2^- will be photodissociated into Cl^- + Cl [18], instead of being photodetached into Cl_2 + e, and the photodetachment cross section of F^- is about three times less than that of Cl^- [6], the current increase in the next section is mainly caused by the photodetachment of Cl^-.

B. Enhancement of Conductivity in CF_2Cl_2-N_2

For the discharge experiment, the CF_2Cl_2-N_2 mixture was discharged between negative point-to-plane electrodes by a dc high voltage. When an ArF laser was used to irradiate the discharge medium, dc discharge current was switched as shown in Fig. 4, where the transient current waveforms were taken at CF_2Cl_2 partial pressures of ~0, 1, and 2 mtorr (see Fig. 4(a), (b), and (c), respectively). The applied voltage was −0.9 kV, the laser energy flux was 30 mJ/cm^2, and the laser beam diameter was 3 mm. Each waveform is the average of 64 pulses. As shown in Fig. 4, the value of dc current decreases with increasing concentration of CF_2Cl_2. This current decrease is due to electron attachment to CF_2Cl_2. For the discharge medium of pure N_2, the discharge current is not affected by the laser irradiation at $t = 0$ as shown in Fig. 4(a). When trace amounts of CF_2Cl_2 are added to the discharge medium, the current increases immediately following the laser irradiation as shown in Fig. 4(b) and (c). This current-increase pulse has a duration of about 1 μs.

The current increase in Fig. 4 is not due to the transient response of the discharge circuit, since the increased current I^+ depends on $[CF_2Cl_2]$ as shown in Fig. 5. The increased current increases linearly with $[CF_2Cl_2]$ at low partial pressures, and then saturates at high partial pressures. The saturation of increased current at high CF_2Cl_2 partial pressure is probably due to the conduction electrons produced by laser photodetachment of Cl^- being reattached to CF_2Cl_2. The current increase is also not due to the photoionization of CF_2Cl_2. Since the ionization energy of CF_2Cl_2 is 12.31 eV [19], it requires at least two ArF laser photons (6.42 eV) or three KrF laser photons (5 eV) to ionize CF_2Cl_2. In Fig. 6, the current increase is linearly proportional to laser power at low energy flux, indicating that the current increase is most likely caused by a single photon process. This assertion was further checked by measuring the multiphoton-ionization coefficient using a parallel-plate drift-tube apparatus. The two-photon-ionization coefficients of several molecules have been measured using this apparatus [20]. No ionization current was detected for $[CF_2Cl_2]$ up to 5-mtorr partial pressure. This result indicates that the multiphoton-ionization coefficient is very small; thus, the process does not produce sufficient electrons to cause the observed current increase. After examining all possibilities, the current increase likely results from the increase of conduction electrons photodetached from the negative ions by laser photons. Similar transient current waveforms were observed in the discharge medium of $SOCl_2$-N_2, when the discharge medium was irradiated by ArF laser pulses [21].

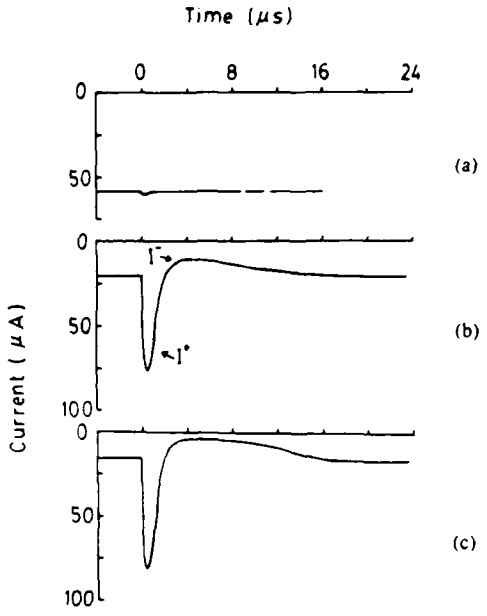

Fig. 4. Transient current waveforms after the discharge medium was irradiated by ArF laser pulses. The partial pressures of CF_2Cl_2 were (a) ~0, (b) 1, and (c) 2 mtorr; the laser energy flux was 30 mJ/cm^2; the laser beam diameter was 3 mm; the applied voltage was −0.95 kV; and the N_2 pressure was about 26 torr. I^+ and I^- indicate the increase and the decrease from the dc current level, respectively.

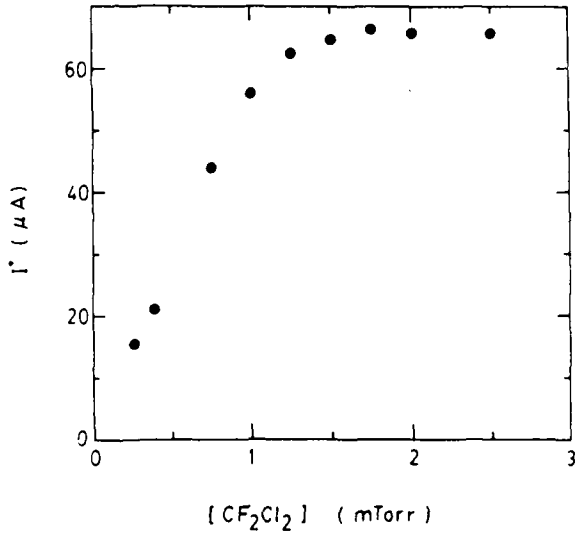

Fig. 5. Maximum value of increased current I^+ as a function of the CF_2Cl_2 concentration.

The current increase versus ArF laser energy flux is shown in Fig. 6, curve (*a*), where $[CF_2Cl_2]$ was ~1.2 mtorr, the applied voltage was −0.95 kV, and the laser beam diameter was 3 mm. The beam diameter was determined from the diameter of the diaphragm in front of the gas cell, the divergence angle of the laser beam, and the distance from the diaphragm to the central region of the gas cell. Since only the central portion of the laser beam was used (the original beam size is about 0.6 × 2 cm^2), the laser flux could be assumed to be spatially uniform. The data in Fig. 6 can be used to derive the photodetachment cross section of negative ions under this discharge condition. The number of negative ions N^- after laser irradiation is given by [22]

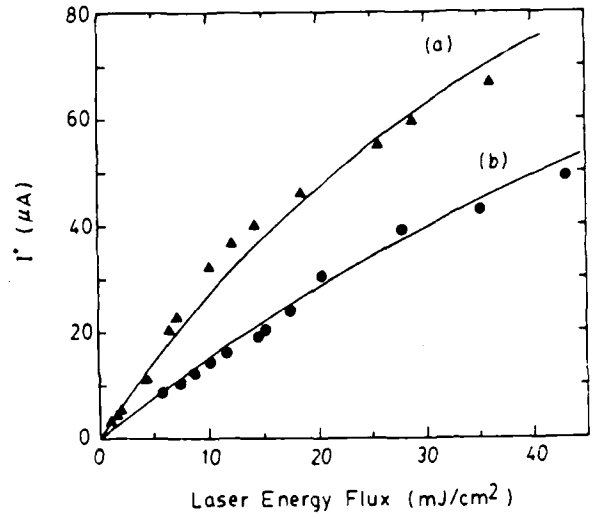

Fig. 6. Values of I^+ as a function of laser energy flux for (*a*) ArF and (*b*) KrF laser irradiation on the discharge medium of CF_2Cl_2 in N_2. The applied voltage was −0.95 kV, $[CF_2Cl_2]$ ~1.2 mtorr, $[N_2]$ ~26 torr, and the laser beam diameter was 3 mm. The solid lines are the best fit to the data using (3).

$$N^- = N_0^- e^{-\sigma J \Delta t} \tag{2}$$

where N_0^- is the number of negative ions before laser irradiation, σ is the photodetachment cross section at the laser wavelength, J is the laser flux at the central region between electrodes, and Δt is the duration of laser pulse. The number of electrons produced by laser photodetachment is

$$\Delta N_e = N_0^- - N^- = N_0^-(1 - e^{-\sigma J \Delta t}). \tag{3}$$

ΔN_e can be determined from the current increase I^+, that is, $I^+ = \Delta N_e \overline{W}$, where $\overline{W}$ is the mean electron drift velocity. $\overline{W}$ may be affected by the change of the local field due to laser irradiation on the discharge medium [5]. However, the current increase was measured at its peak value which is about 0.5 μs after the laser irradiation. At this later time, most of the electrons produced from the laser irradiation have moved away from the laser irradiation region. In this region, the gas property is not affected by the perturbation, and E/N may recover at this later time. Thus, $\overline{W}$ at this later time may be nearly constant, namely, it is not seriously affected by the laser irradiation. Thus, the peak current I^+ is presumably proportional to ΔN_e.

The experimental data of Fig. 6, curve (*a*) were fitted by this equation and represented as a solid line with $\sigma = 2.5 \times 10^{-17}$ cm^2. This uncertainty of the σ value is about ±20 percent of the given value. The photoelectron-detachment cross section of Cl^- has been measured in a Cl^- ion beam experiment by Mandl [6] from the threshold wavelength (~340 nm) to 200 nm. The extrapolated value from [6] at 193 nm is about 2.2×10^{-17} cm^2. This

extrapolated value is close to our result measured under a discharge condition.

The saturation experiment was also performed on the same gas mixture using a KrF laser (248 nm) immediately after the ArF experiment, and the results are shown in Fig. 6, curve (*b*). The experimental conditions, i.e., the discharge parameters, laser beam size, and laser beam position (in the central region between electrodes), were kept the same for both measurements. The experimental data were fitted by (3) with $\sigma = 1 \times 10^{-17}$ cm^2 as shown by the solid line in Fig. 6, curve (*b*). Our value is close to the photodetachment cross section of Cl^- measured at 248 nm by the Cl^- beam experiment [6], which is $\sim 1.3 \times 10^{-17}$ cm^2. The good agreement between these σ values further supports the assertion that Cl^- is the primary negative ion that is photodetached to induce the current increase.

C. Enhancement of Conductivity in CH_3Cl-N_2

Laser-induced enhancement of conductivity was also observed in the discharge medium of CH_3Cl in N_2 buffer gas. Fig. 7 shows the transient current waveforms induced by ArF laser pulses which were taken at CH_3Cl partial pressures of ~ 0, 1.1, and 4.3 mtorr (see Fig. 7(a), (b), and (c), respectively) in an applied voltage of -0.9 kV, a laser energy flux of 40 mJ/cm^2, and a laser beam diameter of 3 mm. As shown in Fig. 7, the value of dc current decreases with increasing $[CH_3Cl]$ due to electron attachment to CH_3Cl; however, this current decrease requires more CH_3Cl gas pressure than that of CF_2Cl_2, because the electron attachment rate constant [10] of the former is less than that of the latter. Similar to the case of CF_2Cl_2-N_2 discharge medium, when trace amounts of CH_3Cl are introduced into the N_2 discharge medium, current increases immediately following the laser irradiation at $t = 0$ as shown in Fig. 7(b), (c). However, in contrast to the case of CF_2Cl_2, the current does not decrease below the dc current level after the current increase. This phenomenon will be further discussed in the next section.

Similar to the case of CF_2Cl_2, the current increase in Fig. 7 is not due to photoionization of CH_3Cl. The ionization energy of CH_3Cl is 11.28 eV [19]. In order to ionize CH_3Cl, it requires two ArF laser photons or three KrF laser photons. The current increase I^+ is linearly proportional to laser power at low laser flux as shown in Fig. 8, curves (*a*) and (*b*) for laser wavelengths of 193 and 248 nm, respectively. The primary negative ion existing in the discharge medium of CH_3Cl-N_2 is expected to be Cl^-, produced by the $CH_3Cl + e \rightarrow CH_3 + Cl^-$ process [23]. The ΔH for this process is -0.1 eV as calculated from the heats of formation for CH_3Cl and CH_3 of 35.62 and -18.1 kcal/mol [14], respectively. Thus, Cl^- can be produced at low electron energy, and it is expected to be the dominant ion in the CH_3Cl-N_2 discharge medium. The photoelectron-detachment of Cl^- is again the cause for the laser-induced current increase.

The data of current increase shown in Fig. 8, curves (*a*) and (*b*) were taken with $[CH_3Cl] \sim 7.3$ mtorr, the applied voltage of -0.9 kV, and the laser beam diameter of 3 mm. These two data sets were measured under the same experimental conditions. The experimental data were fitted by (3) with the σ values of 2.5×10^{-17} cm^2 at 193 nm and 1×10^{-17} cm^2 at 248 nm. These two values coincide with the values obtained from the discharge medium of CF_2Cl_2-N_2. This excellent agreement between the

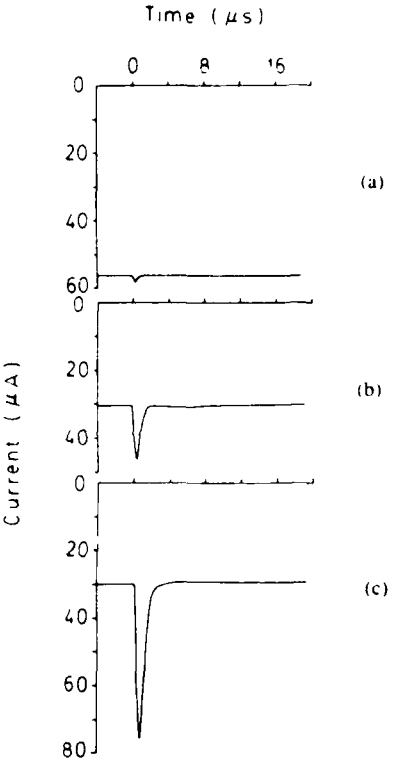

Fig. 7. Transient current waveforms induced by ArF laser irradiation of a discharge medium of CH_3Cl-N_2. The partial pressures of CH_3Cl were (a) ~ 0, (b) 1.1, and (c) 4.3 mtorr, the laser energy flux was 40 mJ/cm^2, the laser beam diameter was 3 mm, the applied voltage was -0.9 kV, and the N_2 pressure was about 26 torr.

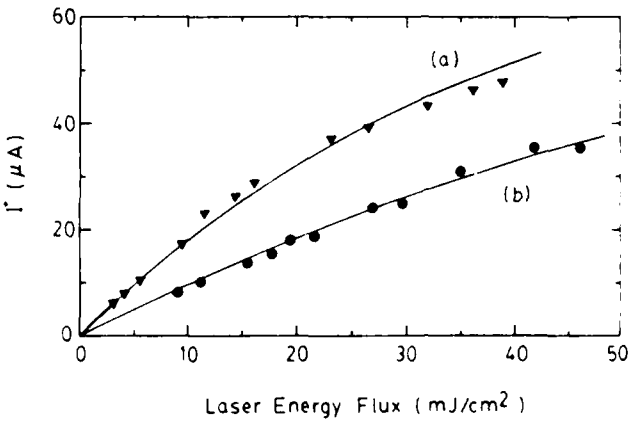

Fig. 8. Current increase I^+, as a function of laser energy flux for (*a*) ArF and (*b*) KrF laser irradiation on the discharge medium of CH_3Cl in N_2. The applied voltage was -0.9 kV, $[CH_3Cl] \sim 7.3$ mtorr, $[N_2] \sim 26$ torr, and laser beam diameter was ~ 3 mm. The solid lines are the best fit to the data using (3).

photoelectron-detachment cross sections measured by different experiments further supports the assertion that the current increase is caused by the photoelectron detachment of Cl^- observed in the discharge media studied.

D. Reduction of Conductivity Observed in Discharge Medium of CF_2Cl_2–N_2

In Fig. 4(b), (c), the discharge current decreased below the dc discharge current level after the initial current increase. This transient current decrease was only observed in CF_2Cl_2 (Fig. 4) but not in CH_3Cl (Fig. 7). This current decrease is a kind of current oscillation phenomenon which will depend on the relative impedances of all circuit components. It is possible that the impedance of the CF_2Cl_2–N_2 discharge medium could be changed by the laser irradiation such that its combination with the external circuit causes a resonance. The impedance of the discharge medium could be changed by electron attachment to the excited state of CF_2Cl_2 and/or to photofragments produced by the laser excitation of CF_2Cl_2. The photoabsorption cross section [24] of CF_2Cl_2 at 193 nm is 4×10^{-19} cm^2. For 2 mtorr of CF_2Cl_2, a concentration of 10^{12} cm^{-3} for the CF_2Cl and Cl radicals could be produced by a laser energy flux of 30 mJ/cm^2. It is expected that vibrationally excited CF_2Cl_2 and excited radicals also exist in the discharge medium, for which the photoabsorption cross sections may be higher than that of CF_2Cl_2 in the ground state. Therefore, the radicals produced by laser irradiation may be much higher than the concentration expected from photodissociation of CF_2Cl_2 in the ground state alone. If the concentration of radicals produced is 10^{13} cm^{-3} and the electron attachment rate constant of this radical is 10^{-7} cm^3/s, then the current decrease due to the attachment by this dissociation product could occur within a microsecond, which is about the time scale for the current decrease in Fig. 4(b), (c).

The ratio of the maximum current decrease I^- to the dc current I is plotted against $[CF_2Cl_2]$ in Fig. 9, curve (*a*). The value of I^-/I increases at low $[CF_2Cl_2]$ but saturates at higher $[CF_2Cl_2]$. Curve (*b*) of Fig. 9 shows the pulsewidth (FWHM) of the transient current as a function of $[CF_2Cl_2]$. The pulsewidth increases at low $[CF_2Cl_2]$ but it saturates at high pressure. It is also observed that the pulsewidth is almost linearly proportional to the laser beam diameter. Present observation indicates that the time for the reduction of a discharge current (duration of I^-) can be controlled by changing laser beam size and concentration of CF_2Cl_2. This effect can, in principle, be used to control the recovery time and repetition rate of a discharge switch.

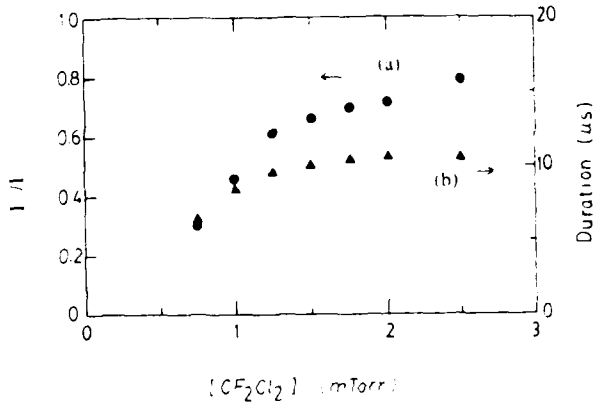

Fig. 9. (*a*) Ratio of the maximum decreased current I^- to the dc discharge current I. (*b*) Duration (FWHM) of the decreased current pulse as a function of CF_2Cl_2 concentration.

IV. Conclusion

Electron attachment rate constants of CF_2Cl_2 in N_2 and Ar buffer gases are measured at various E/N. Such data were used to deduce that the Cl^-, Cl_2^-, and F^- were the dominant negative ions in the discharge media studied. The transient current increase induced by laser irradiation of the discharge medium is attributed to enhanced photoelectron detachment of Cl^- by laser photons. A decrease of transient current below the dc current is also observed in the discharge medium of CF_2Cl_2–N_2, which is likely a kind of current oscillation caused by impedance change of the discharge medium by laser irradiation. For the discharge medium of CH_3Cl–N_2, only the transient current increase, but not the current decrease, was observed. The photodetachment cross sections of Cl^- under a discharge condition were measured to be 2.5×10^{-17} cm^2 at 193 nm and 1.0×10^{-17} cm^2 at 248 nm. These values are close to the data measured by a negative ion beam experiment.

This experiment demonstrates that the discharge current can be switched by laser-induced molecular processes. This information is useful for the development of diffuse-discharge switches.

References

[1] G. Schaefer, P. F. Williams, K. H. Schoenbach, and J. T. Moseley, "Photodetachment as a control mechanism for diffuse discharge switches," *IEEE Trans. Plasma Sci.*, vol. PS-11, p. 263, 1983.

[2] K. H. Schoenbach, G. Schaefer, M. Kristiansen, L. L. Hatfield, and A. H. Guenther, "Diffuse discharge opening switches," in *Electrical Breakdown and Discharges in Gases*, Part b, E. E. Kunhardt and L. H. Luessen, Eds. New York: Plenum, 1983, p. 415.

[3] G. Schaefer and K. H. Schoenbach, "A review of diffuse discharge opening switches," *IEEE Trans. Plasma Sci.*, vol. PS-14, p. 561, 1986.

[4] K. E. Greenberg, G. A. Hebner, and J. T. Verdeyen, "Negative ion densities in NF_3 discharges," *Appl. Phys. Lett.*, vol. 44, p. 299, 1984.

[5] R. A. Gottscho and C. E. Gaebe, "Negative ion kinetics in RF glow discharges," *IEEE Trans. Plasma Sci.*, vol. PS-14, p. 92, 1986.

[6] A. Mandl, "Electron photodetachment cross sections of Cl and Br," *Phys. Rev. A*, vol. 14, p. 345, 1976.
A. Mandl, "Electron photodetachment cross section of the negative ion of fluorine," *Phys. Rev. A*, vol. 3, p. 251, 1971.

[7] D. L. McCorkle, A. A. Christodoulides, L. G. Christophorou, and I. Szamrej, "Electron attachment to chlorofluoromethanes using the electron-swarm method," *J. Chem. Phys.*, vol. 72, p. 4049, 1980.

[8] W. C. Wang and L. C. Lee, "Electron attachment to H_2O in Ar, N_2, and CH_4 in electric field," *J. Appl. Phys.*, vol. 57, p. 4360, 1985.
W. C. Wang and L. C. Lee, "Electron attachment rate constants of $SOCl_2$ in Ar, N_2, and CH_4," *J. Chem. Phys.*, vol. 85, p. 6470, 1986.

[9] S. R. Hunter and L. G. Christophorou, "Electron attachment to the perfluoroalkanes n-C_NF_{N+2} ($N = 1 - 6$) using high pressure swarm techniques," *J. Chem. Phys.*, vol. 80, p. 6150, 1984.

[10] T. G. Lee, "Electron attachment coefficients of some hydrocarbon

flame inhibitors," *J. Phys. Chem.*, vol. 67, p. 360, 1963.

[11] K. M. Bansal and R. W. Fessenden, "Electron disappearance in pulse irradiated fluorocarbon gases," *J. Chem. Phys.*, vol. 59, p. 1760, 1973.

[12] D. Smith, N. G. Adams, and E. Alge, "Attachment coefficients for the reactions of electrons with CCl_4, CCl_3F, CCl_2F_2, $CHCl_3$, Cl_2, and SF_6 determined between 200 and 600 K using the FALP technique," *J. Phys. B: Atmo. Mol. Phys.*, vol. 17, p. 461, 1984.

[13] V. M. Pejcev, M. V. Kurepa, and I. M. Cadez, "Total ionization and electron attachment cross sections of CCl_2F_2 by electron impact," *Chem. Phys. Lett.*, vol. 63, p. 301, 1979.

[14] H. Okabe, *Photochemistry of Small Molecules*. New York: Wiley, 1978.

[15] D. R. Stull and H. Prophet, *JANAF Thermochemical Tables*, 2nd ed. (Nat. Stand. Ref. Data Ser.). Washington, DC: Nat. Bur. Stand., 1971.

[16] A. A. Christodoulides, D. L. McCorkle, and L. G. Christophorou, "Electron attachment processes," in *Electron-Molecule Interactions and Their Applications*, vol. II, L. G. Christophorou, Ed. Orlando, FL: Academic, 1984, p. 478.

[17] R. Schumacher, H. R. Sprunken, A. A. Christodoulides, and R. N. Schindler, "Studies by the electron cyclotron resonance technique. 13. Electron scavenging properties of the molecules CCl_3F, CCl_2F_2, $CClF_3$, and CF_4," *J. Phys. Chem.*, vol. 82, p. 2248, 1978.

[18] L. C. Lee, G. P. Smith, J. T. Moseley, P. C. Cosby, and J. A. Guest, "Photodissociation and photodetachment of Cl_2^-, ClO^-, Cl_3^-, and $BrCl_2^-$," *J. Chem. Phys.*, vol. 70, p. 3237, 1979.

[19] K. Watanabe, T. Nakayama, and J. Mottl, "Ionization potentials of some molecules," *J. Quant. Spectrosc. Radiat. Transfer*, vol. 2, p. 369, 1962.

[20] W. C. Wang and L. C. Lee, "Two-photon-ionization coefficients of CS_2, SO_2, and $(CH_3)_3N$," *J. Appl. Phys.*, vol. 58, p. 3295, 1985.

[21] W. C. Wang and L. C. Lee, "Switching of electron conduction current by photoelectron-detachment and photodissociation processes observed in the discharge medium of $SOCl_2$ in N_2," unpublished, 1986.

[22] J. Taillet, "Determination des concentrations en ions negatifs per photodetachment-eclair," *C. R. Acad. Sci. Paris*, vol. 269, p. 52, 1969.

[23] W. E. Wentworth, R. George, and H. Keith, "Dissociative thermal electron attachment to some aliphatic chloro, bromo, iodo compounds," *J. Chem. Phys.*, vol. 51, p. 1791, 1969.

[24] F. S. Rowland and M. J. Molina, "Chlorofluoromethanes in the environment," *Rev. Geophys. Space Phys.*, vol. 13, p. 1, 1975.

J. Phys. D: Appl. Phys. 21 (1988) 675–682. Printed in the UK

Photodetachment cross sections of negative halogen ions in discharge media

W C Wang and L C Lee

Department of Electrical and Computer Engineering, San Diego State University, San Diego, CA 92182, USA

Received 6 July 1987, in final form 9 December 1987

Abstract. Laser-induced increases of discharge current were observed in the discharge media containing various halogen compounds (F_2, HF, HCl, Cl_2, HBr, CH_3Br, CH_3I and CH_2I_2) in N_2. The increases of transient current were attributed to the photodetachment of negative ions in the discharge media. On the basis of general considerations, the negative ions present in the discharge are assumed to be the atomic halogen negative ions. Photodetachment cross sections were determined from the current increases as a function of laser flux. Photodetachment cross sections of F^-, Cl^-, Br^- and I^- are (0.75, 2.5, 3.3 and 7.0) $\times 10^{-17}$ cm^2 at 193 nm and (0.6, 1.0, 1.5 and 3.0) $\times 10^{-17}$ cm^2 at 248 nm, respectively. These data are compared with the earlier results of negative ion beam experiments and theoretical calculations.

1. Introduction

Photodetachment of negative halogen ions occurs in the atmosphere and in discharge systems (Smirnov 1982). The photodetachment cross sections of negative halogen ions are generally of interest for the studies of laser and plasma physics. Recently, the photodetachment processes of F^- and C^- in discharge media containing NF_3 (Greenberg *et al* 1984), Cl_2 (Gottscho and Gaebe 1986), as well as CF_2Cl_2 and CH_3Cl (Wang and Lee 1987) were studied. These photodetachment data are useful for the development of diffuse discharge switches (Schaefer *et al* 1983, Schaefer and Schoenbach 1986), as well as for understanding the etching and deposition processing of electronic materials.

Photodetachment cross sections of negative halogen ions have been calculated by several investigators (Rescigno *et al* 1978, Ishihara and Foster 1974, Robinson and Geltman 1967, Clodius *et al* 1983, Radojevic *et al* 1987) and also measured by several experiments (Vacquie *et al* 1987, Rothe 1969, Mandl 1971, 1976). Photodetachment cross sections were previously all measured at wavelengths longer than 200 nm (>200 nm for F^-, Cl^-, Br^-; and >300 nm for I^-) without the presence of an electric field.

In this work, the photodetachment cross sections of F^-, Cl^-, Br^- and I^- in discharge media were measured at 193 nm (ArF laser) and 248 nm (KrF laser). The negative halogen ions were produced by DC glow discharges of gas mixtures of various halogen compounds (F_2, HF, HCl, Cl_2, HBr, CH_3Br, CH_3I and CH_2I_2) in N_2 buffer gas. When the discharge media were irradiated by laser pulses, transient current increases were observed. The current increase is attributed to the photodetachment of electrons from negative ions. The photodetachment cross sections of negative ions were determined from the plots of current increase versus laser flux integral. The possible negative ions existing in the discharge media are discussed in this paper. A comparison of the measured photodetachment cross sections with the published experimental data and theoretical values is made.

2. Experimental

The experimental set-up is shown in figure 1, where the gas cell used is a six-way black-anodised aluminium cross of 150 mm OD. Inside the gas cell, the cathode was a steel wire 0.5 mm in diameter with a hemisphere tip, and the anode was a stainless steel plate 5 cm in diameter, they being placed 1.5 cm apart. A DC negative high voltage was applied to the cathode through a 5.6 MΩ resistor. The discharge current was measured by the voltage across a 1000 Ω resistor connecting the anode to ground with an input capacitance of about 10^{-10} F. An excimer laser beam (Lumonics Model 861S) was used to irradiate the discharge medium, where the laser pulse duration (FWHM) was 10 ns with a tail of about 8 ns and the beam size was about 3 mm in diameter. The laser beam size was limited by a

0022-3727/88/050675 + 08 $02.50

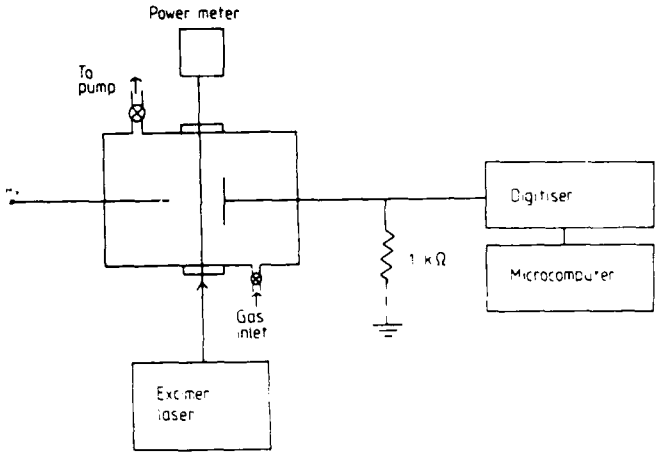

Figure 1. A schematic diagram of the experimental apparatus. The electrode spacing was ≈1.5 cm.

diaphragm placed in front of the gas cell. The actual beam size in the discharge medium is affected by the divergence angle of the laser beam and the distance between the diaphragm and the discharge region. These factors were taken into account in the calculation of laser flux. Since only the central portion of the laser beam was used in the experiment (the original beam size was about $0.6 \times 2\ cm^2$), the laser flux was assumed to be spatially uniform. The laser flux was measured by an energy meter (Scientech Model 365) behind the exit window of the gas cell, where the window transmission is about 90% for KrF and 80% for ArF. The transient current waveforms induced by laser irradiation were monitored by a 150 MHz digital storage oscilloscope (Tektronix 2430) and were subsequently stored in an IBM-PC microcomputer.

The gas pressure was monitored by a MKS-Baratron manometer, where the total pressure was about 25 Torr. All measurements were performed at room temperature. Most of the halogen compounds were premixed in N_2 before being introduced into the gas cell. The purity of N_2 (MG Scientific) was better than 99.998%. The purities of HF, HBr and CH_3Br, supplied by Matheson were 99.9%, 99.8% and 99.5%, respectively. Diluted F_2 (10% in He, Matheson), Cl_2 (2% in He, Matheson), and HCl (20% in He, MG Scientific) were used as delivered. The purities for the liquids of CH_3I and CH_2I_2 (Alfa Products) were better than 99.0%. Each liquid was kept in a Teflon bottle inside a stainless steel container. The liquid in the stainless steel container was continuously pumped for a few hours at the dry ice temperature, before it was introduced into the gas cell.

3. Results and discussion

A point-to-plane discharge was sustained by applying a negative DC high voltage of 700–900 V to the N_2 medium. When a trace amount of halogen compound was introduced into the gas cell, the DC discharge current decreased due to electron attachment to the halogen compound. The amount of current decrease depends on the concentration and species of halogen compounds. The higher the concentration added, the greater was the current decrease. Also, the current decrease increases with the electron attachment rate of halogen compound. For example, the attachment rate constant of HCl at low electron energy is about 10^{-10} $cm^3\ s^{-1}$ (Sze *et al* 1982) and the attachment rate constant of CH_3I at thermal energy is 7×10^{-8} $cm^3\ s^{-1}$ (Christophorou 1976). When 0.2 mTorr of HCl and 0.1 mTorr of CH_3I were added into N_2 discharge media, the DC discharge currents were reduced from 55 μA to 41 μA (see figure 2(*b*)) and to 23 μA (see figure 2(*d*)), respectively. Experimental results indicate that the major negative ions in the discharge media are atomic halogen ions (see the following discussion).

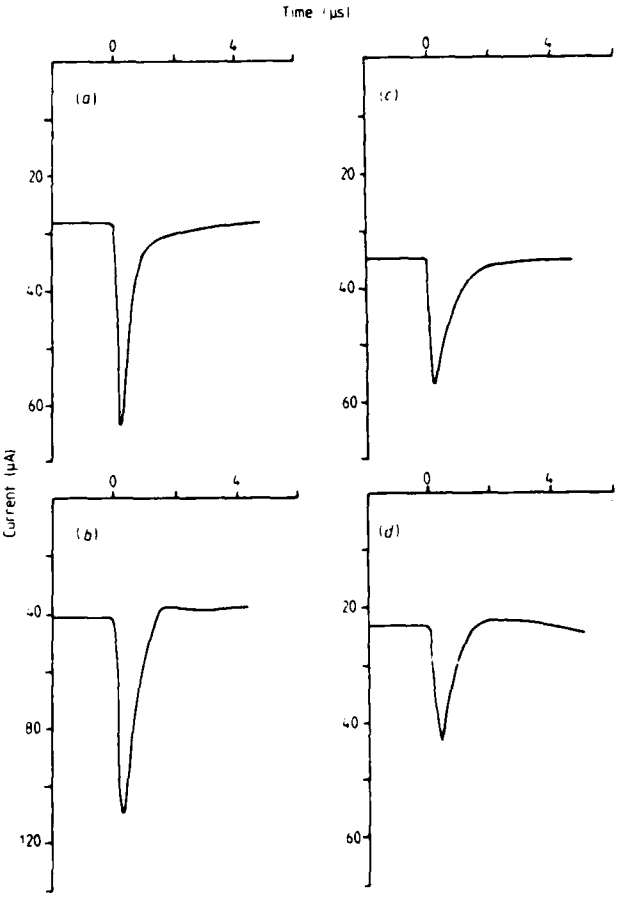

Figure 2. Transient current waveforms produced by the ArF laser irradiation of discharge media. The partial pressures of various halogen compounds were (*a*) $[F_2] \approx 0.15$, (*b*) $[HCl] \approx 0.2$, (*c*) $[HBr] \approx 1.0$, and (*d*) $[CH_3I] \approx 0.1$ mTorr. The energy fluxes of the ArF laser were (*a*) 35, (*b*), 26, (*c*) 14, and (*d*) 30 mJ cm^{-2}. The applied voltages were (*a*) −0.7, (*b*) −0.9, (*c*) −0.8, and (*d*) −0.9 kV. The N_2 pressure was about 25 Torr and the laser beam diameter was ≈3 mm.

When the discharge media were irradiated by excimer laser pulses, the discharge current increased initially and then recovered to the original DC level

after a few μs, as can be seen from figures 2(*a*) and 2(*c*) for the discharge media of F_2 and HBr, respectively. For the discharge media of HCl (figure 2(*b*)) and CH_3I (figure 2(*d*)), the discharge current did not recover to the DC level after a few μs, but showed a kind of current oscillation. This oscillation could be due to the impedance change of the discharge medium caused by laser irradiation.

The transient current increase depends on the partial gas pressure of the halogen compound as shown in figure 3. The increased current increases linearly with

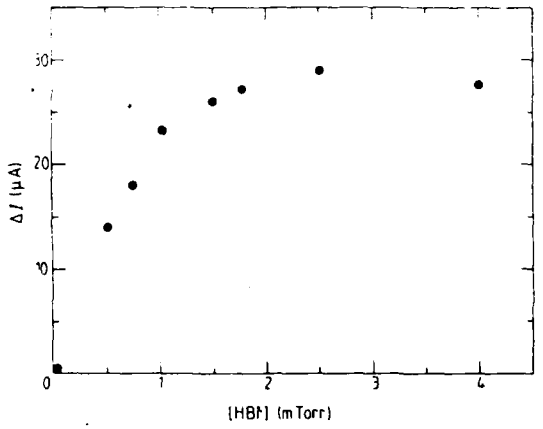

Figure 3. The peak values of the transient current increase, ΔI, as a function of the partial pressure of HBr, where the ArF laser energy is $\simeq 14\ mJ\ cm^{-2}$.

[HBr] at low partial pressures but saturates at high partial pressures. The saturation of increased current (or the negative ion) at high HBr partial pressure may be due to conduction electrons being mostly attached to HBr. Since the increased current depends on [HBr] as shown in figure 3, the transient current increase is thus not due to the transient noise induced by the laser discharge. The current increase is also not due to the photo-ionisation of halogen compounds except for the case of Cl_2 (see § 3.4). For the molecules studied, the ionisation energies are in the 9.5–16 eV range, for example, the ionisation energies are 9.54 eV for CH_3I and 15.77 eV for HF (Watanabe *et al* 1962). It requires at least two ArF (or KrF) laser photons to ionise these halogen compounds, namely, by a multiphoton ionisation process. The current increases in most discharge media are linearly proportional to laser power at low laser power (see figures 4 and 5), indicating that the current increase is caused by a single photon process. The assertion that the current increase is not caused by photo-ionisation of the halogen compound is further checked by measuring the two-photon ionisation coefficient using a parallel-plate drift-tube apparatus (Wang and Lee 1985). Except for Cl_2 irradiation by an ArF laser (see § 3.4), no currents due to ionisation of neutrals were detected with exposure of the studied molecules to 193 and 248 nm radiation. From the above experimental facts, it is concluded that the current increase is produced only by the photodetachment process. Thus, the current increase as a function of laser flux can be used to derive the photodetachment cross section as described below.

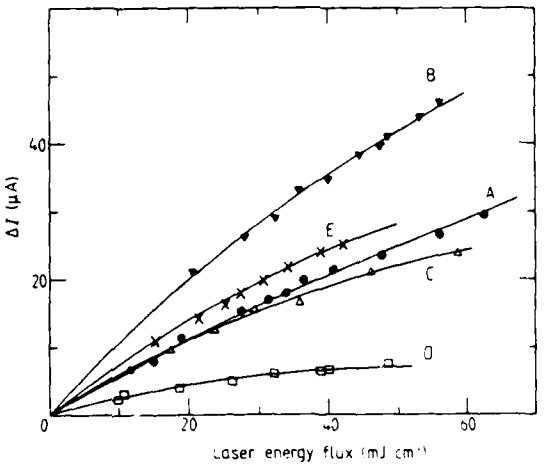

Figure 4. The peak values of current increase versus the energy fluxes of the KrF laser (248 nm) in the discharge media containing F_2 (curve A), HCl (curve B), HBr (curve C), CH_3I (curve D), and Cl_2 (curve E). The applied voltages were −0.7, −0.9, −0.8, −0.9 and −0.9 kV, respectively; and the partial pressures of the halogen compounds were 0.15, 0.2, 1.0, 0.1, and 0.8 mTorr, respectively. The full curves are the best fit to the data using equation (2).

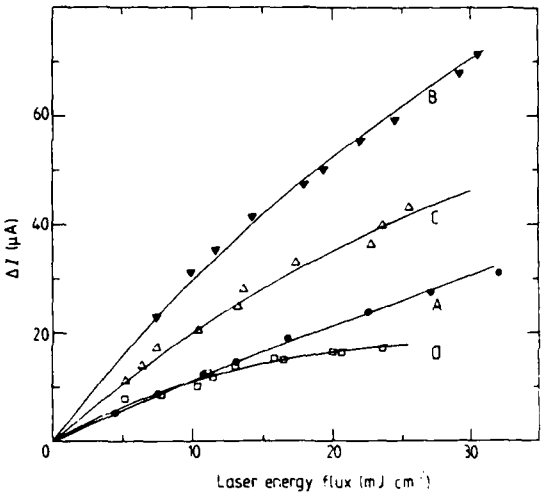

Figure 5. The peak current increases versus the energy fluxes of the ArF laser (193 nm) in the discharge media containing F_2 (curve A), HCl (curve B), HBr (curve C), and CH_3I (curve D). The applied voltages were −0.7, −0.9, −0.8, and −0.9 kV respectively, and the partial pressures of the halogen compounds were 0.15, 0.2, 1.0, and 0.4 mTorr, respectively. The full curves are the best fit to the data using equation (2).

The number of negative ions, N^-, after laser irradiation is obtained by integration of an expression given by (Taillet 1969)

$$N^- = N_0\ e^{-\sigma J \Delta t} \qquad (1)$$

where N_0^- is the number of negative ions before laser irradiation, σ is the photodetachment cross section at the laser wavelength, J is the laser flux, and Δt is the duration of laser pulse. The number of electrons produced by laser photodetachment is

$$\Delta N_e = N_0^- - N^- = N_0^-(1 - e^{-\sigma J \Delta t}). \quad (2)$$

Here, ΔN_e can be determined from the current increase, ΔI, that is, $\Delta I \propto \Delta N_e \bar{W}$, where $\bar{W}$ is the mean electron drift velocity. It should be noted that $\bar{W}$ could be affected by the change of local field due to laser irradiation of the discharge medium (Gottscho and Gaebe 1986). In our experiment, the current increase was measured at its peak which is about 0.3 μs after laser irradiation (see figure 2). At this later time, most of the photodetachment electrons have moved away from the laser irradiation region to enter a region where the gas property is not seriously affected by the perturbation. Also, the electric field that may be disturbed by the laser irradiation will recover at this later time. Thus, the $\bar{W}$ at this later time is expected to be nearly constant, and the peak current, ΔI, is thus proportional to ΔN_e.

The other sources of uncertainty relevant to equation (2) are the laser beam profile and secondary reaction processes (Gottscho and Gaebe 1986). In deriving (2), the laser beam intensity was assumed to be uniform. Thus was justified by using only the central portion of the laser beam for the experiment. The secondary reaction processes should not be important in our experiment because the concentration of halogen compound was small. As an example, the electron attachment rate constant of CH_3I, which is the highest among the halogen compounds we investigated, is 7×10^{-8} cm^3 s^{-1} (Christophorou 1976) at thermal energy. For 0.1 mTorr of CH_3I, its maximum attachment rate is 2.3×10^5 s^{-1} and the reaction time is about 4 μs which is much longer than the duration of the laser pulse and the current-increase pulse. Thus, the electron attachment process does not affect the measurement of ΔN_e.

In figure 2, there is about a 0.3 μs delay in the observation of peak current increase. This delay time may be the combination of the RC time constant ($\simeq$ 0.1 μs) of the input circuit, the relaxation time for the photodetached electrons to reach an equilibrium state, and the drift time of the photodetached electrons to the anode. The rapid current drop after the peak is likely due to the absorption of electrons by the anode, but not charge recombination or electron attachment. The charge recombination coefficient of N_2^+ at room temperature is about 3×10^{-7} cm^3 s^{-1} (Kasner 1967). For an ion density of approximately 10^{11} cm^{-3} in our discharge system, the recombination rate is 3×10^4 s^{-1}, which is much slower than the current drop rate. CH_3I has a maximum electron attachment rate of 2.3×10^5 s^{-1} which is the highest for all the molecules we studied. This is also much smaller than the current drop rate.

The σ-values are determined by the best fit of experimental data of ΔI versus laser flux with equation (2) as shown in figures 4 and 5. The photodetachment cross sections are listed in table 1 for both the KrF (248 nm) and ArF (193 nm) laser wavelengths. The

Table 1. Photodetachment cross sections of negative halogen ions at 248 and 193 nm (in units of 10^{-18} cm^2).

		248 nm			193 nm	
Ions	Compounds studied	This work	Other experimental values	Theoretical values	This work	Theoretical values
F^-	F_2	6	5.5[a]	6.5[b], 5.5[c]	8	7.3[b], 9.4[d]
	HF	6		7.8[d], 7.3[e] 6.7[g]	7	7.8[g]
Cl^-	HCl	10			25	27[d], 20[g]
	Cl_2	10	14[f]	17[d], 16[g]		
	CF_2Cl_2	10[h]			25[h]	
	CH_3Cl	10[h]			25[h]	
Br^-	HBr	15	19[f]	28[d], 20[g]	30	44[d], 26[g]
	CH_3Br	15			35	
I^-	CH_3I	30		49[d], 31[g]	75	83[d], 40[g]
	CH_2I_2				65	

[a] Mandl (1971).
[b] Rescigno *et al* (1978).
[c] Ishihara and Foster (1974).
[d] Robinson and Geltman (1967).
[e] Clodius *et al* (1983).
[f] Mandl (1976).
[g] Radojevic *et al* (1987).
[h] Wang and Lee (1987).

experimental data (Mandl 1971, 1976) and the theoretical calculated values (Rescigno *et al* 1978, Ishihara and Foster 1974, Robinson and Geltman, 1967, Clodius *et al* 1983, Radojevic *et al* 1987) are also listed in table 1 for comparison. The uncertainty of the σ-values is estimated to be about $\pm 20\%$ of the given value. The current increases of the iodine discharge media are almost saturated at high laser power, so the uncertainty is small ($\pm 10\%$). However, for F^-, the uncertainty is large ($\pm 30\%$) because the current increases are not quite saturated at high laser power density.

The magnitude of the transient current increase depends on the interaction position of the laser beam and plasma. Near the cathode, the field is highly inhomogeneous and $\bar{W}$ may vary with position. The current increase is higher when the laser beam is close to the cathode than that at the central region between electrodes. This is due to the variation of negative ion concentration and electron drift velocity inside the plasma. Although the magnitude of current increase changes with position, the photodetachment cross sections measured at different positions are the same for *all gas mixtures studied, except for* $HF-N_2$. For the discharge medium of $HF-N_2$, two different apparent photodetachment cross sections were obtained at different positions; we assume that the composition of the negative ion population was different at different positions. The results for various discharge media are discussed below.

3.1. F_2

The transient current waveform produced by ArF laser irradiation of the discharge medium of F_2-N_2 is shown in figure 2 (*a*), where the waveform was the average of 64 pulses. The peak current increases versus ArF and ArF laser energy flux are shown in figures 4 (curve A) and 5 (curve A), respectively. The full curves in these figures are the best fit of the experimental data with equation (2), from which the photodetachment cross sections were determined and listed in table 1.

The electron attachment to F_2 has the highest attachment rate constant of $\sim 5.0 \times 10^{-9}\,cm^3\,s^{-1}$ near the thermal energy (Tam and Wong 1978, Chen *et al* 1977). The electron attachment to F_2 is mainly by the dissociative attachment process that produces the only stable negative ion, F^-. In our experiment, when a trace amount of F_2 was introduced into the discharge medium of N_2, the DC current decreased due to electron attachment to F_2. Since the electron-impact excitation of F_2 mainly dissociates into $F + F^-$, it is presumed that F^- is the major negative ion in the discharge medium. Although other negative ions may be produced through processes such as the three-body electron attachment process and ion–molecule reactions, the concentrations of these ions are expected to be small when compared with F^-. For example, the second most dense ion in the discharge medium is likely to be F_2^-. However, F_2^- can not be produced by the charge transfer of F^- to F_2, because the electron affinity (EA) of F (3.4 eV) is higher than that of F_2 (2.9 eV) (Christodoulides *et al* 1984). F_2^- can be only produced by a three-body attachment process for which the attachment rate is usually much smaller than the two-body process that leads to F^-. In order to confirm that our measurement is indeed due to F^-, we also studied the discharge medium of HF needed to produce F^- as discussed in the next section. The good agreement between these systems supports the theory that the measured photodetachment cross section associates with F^-.

At 248 nm, our data agree with the earlier data measured by the negative ion beam experiment (Mandl 1971) and the theoretical values as listed in table 1. At 193 nm, no experimental data are available, but our value is consistent with the theoretical calculations as also listed in table 1. This good agreement suggests that the photodetachment cross section of negative ions in the F_2-N_2 discharge medium really associates with F^-. The good agreement seems also to indicate that this determination of the photodetachment cross section is not significantly affected by the electric field in the discharge medium.

3.2. HF

The photodetachment cross section of the negative ion in the discharge medium of $HF-N_2$ was determined to compare with that of the F_2-N_2 system. However, for *this mixture, the apparent photodetachment* cross section depends on laser beam position. When the laser beam axis was about 0.5 cm away from the cathode (the electrode spacing was 1.5 cm and the beam diameter was 0.3 cm), the measured photodetachment cross sections are $7.0 \times 10^{-18}\,cm^2$ at 193 nm and $6.0 \times 10^{-18}\,cm^2$ at 248 nm, in agreement with those values measured from the F_2-N_2 discharge medium. However, when the laser beam is moved to the centre between the electrodes, the photodetachment cross sections become as large as $4.0 \times 10^{-17}\,cm^2$ at 193 nm and $2.5 \times 10^{-17}\,cm^2$ at 248 nm. As an illustration of the difference, the current increases versus ArF laser energy fluxes measured at the laser beam about 0.5 cm away from the cathode (curve A) and the centre of the electrodes (curve B) are shown in figure 6. The photodetachment cross section deduced from curve A in figure 6 is much smaller than that from curve B in figure 6. The results show that two different kinds of negative ions exist in the discharge medium of $HF-N_2$, which is further discussed below.

The possible electron attachment processes for HF are

$$HF + e \rightarrow F^- + H \qquad \Delta H \approx 2.5\,eV \qquad (3a)$$

$$HF + e \rightarrow H^- + F \qquad \Delta H \approx 5.1\,eV \qquad (3b)$$

where the thermochemical energies, ΔH, were taken from the dissociation energy (DE) of 5.86 eV for HF (Okabe 1978), and the electron affinities (EA) of 3.4 and 0.8 eV for F and H (Christodoulides *et al* 1984).

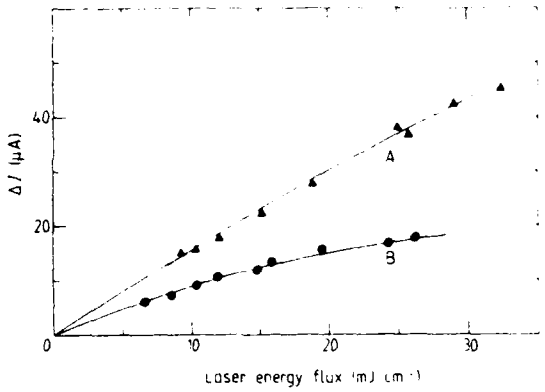

Figure 6. The peak values of current increase versus the ArF laser (193 nm) energy fluxes in the discharge medium of $HF–N_2$, where the laser beam position was 0.5 cm away from the cathode (curve A) and at the centre between the electrodes (curve B). The electrode spacing was 1.5 cm and the beam diameter was 0.3 cm. The partial pressure of HF was 0.3 mTorr.

The electron attachment cross section of HF (Abouaf and Teillet-Billy 1980) shows that F^- is produced in the energy range of 2.3 to 3.5 eV. In a glow discharge system, the closer to the cathode, the higher is the electrode field (Doughty *et al* 1984, 1985); thus, the electron energy near the cathode is expected to be higher than that in the plasma region where the electric field is relatively small. According to the results of figure 6, F^- was produced more near the cathode (sheath) region than in the central region (plasma region). Since the electron energy required to produce H^- is higher than 5 eV, the concentration of H^- is expected to be small. A further investigation of the ion species in the plasma region is of interest.

3.3. HCl

Electron-impact excitation of HCl will produce Cl^- ($\Delta H \simeq 0.76$ eV) or H^- ($\Delta H \simeq 3.63$ eV), where the ΔH-values are taken from the DE of 4.43 eV for HCl (Okabe 1978) and the EA of 3.67 eV for Cl (Christodoulides *et al* 1984). Cl^- is produced in the energy range of 0.5 to 1.5 eV, while H^- is produced in the range ≈6 to 11 eV (Azria *et al* 1974, 1980). Because the mean electron energy in N_2 is usually low, Cl^- is expected to be the dominant negative ion in the discharge medium of $HCl–N_2$. The measured photodetachment cross sections should thus associate with Cl^-. Our value at 248 nm (derived from figure 4 (curve B)) is close to the measurement of Mandl (1976) by beam experiment as listed in table 1. At 193 nm, no experimental data are available, but our value is consistent with the theoretical calculation as listed in table 1.

3.4. Cl_2

Similar to F_2, electron attachment to Cl_2 is a dissociative attachment process; thus, Cl^- should be the dominant negative ions in the $Cl_2–N_2$ discharge medium. At 248 nm, the photodetachment cross section of Cl^- in the discharge medium of $Cl_2–N_2$ (derived from figure 4 (curve E)) was determined to be 1.0×10^{-17} cm^2 which is consistent with the values determined from other chlorine compounds. At 193 nm, the current increase perisistently increases with laser flux without saturation; thus, the photodetachment cross section can not be determined.

The current increase at 193 nm is partly caused by the two-photon ionisation process. The ionisation energy of Cl_2 is 11.48 eV (Watanabe *et al* 1962). At 193 nm (6.42 eV), two-photon ionisation of Cl_2 is energetically possible. This multiphoton process is supported by the observation that (i) the current increase pulse occurs even though the gas medium is not discharged, and (ii) the current increase is proportional to the square of laser power density as shown in figure 7. Because of interference by this multiphoton process, the photodetachment cross section of Cl^- can not be determined from the $Cl_2–N_2$ discharge medium.

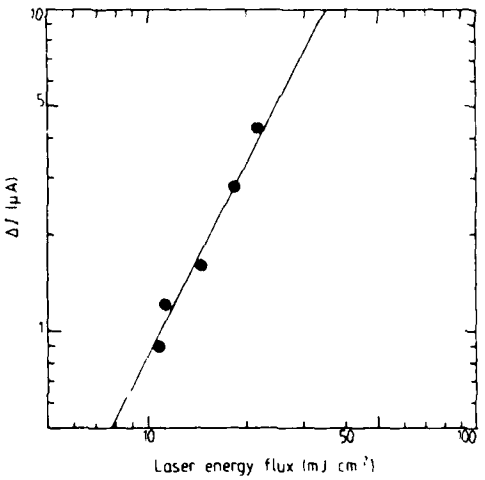

Figure 7. The two-photon ionisation signal versus the energy flux of the ArF laser (193 nm) for Cl_2 in N_2 where a parallel-plate drift-tube apparatus was used. The DC current was zero, the applied voltage was 0.6 kV, and the partial pressure of Cl_2 was 0.2 mTorr.

The photodetachment cross sections of negative ions in the discharge media of $CF_2Cl_2–N_2$ and $CH_3Cl–N_2$ have been measured before (Wang and Lee 1987). The dominant negative ions responsible for photodetachment in these two discharge media were taken to be Cl^-, for which the photodetachment cross sections are also listed in table 1 for comparison. The photodetachment cross sections of Cl^- measured from these two discharge media are the same as those measured with HCl and Cl_2 in N_2.

3.5. HBr

Electron attachment to HBr will produce Br^- ($\Delta H \simeq 0.39$ eV) or H^- ($\Delta H \simeq 2.95$ eV), where the DE of

3.75 eV for HBr (Okabe 1978) and the EA of 3.36 eV for Br (Christodoulides *et al* 1984) give ΔH. The electron attachment cross section of HBr shows that Br^- is produced at an energy below approximately 2 eV (Abouaf and Teillet-Billy 1980) and H^- is produced in the 5–11 eV range (LeCoat *et al* 1982). H^- is again less likely to be produced in the N_2 discharge medium because of its high energy threshold. The photodetachment cross section measured in the discharge medium of HBr–N_2 thus presumably associates with Br^-. Our value at 248nm is close to the measurement of Mandl (1976) as listed in table 1. At 193 nm, no experimental data are available. Our data are again consistent with the theoretical calculation as listed in table 1.

3.6. CH_3Br

The photodetachment cross sections of negative ions in the CH_3Br–N_2 discharge medium were measured to be 3.5×10^{-17} and 1.5×10^{-17} cm^2 at 193 and 248 nm, respectively. The electron attachment process in CH_3Br is

$$CH_3Br + e \rightarrow Br^- + CH_3 \quad \Delta H \simeq -0.39\,eV \quad (4)$$

where ΔH is the difference between the DE of 2.97 eV for CH_3–Br (Okabe 1978) and the EA of 3.36 eV for Br (Christodoulides *et al* 1984). Since the EA of CH_3 is $\simeq 0$ eV, CH_3^- may not be stable, and it is thus unlikely to be produced in the CH_3Br–N_2 discharge medium. Therefore, the measured photodetachment cross sections are attributed to Br^-.

3.7. CH_3I

I^- is presumably the dominant negative ion in the discharge medium of CH_3I–N_2. The determined photodetachment cross section in the discharge medium of CH_3I–N_2 is attributed to I^-. The photodetachment cross sections of I^- at wavelengths shorter than 300 nm have not been reported before. Our values are consistent with the theoretical calculations as listed in table 1.

3.8. CH_2I_2

The photodetachment cross sections of negative ions in the discharge medium of CH_2I_2–N_2 were determined at 193 nm. Since the electron attachment rate constant of CH_2I_2 is very small (DeCorpo *et al* 1971), the concentrations of negative ions in the discharge medium of CH_2I_2–N_2 are quite low. The current of photodetached electrons observed at 193 nm was so small that the experimental uncertainty was high. At 248 nm, the signal was even smaller.

I^- is presumably the dominant negative ion produced from electron-impact excitation of CH_2I_2 at low electron energy. The value of 6.5×10^{-17} cm^2 measured at 193 nm is consistent with the value measured with CH_3I.

4. Conclusion

The transient current increases due to photodetachment of negative ions in the discharge media of halogen compounds in N_2 were investigated using ArF or KrF laser photons. The major negative ions in the various discharge media are attributed to atomic halogen ions. Our data seem generally to agree with the existing experimental data and theoretical calculations. The agreement seems to indicate that the effect of the electric field on the determination of the photodetachment cross sections is not large. The knowledge of photodetachment cross sections is useful for measuring the concentrations of negative ions and for the modelling of diffuse discharge switches.

Acknowledgment

This work is supported by the Air Force Office of Scientific Research under Grant No AFOSR-86-0205.

References

Abouaf R and Teillet-Billy D 1980 *Chem. Phys. Lett.* **73** 106–9
Azria R, LeCoat Y, Simon D and Tronc M 1980 *J. Phys. B: At. Mol. Phys.* **13** 1909–18
Azria R, Roussier L, Paineau R and Tronc M 1974 *Rev. Phys. Appl.* **9** 469–73
Chen H L, Center R E, Trainor D W and Fyfe W I 1977 *Appl. Phys. Lett.* **30** 99–101
Christodoulides A A, McCorkle D L and Christophorou L G 1984 *Electron-Molecule Interactions and Their Applications* vol II, ed. L G Christophorou (Orlando: Academic) p 478
Christophorou L G 1976 *Chem. Rev.* **76** 409–23
Clodius W B, Stehman R M and Woo S B 1983 *Phys. Rev.* A **27** 333–44
DeCorpo J J, Bafus D A and Franklin J L 1971 *J. Chem. Phys.* **54** 1592–7
Doughty D K, DenHartog E A and Lawler J E 1985 *Appl. Phys. Lett.* **46** 352–4
Doughty D K, Salih S and Lawler J E 1984 *Phys. Lett.* **103A** 41–4
Gottscho R A and Gaebe C E 1986 *IEEE Trans. Plasma Sci.* **PS-14** 92–102
Greenberg K E, Hebner G A and Verdeyen J T 1984 *Appl. Phys. Lett.* **44** 299–300
Ishihara T and Foster T C 1974 *Phys. Rev.* A **9** 2350–5
Kasner W H 1967 *Phys. Rev.* **164** 194–200
LeCoat Y, Azria R and Tronc M 1982 *J. Phys. B: At. Mol. Phys.* **15** 1569–79
Mandl A 1971 *Phys. Rev.* A **3** 251–5
—— 1976 *Phys. Rev.* A **14** 345–8
Okabe H 1978 *Photochemistry of Small Molecules* (New York: Wiley)
Radojevic V, Kelly H P and Johnson W R 1987 *Phys. Rev.* A **35** 2117–21
Rescigno T N, Bender C F and McKoy B V 1978 *Phys. Rev.* A **17** 645–9
Robinson E J and Geltman S 1967 *Phys. Rev.* **153** 4–8
Rothe D E 1969 *Phys. Rev.* **177** 93–9
Schaefer G and Schoenbach K H 1986 *IEEE Trans. Plasma Sci.* **PS-14** 561–74

Schaefer G, Williams P F, Schoenbach K H and Moseley J T 1983 *IEEE Trans. Plasma Sci.* **PS-11** 263–5
Smirnov B M 1982 *Negative Ions* (New York: McGraw-Hill) ch 6
Sze R C, Green A E and Brau C A 1982 *J. Appl. Phys.* **53** 1312–6
Taillet J 1969 *C. R. Acad. Sci., Paris* **269** 52–4
Tam W C and Wong S F 1978 *J. Chem. Phys.* **68** 5626–30
Vacquie S, Gleizes A and Sabsabi M 1987 *Phys. Rev.* A **35** 1615–20
Wang W C and Lee L C 1985 *J. Appl. Phys.* **58** 3295–301
—— 1987 *IEEE Trans. Plasma Sci* **PS-15** 460–6
Watanabe K, Nakayama T and Mottl J 1962 *J. Quant. Spectrosc. Radiat. Transfer* **2** 369–82

Electron attachment rate constants of HBr, CH_3Br, and C_2H_5Br in N_2 and Ar

W. C. Wang and L. C. Lee
Department of Electrical and Computer Engineering, San Diego State University, San Diego, California 92182

(Received 28 September 1987; accepted for publication 20 January 1988)

The electron attachment rate constants of bromine compounds in the buffer gases of N_2 and Ar ($\sim$250 Torr) were measured as a function of E/N (or mean electron energy). The measured electron attachment rate constants of HBr, CH_3Br, and C_2H_5Br show maximum values of 1.05×10^{-9}, 1.08×10^{-11}, and 9.3×10^{-11} cm^3/s at mean electron energies of 0.55, 0.4, and 0.8 eV, respectively. The electron drift velocities for the gas mixtures of CH_3Br in N_2 and Ar were also measured.

I. INTRODUCTION

The published electron attachment rate constants of HBr and CH_3Br exhibit a large discrepancy. For example, the electron attachment rate constant of CH_3Br at thermal energy measured by Christodoulides and Christophorou[1] is about three orders of magnitude higher than the values given by Bansal and Fessenden,[2] Wentworth, George, and Keith,[3] Mothes, Schultes, and Schindler,[4] and Alge, Adams, and Smith.[5] Another example, the electron attachment rate constant of HBr measured by Christophorou, Compton, and Dickson[6] increases with decreasing mean electron energy, indicating that a maximum occurs at thermal energy. This is different from the result of Trainor and Boness[7] that the attachment rate constant has a maximum at about 0.6 eV. The absolute value reported by Christophorou and coworkers[6] is also quite different from that of Mothes and coworkers and Trainor and Boness.[7] Measurements of these electron attachment rate constants are of interest for elucidating these discrepancies.

The electron attachment rate constants of bromine compounds are also needed for many practical applications. Current switching due to laser irradiation of the discharge media containing halogen compounds has been recently observed in our laboratory.[8] The current switching can be used for the development of gaseous discharge switches. Electron attachment rate constants over a wide range of electron energy are needed for such development. Also, bromine compounds are often used in plasma etching of electronic materials. The electron attachment data are needed for modeling of the etching process.

The electron attachment rate constants were measured by a parallel-plate drift-tube electron-swarm technique, which has been applied to measure the electron attachment rate constants of many molecules.[9] In this paper, we report the measurements of HBr, CH_3Br, and C_2H_5Br in N_2 and Ar at various E/N. The published attachment rate constants of C_2H_5Br are less controversial than those of HBr and CH_3Br. A comparison between current measurements and published data is included in this paper. The electron drift velocities for the gas mixtures of CH_3Br in N_2 and Ar were also measured at various E/N. The electron drift velocity of a gas mixture is usually different from that of a pure buffer gas.

II. EXPERIMENT

The experimental setup has been described in previous papers.[9] In brief, the gas cell was a six-way, black anodized aluminum cross of 6-in. o.d. The electrodes were two parallel uncoated stainless-steel plates of 5 cm in diameter and 2.5 cm apart. The electron swarm was produced by irradiation of the cathode with a KrF (Lumonics 861S) laser beam at a wavelength of 248 nm (5.0 eV). The laser pulse duration was about 10 ns with a beam size reduced to 3 mm in diameter by a diaphragm.

A negative high voltage was applied to the cathode to maintain an electric field between the electrodes. The conduction current induced by the electron motion between the electrodes was measured by a transient voltage pulse across a resistor (1000 Ω) connecting the anode to ground. Each transient waveform was monitored by a 150-MHz digital storage oscilloscope (Tektronix 2430). The averaged waveform was stored in a microcomputer, and subsequently analyzed. All measurements were performed at room temperature.

Diluted mixtures of HBr (2%–10%) and C_2H_5Br (<3.5%) in N_2 or Ar were premixed before being introduced into the gas cell. The gas mixture in the gas cell was slowly pumped. The purities of N_2 and Ar (MG Scientific) were better than 99.999% and 99.998%; and the purities of CH_3Br and HBr (Matheson) were 99.5% and 99.8%, respectively. These gases were used as delivered. The C_2H_5Br liquid (Alfa Products, better than 98% purity) was kept in a Teflon bottle inside a stainless-steel container, which was continuously pumped for 1 h at the dry ice temperature before it was premixed with N_2 or Ar.

III. RESULTS AND DISCUSSION

A. CH_3Br

The waveforms of transient voltage pulses observed in the CH_3Br-N_2 mixture at $E/N = 7.8$ Td (1 Td = 10^{-17} V cm^2) are shown in Fig. 1, where the partial pressures of CH_3Br were (a) 0 and (b) 2.1 Torr in a total pressure of 255 Torr. Each waveform is the average of about 90 transient pulses. The voltage shown in Fig. 1(a) decreases slightly after the first peak which is probably caused by the loss of

 0021-8979/88/104905-06$02.40

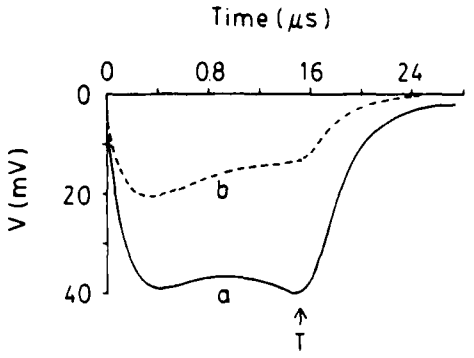

FIG. 1. The waveforms of transient voltage pulses produced from electron motion in 255 Torr of N_2 with CH_3Br (a) 0 and (b) 2.1 Torr. Electrons were produced from irradiation of the cathode by KrF laser photons. The E/N was fixed at 7.8 Td, the electrode spacing was 2.5 cm, and the external resistor was 1000 Ω.

electrons due to back diffusion to the cathode.[10] After the peak, the voltage remains fairly constant until the electrons arrive at the anode. The voltage shows a slight increase before it drops. This increase is likely due to the increase of electron drift velocity caused by the anode, similar to the effect that electron energy distribution is distorted in the vicinity of anode.[11] This increase serves as an indication that electrons arrive at the absorbing electrode.

The value of R used in this experiments was chosen to be as large as possible in order to improve the signal-to-noise ratio. However, the peak of the waveform due to back diffusion is broadened when R is large, as can be seen from Fig. 1, which could be taken as an indication that the rest of the waveform was also modified. We have performed measurements of the attachment rates for several values of R and selected the largest value for which no changes of the attachment rate were observed under conditions of the largest difference in shape between the waveforms with and without the attaching gas.

The electron drift time T is measured from the laser pulse to where $V(t)$ starts to drop as shown in Fig. 1. The T value included the uncertainty caused by electron diffusion as well as the electrical noise of the laser discharge. The electron drift velocity is determined by d/T, where d is the separation between electrodes. The electron drift velocities for the gas mixtures of CH_3Br-N_2 and CH_3Br-Ar were measured as a function of E/N at different CH_3Br partial pressures as shown in Figs. 2 and 3, respectively. The uncertainty for the measured electron drift velocity is estimated to be about ± 10% of the given value. For pure N_2, our data agree with Lowke's values[12] within the experimental uncertainty. For pure Ar, our data agree with the values of Levine and Uman,[13] and Nielsen[14] within the experimental uncertainty, but they are about 15% lower than that of Herreng.[15]

When CH_3Br was added to the gas cell, the electron drift velocity increases as shown in Figs. 2 and 3. The increase of electron drift velocity in N_2 is not significant, but the increase in Ar is dramatic. The electron drift velocity increases with the partial pressure of CH_3Br. The measurements for the CH_3Br-Ar mixture were stopped at the E/N where the ionization started to occur. At high partial pressure of CH_3Br in Ar, the electron drift velocity shows a peak

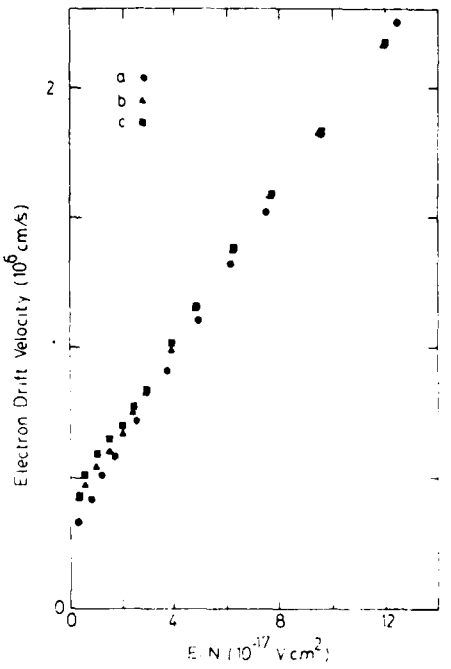

FIG. 2. The electron drift velocities in the CH_3Br-N_2 mixtures as a function of E/N. The ratios of $[CH_3Br]/[N_2]$ are (a) 0%, (b) 0.35%, and (c) 0.52%.

at low E/N in Fig. 3(d), which is similar to that of CH_4.[9,16] The negative differential conductivity (decreasing electron drift velocity with increasing electric field strength) has been observed in many gases. Petrović, Crompton, and Haddad[17] have recently explained this phenomena by the combination effect of elastic and inelastic cross sections and the threshold energy of the inelastic process.[18]

When CH_3Br was added, the pulse amplitude decreased as shown in Fig. 1(b). This decrease is caused by the electron attachment to the electronegative gas, which can be used to determine the electron attachment rate.[9] The transient vol-

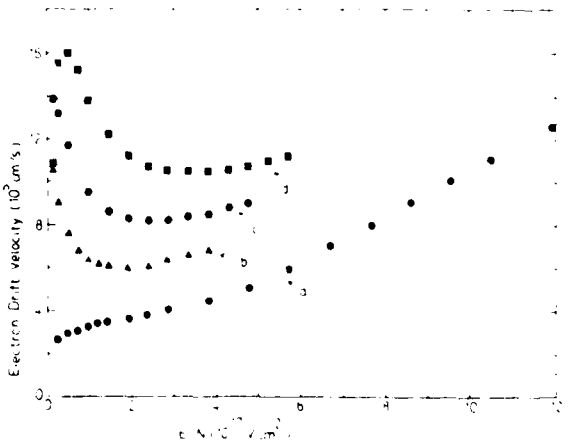

FIG. 3. The electron drift velocities in the CH_3Br-Ar mixture as a function of E/N. The ratios of $[CH_3Br]/[Ar]$ are (a) 0%, (b) 0.16%, (c) 0.41%, and (d) 0.81%.

tage induced by electron motion as shown in Fig. 1(a) can be represented by [9,10]

$$V(t) = f(t)\,\mathrm{Re}\; WN_e/d\,, \tag{1}$$

where N_e is the number of electrons between the electrodes, W is the electron drift velocity, d is the electrode spacing, R is the resistor connecting the anode to ground, $f(t)$ is the response function of the detection system, and t is the electron drift time. When CH_3Br is added, the transient voltage becomes

$$V'(t) = f(t)\,\mathrm{Re}\; W'N_e' \exp(-\nu_a t)/d\,, \tag{2}$$

where ν_a is the electron attachment rate (frequency) of the mixture containing CH_3Br. The electron attachment rate at a fixed CH_3Br concentration can be obtained from the slope of $\ln[V'(t)/V(t)]$ vs t,

$$\ln[V'(t)/V(t)] = \ln(N_e'W'/N_eW) - \nu_a t\,, \tag{3}$$

where the $\ln(V'/V)$ value is either negative or positive, depending on the constant of

$$\ln(N_e'W'/N_eW) \sim \ln(W'/W)\,.$$

For the case that electron drift velocity is not significantly affected by the gas added (see Fig. 1), the plot of $\ln[V'(t)/V(t)]$ vs t is a straight line as shown in Fig. 4(a). For the case of CH_3Br-Ar (and CH_3Br-N_2 at low E/N), the electron drift velocity becomes much faster when CH_3Br is added (see Figs. 2 and 3), and the plot of $\ln[V'(t)/V(t)]$ vs t deviates from the straight line when t is close to T', the electron drift time for the gas mixture. This deviation is the result of the fact that under those circumstances comparison in Eq. (3) is made between the points of the waveforms that correspond to different positions of the swarms between the electrodes, and consequently the deviation from the straight line is the result of comparison between the points corresponding to the second peak on one waveform with a point that is not on the peak. This effect can be corrected by comparing V' and V at a same position, namely, comparing $V'(t)$ with $V(tT/T')$. With this correction, the plot of $\ln[V'(t)/V(tT/T')]$ is linear with t even at $t = T'$ as shown in Fig. 4(b).

The measured electron attachment rate increases approximately linearly with an increased partial pressure of CH_3Br, but it is independent on the buffer gas pressure. This result indicates that the electron attachment is a two-body dissociative process so that the attachment rate constant can be determined by the ratio of $\nu_a/[CH_3Br]$. Departures from linearity were both positive and negative, and they were caused by the influence of a small amount of molecular gas on the electron energy distribution in buffer gases. (CH_3Br is a polar molecule and therefore its cross sections are significantly larger than the corresponding cross sections for nitrogen.) To check this effect, the $\nu_a/[CH_3Br]$ values were measured as a function of $[CH_3Br]/[Ar]$ and $[CH_3Br]/[N_2]$ as shown in Fig. 5. For CH_3Br-Ar [Fig. 5(a)], $\nu_a/[CH_3Br]$ increases largely with increasing $[CH_3Br]/[Ar]$, indicating that the electron energy distribution is significantly affected by the addition of CH_3Br. This concurs with the observation that the electron drift velocity in Ar changes dramatically when CH_3Br is added as shown in Fig. 3. For CH_3Br-N_2 [Figs. 5(b)–5(f)], $\nu_a/[CH_3Br]$ decreases with increasing $[CH_3Br]/[N_2]$ at a mean electron energy lower than 0.4 eV, but it increases at higher mean electron energy. The mean electron energies were adopted from the calculation of Hunter and Christophorou.[19] The change of $\nu_a/[CH_3Br]$ could be used as an indicator for the shift of electron energy distribution (to be discussed later).

The electron attachment rate constants k_a determined from the extrapolated values of $\nu_a/[CH_3Br]$ at $[CH_3Br] \to 0$ in N_2 are shown in Fig. 6(a) for E/N from 0.5 to 10 Td. The k_a values are replotted in Fig. 6(b) as a function of mean electron energy. For the CH_3Br-Ar mixture, the $\nu_a/[CH_3Br]$ value at $[CH_3Br]/[Ar] \to 0$ is very small; thus, the k_a value cannot be determined with certainty at high E/N. The attachment rate constant obtained for the

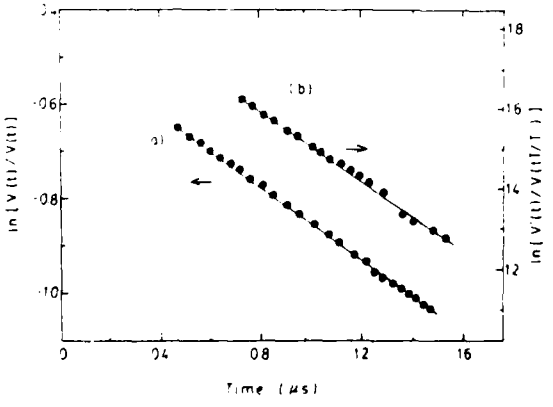

FIG. 4. The ratios of the transient voltages measured with and without CH_3Br in buffer gas as a function of the elapsed time after laser pulse. (a) The ratio of the two waveforms in Fig. 1 where the electron drift times for both pulses are almost the same; (b) the ratio of $V'(t)$ (with 1 Torr of CH_3Br in Ar) to $V(tT/T')$ (pure Ar), with $E/N = 0.342$ Td and $T/T' \sim 3.9$, where T and T' are the electron drift times without and with CH_3Br added to Ar.

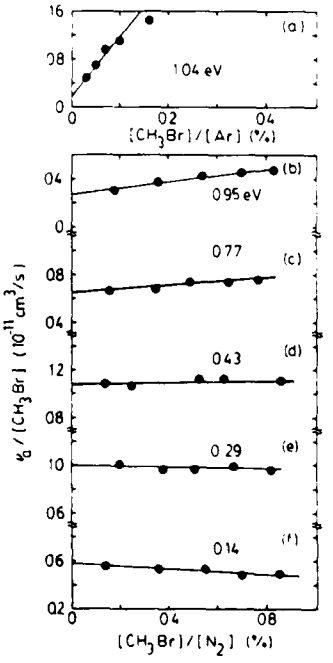

FIG. 5. The $\nu_a/[CH_3Br]$ values as a function of $[CH_3Br]/[Ar]$ (a) and $[CH_3Br]/[N_2]$ (b)–(f) at various mean electron energies.

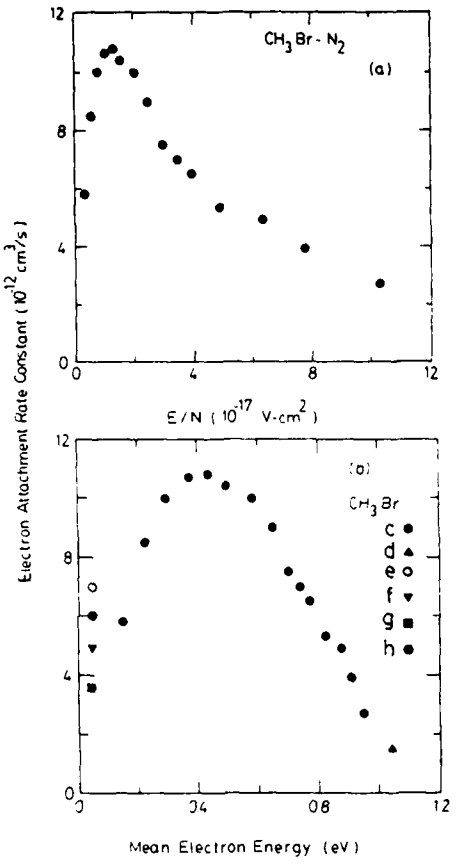

FIG. 6.(a) Electron attachment rate constant as a function of E/N for CH_3Br in N_2. The total pressure of N_2 was ~255 Torr. (b) Electron attachment rate constant as a function of mean electron energy for CH_3Br in N_2 (c) and in Ar (d). (e) The thermal energy data given by Bansal and Fessenden (Ref. 2) and Petrović and Crompton (Ref. 20), (f) Wentworth and co-workers (Ref. 3), (g) Mothes and co-workers (Ref. 4), and (h) Alge and co-workers (Ref. 5) are also shown for comparison.

CH_3Br-Ar mixture at $E/N = 0.179$ Td ($\langle\epsilon\rangle \sim 1.04$ eV) is shown in Fig. 6(b), which matches well with the data of N_2. This match has been observed in many gases.[9]

The electron attachment rate constants of CH_3Br at thermal energy measured by various investigators[2-5,20] are also shown in Fig. 6(b) for comparison. The recent result of Petrović and Crompton[20] agrees with the value of Bansal and Fessenden.[2] Our result is consistent with these thermal energy data within experimental uncertainties. The current result that k_a has a maximum value around 0.4 eV is consistent with the electron attachment cross section of CH_3Br which shows a maximum at 0.35 eV.[21] In contrast, our result is quite different from the data of Christodoulides and Christophorou[1] in which the electron attachment rate constants increase with decreasing mean electron energy with a value as high as 7×10^{-9} cm^3/s at thermal energy. Their values[1] are larger than the current data by three orders of magnitude.

The electron attachment is likely due to the two-body dissociative process,

$$CH_3Br + e \rightarrow CH_3 + Br^- . \quad (4)$$

The thermochemical threshold for this process is -0.30 eV as calculated from the electron affinity of Br (3.36 eV)[22] and the heats of formation of -0.39, 1.51, and 1.16 eV for CH_3Br,[23] CH_3,[24] and Br,[24] respectively. The small electron attachment rate constant at thermal energy indicates that this process has a high potential barrier. Wentworth and co-workers[3] determined the potential barrier from the difference between the repulsive potential curve for process (4) and the zero-point energy of CH_3Br to be 0.25 eV. Petrović and Crompton[20] determined the activation energy from the Arrhenius plot of k_a vs $1/T$ to be 0.260 eV, which agrees with the result of Alge and co-workers[5] of 0.30 eV. The current data that the electron attachment rate constant has a maximum at 0.4 eV are consistent with these early results. The uncertainty for the heat of formation of CH_3Br is quite high, for example, the value is listed as -0.20 eV.[25] This uncertainty may make the calculated threshold energy appear low.

As shown in Fig. 5(a), $\nu_a/[CH_3Br]$ increases with increasing $[CH_3Br]/[Ar]$. This result indicates that the mean electron energy shifts to a low value as the partial pressure of CH_3Br increases, because at 0.9 eV the k_a value increases with decreasing mean electron energy [see Fig. 6(b)]. The results for the CH_3Br-N_2 mixture also suggest that the mean electron energy shifts to a low value when CH_3Br is added. This is because $\nu_a/[CH_3Br]$ increases with increasing $[CH_3Br]/[N_2]$ when the mean electron energy is higher than 0.4 eV [see Figs. 5(b) and 5(c)], and vice versa when the mean electron energy is lower than 0.4 eV [see Figs. 5(e) and 5(f)]. At the mean electron energy of 0.43 eV, the attachment rate constant has a broad peak such that it is not sensitive to the addition of CH_3Br as shown in Fig. 5(d). $\nu_a/[CH_3Br]$ in N_2 does not change as much as that of Ar, indicating that the mean electron energy is not significantly affected by the added CH_3Br. This is consistent with the small change of electron drift velocity when CH_3Br is added to N_2.

B. HBr

Since the attachment rate constant of HBr is much larger than that of the other two gases studied, a smaller amount of HBr was used and consequently the effect on the drift velocity was insignificant. The electron attachment rate constants of HBr in N_2 and Ar buffer gases were measured as a function of E/N. The electron attachment rate increases with the HBr partial pressure, but it is independent on the buffer gas pressure; thus, the attachment is a two-body dissociative process. Similar to the case of CH_3Br, $\nu_a/[HBr]$ varies with [HBr], but the effects are much smaller as can be predicted from the fact that the drift velocity is not seriously affected. The attachment rate constant of HBr was determined by extrapolation of $\nu_a/[HBr]$ at $[HBr]\rightarrow0$, for which the electron energy distribution is associated with pure N_2 (or Ar). The measured k_a values are shown in Fig. 7(a) as a function of E/N and in Fig. 7(b) as a function of mean electron energy. The electron attachment rate constant has a maximum of 1.06×10^{-9} cm^3/s at 0.55 eV.

The current results agree reasonably well with the data of Trainor and Boness[7] and Mothes, Schultes, and Schindler[4], which are also shown in Fig. 7(b) for comparison. However, the current results are significantly lower

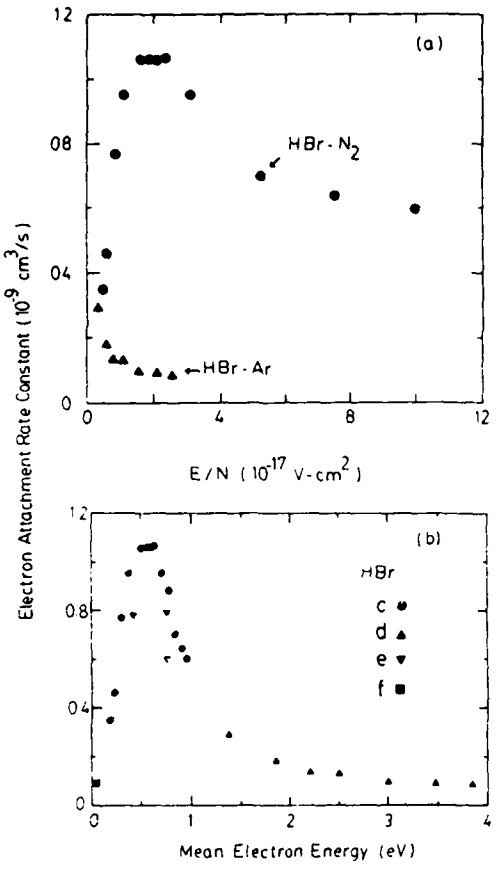

FIG. 7. (a) Electron attachment rate constant as a function of E/N for HBr in N_2 and Ar, where the total pressure was ~250 Torr. (b) Electron attachment rate constant as a function of mean electron energy for HBr in (c) N_2 and (d) in Ar. (e) The data reported by Trainor and Boness (Ref. 7) and (f) Mothes and co-workers (Ref. 4) are plotted for comparison.

than the data of Christophorou and co-workers[6]; for example, a value of 1.0×10^{-8} cm^3/s was reported at 0.2 eV, which is about two orders of magnitude higher than the current value. The electron attachment cross section of HBr measured with electron beam technique by Ziesel, Nenner, and Schulz[26] and Abouaf and Teillet-Billy[27] shows a maximum at 0.4 eV. Our result concurs with these data.

The electron attachment is caused by the two-body dissociative process,

$$HBr + e \rightarrow H + Br^- . \quad (5)$$

The thermochemical threshold for this process is 0.39 eV, which is the difference between the electron affinity of Br (Ref. 22) and the dissociation energy of HBr (3.75 eV).[25] Other dissociative processes may not contribute significantly to the observed attachment, because they require much higher electron energy. For example, the thermochemical threshold for the dissociative electron attachment process,

$$HBr + e \rightarrow H^- + Br \quad (6)$$

is 2.98 eV, where the electron affintiy of H used in the calculation is 0.77 eV.[22]

Because the electron attachment process of HBr requires substantial electron energy, the attachment rate constant at thermal energy is expected to be small. The value of 9.6×10^{-11} cm^3/s given by Mothes and co-workers[4] is on line with this expectation. On the other hand, the result of Christophorou and co-workers[6] is not consistent with this expectation.

C. C_2H_5Br

For C_2H_5Br, the electron drift velocity in N_2 (or Ar) did not change significantly when a small amount of C_2H_5Br was added. The electron attachment rate constants of C_2H_5Br in N_2 and Ar buffer gases were measured at various E/N. The electron attachment is a two-body dissociative process. In contrast to the cases of CH_3Br and HBr, $\nu_a/[C_2H_5Br]$ does not vary significantly with $[C_2H_5Br]$. The k_a values determined by $\nu_a/[C_2H_5Br]$ at $[C_2H_5Br]\rightarrow0$ are plotted in Fig. 8(a) as a function of E/N and in Fig. 8(b) as a function of mean electron energy. The data measured by Christodoulides and Christophorou[1] at a total gas pressure of 400 Torr and the data at thermal energy measured by Bansal and Fessenden[2] are also shown in Fig. 8(b) for comparison. The current results are consistent with these earlier measurements.[1,2]

The electron attachment is likely due to the two-body dissociative process,

$$C_2H_5Br + e \rightarrow C_2H_5 + Br^- . \quad (7)$$

The thermochemical threshold is -0.41 eV as calculated from the heats of formation[24] of -0.64 and 1.15 eV for C_2H_5Br and C_2H_5. Similar to the case of CH_3Br, this process may also have a high potential barrier such that the electron attachment rate constant at thermal energy is small. The potential barrier could be estimated from the current data to be smaller than 0.8 eV.

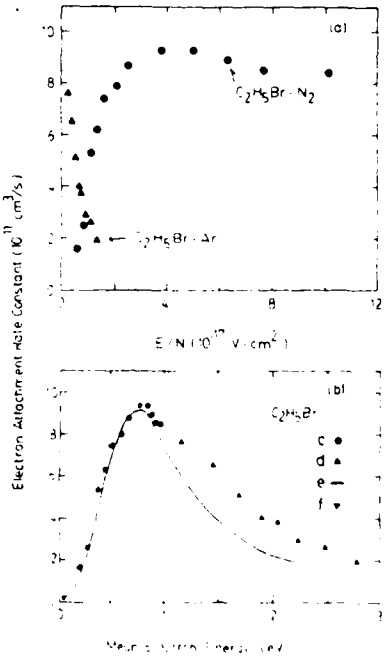

FIG. 8. (a) Electron attachment rate constant as a function of E/N for C_2H_5Br in N_2 and Ar, where the total pressure was ~250 Torr. (b) Electron attachment rate constant as a function of mean electron energy for C_2H_5Br in (c) N_2 and in (d) Ar. The data from (e) Ref. 1, and from (f) Ref. 2 are plotted for comparison.

IV. CONCLUSION

The electron attachment rate constants of HBr, CH_3Br, and C_2H_5Br in N_2 and Ar were measured at various E/N (or mean electron energy). The method for measuring the electron attachment rate constant of a gas mixture that has an electron drift velocity significantly different from that of the buffer gas is described. All studied molecules show small attachment rate constants at thermal energy, maximum values at energy less than 1 eV, and small values at higher energy. The electron attachment is a two-body dissociative process that leads to the production of Br^-. The current results are reasonably consistent with the published data, except for the data of CH_3Br reported in Ref. 1 and that of HBr reported in Ref. 6. The electron drift velocities of the gas mixtures were also investigated, and the results for the CH_3Br-N_2 and Ar mixtures are reported in this paper.

ACKNOWLEDGMENTS

The authors wish to thank Z. Lj. Petrović for useful comments. This work is supported by the Air Force Office of Scientific Research under Grant No. AFOSR-86-0205.

[1] A. A. Christodoulides and L. G. Christophorou, J. Chem. Phys. **54**, 4691 (1971); L. G. Christophorou, D. L. McCorkle, and A. A. Christodoulides, in *Electron-Molecule Interactions and Their Applications*, Vol. I, edited by L. G. Christophorou (Academic, Orlando, FL, 1984), p. 541.
[2] K. M. Bansal and R. W. Fessenden, Chem. Phys. Lett. **15**, 21 (1972).
[3] W. E. Wentworth, R. George, and H. Keith, J. Chem. Phys. **51**, 1791 (1969).
[4] K. G. Mothes, E. Schultes, and R. N. Schindler, J. Phys. Chem. **76**, 3758 (1972).
[5] E. Alge, N. G. Adams, and D. Smith, J. Phys. B **17**, 3827 (1984).
[6] L. G. Christophorou, R. N. Compton, and H. W. Dickson, J. Chem. Phys. **48**, 1949 (1968).
[7] D. W. Trainor and M. J. W. Boness, Appl. Phys. Lett. **32**, 604 (1978).
[8] W. C. Wang and L. C. Lee, *IEEE Trans. Plasma Sci.* **PS-15**, 460 (1987).
[9] L. C. Lee and F. Li, J. Appl. Phys. **56**, 3169 (1984); W. C. Wang and L. C. Lee, **57**, 4360 (1985); **58**, 184 (1985); J. Chem. Phys. **84**, 2675 (1986); **85**, 6470 (1986).
[10] L. G. H. Huxley and R. W. Crompton, *The Diffusion and Drift of Electrons in Gases* (Wiley, New York, 1974), pp. 298–303.
[11] G. L. Braglia and J. J. Lowke, J. Phys. D **12**, 1831 (1979).
[12] J. J. Lowke, Aust. J. Phys. **16**, 115 (1963).
[13] N. E. Levine and M. A. Uman, J. Appl. Phys. **35**, 2618 (1964).
[14] R. A. Nielsen, Phys. Rev. **50**, 950 (1936).
[15] P. Herreng, Compt. Rend. **217**, 75 (1943).
[16] G. S. Hurst, J. A. Stockdale, and L. B. O'Kelly, J. Chem. Phys. **38**, 2572 (1963).
[17] Z. Lj. Petrović, R. W. Crompton, and G. N. Haddad, Aust. J. Phys. **37**, 23 (1984).
[18] A. G. Robertson, Aust. J. Phys. **30**, 39 (1977).
[19] S. R. Hunter and L. G. Christophorou, J. Chem. Phys. **80**, 6150 (1984).
[20] Z. Lj. Petrović and R. W. Crompton, J. Phys. B **20**, 5557 (1987).
[21] J. A. Stockdale, F. J. Davis, R. N. Compton, and C. E. Klots, J. Chem. Phys. **60**, 4279 (1974).
[22] A. A. Christodoulides, D. L. McCorkle, and L. G. Christophorou, in *Electron-Molecule Interactions and Their Applications*, Vol. II, edited by L. G. Christophorou (Academic, Orlando, FL, 1984), p. 481.
[23] S. W. Benson, *Thermochemical Kinetics* (Wiley, New York, 1976).
[24] M. W. Chase, Jr., C. A. Davies, J. R. Downey, Jr., D. J. Frurip, R. A. McDonald, and A. N. Syverud, J. Phys. Chem. Ref. Data **14**, Suppl. No. 1, 1 (1985).
[25] H. Okabe, *Photochemistry of Small Molecules* (Wiley, New York, 1978).
[26] J. P. Ziesel, J. Nenner, and G. J. Schulz, J. Chem. Phys. **63**, 1943 (1975).
[27] R. Abouaf and D. Teillet-Billy, Chem. Phys. Lett. **73**, 106 (1980).

Attachment of low-energy electrons to HCl

Z. Lj. Petrović,[a] W. C. Wang, and L. C. Lee
Department of Electrical and Computer Engineering, San Diego State University, San Diego, California 92182-0190

(Received 4 February 1988; accepted for publication 26 April 1988)

The electron-attachment rate constants of HCl diluted in Ar and N_2 were measured as a function of the reduced electric field E/N. These data were converted to the electron-attachment cross section of HCl using the electron-energy distribution functions of pure Ar and N_2. The dependence of the electron-attachment rate constant and the mean electron energy on the fraction of HCl in each buffer gas was investigated. A comparison of the current result with both available experimental data and theoretical calculations is made.

I. INTRODUCTION

Dissociative attachment of chlorine-containing molecules in gas discharges is frequently used for many applications. This is especially true for excimer (XeCl) lasers,[1,2] plasma etching,[3,4] and possibly optically controlled diffuse discharge switches.[5,6] Electron-attachment data are needed for these applications.

In this paper we present our experimental data for the electron-attachment coefficients of HCl in dilute HCl-Ar and HCl-N_2 mixtures. These data are then converted to the absolute values of the low-energy-electron-attachment cross section. Electron-attachment data of chlorine-containing molecules[7,8] are not well measured and the available data are in serious disagreement.

HCl was experimentally studied several times by both swarm and beam methods. Earlier publications of the HCl data, which include the work of Buchel'nikova[9] and Christophorou, Compton, and Dickson,[10] were reviewed by Christophorou,[11] who measured the electron-attachment rate constants of hydrogen halides and their deuterated compounds using N_2 as the buffer gas. However, their measurements covered only relatively low values of E/N. Towards the zero value of E/N they observed an unusual increase of attachment. No satisfactory explanation for this effect has been given.[8]

Recently, attachment coefficients for nonthermal electrons were measured by Kligler, Rozenberg, and Rokni[12] and Sze, Greene, and Brau[13] in HCl-Ar, HCl-N_2, and HCl-Ar-H_2 mixtures as well as in pure HCl by Davies.[14] Thermal attachment rate constants were also measured.[15,16] These data are consistent with the results measured by swarm and beam techniques but are 3 orders of magnitude lower than the results inferred from the associative detachment data.[15,17,18]

Dissociative attachment cross sections were measured by beam techniques producing both relative[19–21] and absolute[10,21] values. The general shapes of the electron excitation spectra are in good agreement, but there is significant scatter of the absolute values. Theoretical calculations of the cross sections agree with the swarm and beam data in shapes, but the absolute values[22,23] are different by a factor of up to 3.

The large data scatter of both attachment rate coefficients and cross sections can only be resolved by new measurements with alternative techniques. The previous data measured by swarm methods at varied E/N are not consistent with the shape of the cross sections obtained by beam methods. The results presented in this paper are consistent with the beam data, which can be used for their absolute calibration. Determination of the cross section from our data is based on the electron-energy distribution functions calculated for pure buffer gases N_2 and Ar. We have also analyzed the influence of small amounts of HCl on attachment rate coefficients and mean electron energies in buffer gases in order to justify the experimental procedure.

II. EXPERIMENT

A. Experimental setup

The experimental setup has been described in previous papers.[24–27] Two parallel, flat, stainless-steel electrodes (5 cm in diameter) were placed 2.5 cm apart inside the vacuum chamber, which was a six-way black anodized aluminum cross 15 cm in diameter (see Fig. 1). Initial electrons were produced by irradiating the uncoated cathode surface with a KrF excimer laser beam (Lumonics 861S) at 248 nm (5 eV). The diameter of the beam was reduced by an aperture to 3 mm in order to make sure that the electron swarm does not extend outside the region of homogeneous field. Duration of the laser pulse is about 10 ns, which is significantly shorter than the transit time of electrons. The laser was operated at 5 Hz.

This experiment belongs to the class of pulsed Townsend experiments.[28,29] The cathode is connected to a high negative voltage (known to $\pm 1\%$), while the anode is connected to the ground through a resistor (R). One option[30] is to select R to be rather high, which means that RC is greater than the electron transit time and thus the voltage on the resistor $V(t)$ is proportional to the integral of the current. The other option, which was adopted in the present experiment, was to select R to be low ($R = 1000\ \Omega$) so that RC is lower than the transit time and $V(t)$ is proportional to the displacement current between the electrodes. Transient voltage waveforms were monitored by a 150-MHz digital storage oscilloscope (Tektronix 2430). An averaged waveform of at least 100 pulses was transferred to a microcomputer for subsequent analysis.

[a] Permanent address: Institute of Physics, University of Belgrade, P. O. Box 57, 11001 Belgrade, Yugoslavia.

 0021-8979/88/161625-07$02.40

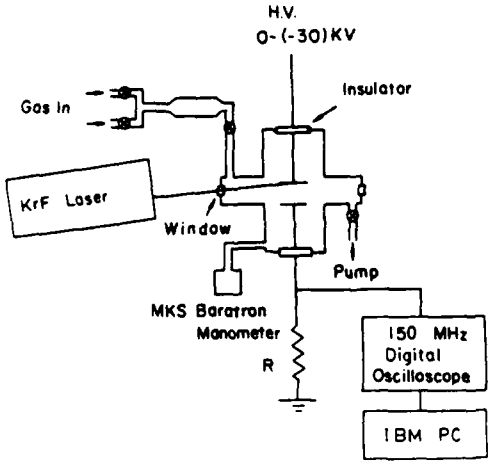

FIG. 1. Schematic diagram for experimental apparatus.

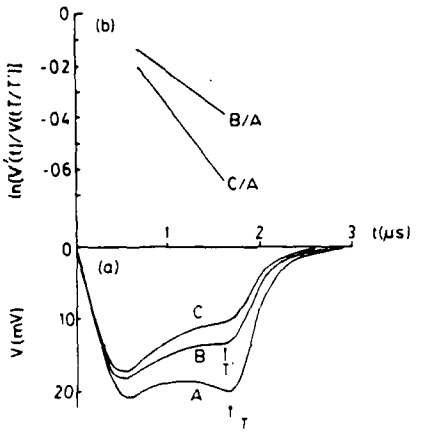

FIG. 2. (a) Waveforms of transient voltage pulses produced by electron motion in N_2 and in HCl-N_2 mixtures. Curve A, 0 mtorr; Curve B, 30 mtorr. Curve C, 50 mtorr of HCl in 245 torr of N_2, $E/N = 8.55$ Td; (b) $\ln[V'(t)/V(tT/T')]$ between the waveforms in (a).

In order to avoid a buildup of impurities, loss of polar molecules due to adsorption, and buildup of excited species and dissociation products, the gas mixtures were operated in a flow system. Buffer gases N_2 and Ar (MG Scientific) of purities greater than 99.999% and 99.998%, respectively, were used as delivered. HCl was premixed (20%) with He (MG Scientific). The attaching gas was diluted further with the buffer gas by using calibrated gas-flow meters. The uncertainty of the mixture composition was expected to be less than 3%. The gas pressure was determined by a calibrated capacitance manometer (MKS Baratron), and the uncertainty of the gas number density was believed not to exceed $\pm 0.5\%$. All measurements were performed at room temperature (298 ± 2 K).

B. Experimental procedure

The largest experimental difficulty in performing the pulsed Townsend experiment with low values of R (i.e., $RC \ll d/W$, where d is the distance between electrodes and W is the drift velocity) is to reduce the noise. Therefore, precaution was taken to reduce any possible noise, especially the noise generated by the discharge of the excimer laser.

Typical voltage waveforms are shown in Fig. 2(a). After the maximum is reached, the voltage drops due to back-diffusion.[29,31] Then, the voltage is approximately constant [if there is no attachment or ionization as shown in curve A of Fig. 2(a)], and as electrons reach the anode, it starts to drop again. The small increase and the following rapid decrease serve as an indication of the arrival of electrons to the anode, i.e., the end of the drift period (T), which can be used to determine the drift velocity $W = d/T$.

Our method for measuring attachment rate coefficients is to compare the voltage waveforms obtained under identical conditions in the pure buffer gas and in the buffer gas mixed with a small amount of attaching gas.[24-27,32] The transient voltage induced by electron motion is given by[29]

$$V(t) = f(t) Re W N_e(t)/d , \tag{1}$$

where $f(t)$ is the response function of the detection system, d is the spacing between electrodes, and $N_e(t)$ is the number of electrons between electrodes. $N_e(t)$ is given by[29]

$$N_e(t) = (N_0/\sqrt{\pi} W t)\left[\int_0^d \left(\frac{z}{(4D_L t)^{1/2}}\right) \exp\left(\frac{-(z-Wt)^2}{4D_L t}\right) dz + \int_0^d \left(\frac{z-2d}{(4D_L t)^{1/2}}\right) \exp\left(\frac{dW}{D_L} - \frac{(z-2d-Wt)^2}{4D_L t}\right) dz\right] \exp(-\nu_a t) , \tag{2}$$

where the electric field is along the z axis, D_L is the longitudinal diffusion coefficient, ν_a is the attachment collision frequency, and N_0 is the number of electrons produced by laser irradiation on the cathode surface.

The ratio of the voltage waveforms for the conditions with (denoted by a prime) and without attachment is

$$V'(t)/V(t) = [N_e'(0) W'/N_e(0) W] \exp(-\nu_a t) \tag{3}$$

or

$$\ln[V'(t)/V(t)] = \ln[N_e'(0) W'/N_e(0) W] - \nu_a t . \tag{4}$$

The attachment rate coefficient can be determined from the slope of $\ln[V'(t)/V(t)]$ versus time as shown in Fig. 2(b), where lines B/A and C/A are determined from the ratios of curves B and C to curve A of Fig. 2(a), respectively.

Under some circumstances, however, the addition of an attaching gas may affect the energy balance and/or momentum balance of electrons. Such situations are not desirable, because it then becomes difficult to assign a known value of average electron energy (also the attachment rate coefficient and electron-energy distribution function) to the E/N value used in the measurements. Data obtained in argon are sensitive to the addition of small amounts of impurities. Most of all, drift velocities[33] can be subject to dramatic changes. In pure argon, the electron-energy balance is determined by elastic collisions that are not very efficient in dissipating energy, so the mean energy is relatively high. Therefore, even a very small amount of molecular gas impurities can reduce the average electron energy. Since the momentum-transfer cross section above the Ramsauer–Townsend minimum changes extremely rapidly,[34] the corresponding effects on W will be significant.[35,36] Therefore, changes of W, when the attaching gas is introduced, indicate that the electron-energy distribution function (EEDF) is not identical to the EEDF of the pure buffer gas. However, even under those circumstances it might still be possible to perform a meaningful extrapolation of the attachment data to the zero abundance of the attaching gas. Under those circumstances, comparison of the voltage waveforms should be performed at times that correspond to the same position of the traveling swarm between the electrodes, that is, the attachment rate coefficient is determined from

$$-\nu_a t = \ln[V'(t)/V(tT/T')] - \ln[N_c'(0)W'/N_c(0)W]\,. \quad (5)$$

Such treatment gives a linear plot even in the region of nonequilibrium i.e., at $t \cong T'$ [see Fig. 2(b)].

III. EXPERIMENTAL RESULTS

Voltage waveforms were first measured in a pure buffer gas at a given pressure and E/N. Drift velocities obtained from these measurements were compared to some available experimental data,[32,37–39] and good agreement[40] (to within the error bounds of the present technique for measuring W to be about 10%) was taken as an indication of sufficient purity of the gas and adequate calibration of the system.

When the attaching gas was added to the buffer gas, voltage waveforms changed as shown in Fig. 2(a), curves B and C. Comparison of the waveforms gave the attachment rate constant k_a, for that particular mixture (normalized by the partial pressure of the attacher). In order to check whether there is any influence of the attaching gas on the EEDF, measurements were performed at several partial pressures, for which some examples are shown in Fig. 3. Keeping the experimental uncertainty and the statistical scatter of the data in mind, the linear extrapolation to the zero partial pressure was found to be adequate in all cases. Further discussion of this procedure will be given in Sec. IV D. The uncertainty introduced by extrapolation is believed to be within $\pm$ 5% of the given value.

The electron-attachment rate constants obtained by this procedure were found to be independent of the buffer-gas pressure and laser power, indicating that the data do not depend on electron-conduction currents. Data for HCl in N_2 and in Ar are, respectively, shown in Figs. 4 and 5, together

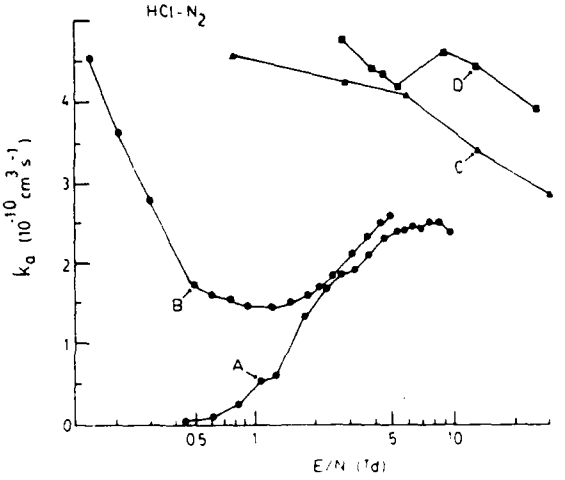

FIG. 4. Electron-attachment rate constants of HCl in N_2 as a function of E/N. Curve A, present results; Curve B, Christophorou, Compton, and Dickson (Ref. 10); Curve C, Kligler, Rozenberg, and Rokni (Ref. 12); Curve D, Sze, Greene, and Brau (Ref. 13).

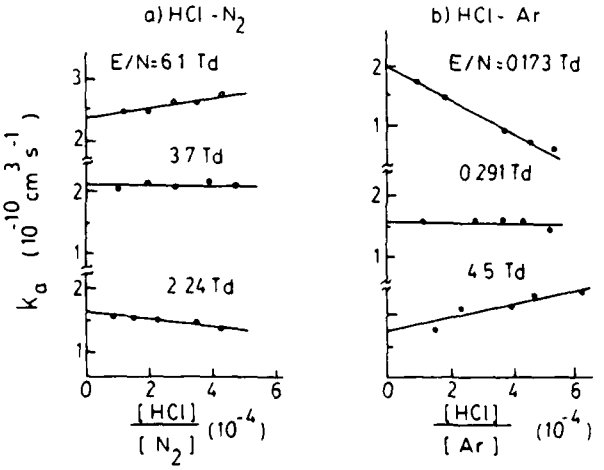

FIG. 3. Electron-attachment rate constants as a function of partial pressure of HCl in (a) N_2 and (b) Ar at varied E/N.

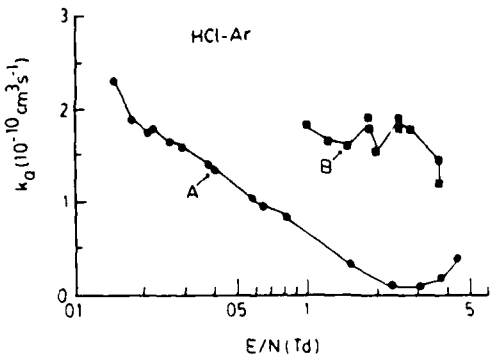

FIG. 5. Electron-attachment rate constants of HCl in Ar as a function of E/N. Curve A, present results; Curve B, Sze, Greene, and Brau (Ref. 13).

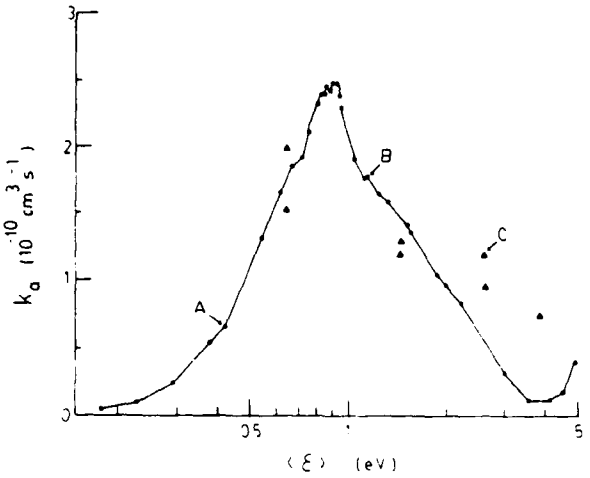

FIG. 6. Electron-attachment rate constants of HCl as a function of the mean energy of the electron swarm with Curve A N_2 and Curve B Ar as the buffer gas. Experimental data of Kligler, Rozenberg, and Rokni (Ref. 12) for Ar-H_2 mixture are shown as triangles (C).

with some other available data.[10,12] The upper limit of the E/N values was determined by the onset of ionization in the buffer gas. Figure 6 shows the data obtained in N_2 and Ar as a function of the mean electron energy. The mean electron energies were calculated as explained in Sec. IV B and were found to be in good agreement with the results of Hunter and Christophorou.[32]

The overall uncertainty of the attachment rate constant is estimated to be within $\pm$ 10% of the given value. It is difficult to account for each possible individual source of error, and instead a sum of errors is estimated. The main causes of data uncertainty are the extrapolation procedure in conjunction of with scatter of data, a possible weak nonlinear dependence of k_a on the partial pressure of HCl (see Sec. IV D), and the determination of the partial pressure.

IV. DISCUSSION

A. Comparison of experimental data

Dissociative attachment to HCl proceeds through two possible channels:

$$HCl + e \rightarrow H + Cl \quad (6)$$

$$\rightarrow H^- + Cl. \quad (7)$$

The first process peaks between 0.8 and 0.9 eV and the absolute cross sections[9,10,21-23] were found to be (3.9–30) $\times$ 10^{-18} cm^2. The ion appearance potential was found to be 0.64 eV.[11] The vibrationally excited states of HCl have significantly lower thresholds, and the corresponding cross sections are more than 1 (for $v = 1$) and 2 (for $v = 2$) orders of magnitude larger than the cross section for the ground state.[22,41] Production of H^- ions begins at higher energies with peaks at 7.1 and 9.05 eV (Ref. 21) with a maximum cross section of the order of 2×10^{-18} cm^2. This process is outside the energy range of our measurements, and only at the highest values of E/N in Ar there is some indication of H^- production.

Our experimental data are compared with other available data in Figs. 4–6. In N_2 (Fig. 4), the agreement with the results of Christophorou, Compton, and Dickson[10] is good above $E/N = 2$ townsends (Td), but we do not observe an increase of k_a at low values of E/N. Attachment rate constants of Kligler, Rozenberg, and Rokni[12] and Sze, Greene, and Brau[13] are significantly larger than the current data. Their data are significantly larger than the predictions of cross sections obtained by beam methods. Apparatuses used by Kligler, Rozenberg, and Rokni and by Sze, Greene, and Brau are quite similar and so is the analysis. Also, both groups have failed to observe the energy (E/N) dependence of k_a that would be consistent with the shape of the available cross sections. It is hard to explain the discrepancy, but it is possible that some other electron-loss processes were present in their apparatus, such as losses due to electron drift. In addition, these authors[13] observed significant dissociation (50%) of HCl in their mixtures of several ppm of HCl in the buffer gas. Surprisingly, the results for attachment rates in Ar-H_2 mixture obtained by Kligler, Rozenberg, and Rokni[12] agree in magnitude with our data.

It is not possible to make a meaningful comparison with the available data for thermal attachment rates such as those obtained by Miller and Gould,[45] who have performed measurements in the temperature range 1730–2475 K. While the mean energies covered by them overlap with the mean energies covered in the present analysis, one could expect a large population of vibrationally excited molecules, and also the Maxwellian distribution function would be quite different from the electron energy distribution function at the corresponding E/N in N_2.

B. Calculation of electron-energy distribution functions

Electron-energy distribution functions (EEDFs) were calculated from the Boltzmann equation using a standard two-term procedure that takes into account superelastic collisions.[42] Sets of electron-scattering cross sections for N_2 (Ref. 43) and Ar (Refs. 34 and 44) were compiled. Inelastic processes were also included for Ar, even though in conditions of the present measurements their contribution was negligible.[45] Calculations of transport coefficients for pure buffer gases were in good agreement with the available experimental data.[29,42] Several attachment cross sections of Hunter and Christophorou[32] were also used to check the performance of the computer code and adequacy of the selected cross sections.

Our measurements in N_2 extended only up to 10 Td. Multiterm corrections to mean electron energy (ϵ) and other transport coefficients are very small at these values of E/N. Pitchford and Phelps,[43,46] however, found that rate coefficients calculated by the two-term theory could be very much in error even when other coefficients were determined accurately.[46] This is the result of the fact that when the two-term theory starts breaking down, the high-energy tail of the EEDF will be affected the most. Therefore, the calculation of rate coefficients for processes with inelastic thresholds significantly higher than $\langle\epsilon\rangle$ is the least accurate. This was not the case in our calculations for most high E/N data, since the inelastic energy losses and sometimes even energy corresponding to the maximum of the cross section were normally

lower than $\langle\epsilon\rangle$. Thus, k_a was determined by the bulk of EEDF and therefore subject to inaccuracy due to application of the two-term theory, which is comparable to the inaccuracy in $\langle\epsilon\rangle$. At low E/N, the $\langle\epsilon\rangle$ values were significantly (up to 4 times) smaller than the inelastic threshold. However, at these energies the two-term theory performs very well even for the high-energy tail. Also, the cross sections were determined from a wide range of data, so we can conclude that our results are not affected by the breakdown of the two-term theory.

It is generally believed that the two-term theory is applicable for pure atomic gases well below the onset of inelastic processes.[47] Although the calculation of the transverse diffusion coefficient was recently questioned,[48] such effects would not affect[49] our calculations. Finally, it should be noted that in order to make a comparison with the data of Kligler, Rozenberg, and Rokni[12] (see Fig. 6), mean electron energies in the 5% H_2-Ar mixture were calculated using the best available set of cross sections for low-energy electrons in H_2 (Ref. 50).

C. Electron-attachment cross section

Recently, analyses of electron transport in pure HCl and gas mixtures of HCl have been performed by Davies[14] and by Penetrante and Bardsley.[51] Davies used a two-term solution to the Boltzmann equation, while Penetrante and Bardsley applied the Monte Carlo procedure. In both cases, the ranges of transport coefficients (k_a and W for pure HCl and k_a for HCl-N_2 mixtures as measured by Sze, Greene, and Brau[13] and Kligler, Rozenberg, and Rokni[12]) were, however, insufficient to determine the entire set of electron scattering cross sections uniquely. Nevertheless, the mixture data provide a sufficient basis to determine uniquely the absolute values of the electron-attachment cross section. On the other hand, it was found by Penetrante and Bardsley[51] that attachment rates in pure HCl are very sensitive to the vibrational excitation cross section. These authors had to significantly increase the vibrational excitation cross sections of Davies in order to fit both the attachment rates in pure and gas mixtures of HCl. Alterations of the attachment cross section had little effect on the corresponding rates in pure HCl due to a "hole-burning" effect at the local minimum of the EEDF. The determination of the cross section for attachment on the basis of the mixture data does not suffer from this problem since the energy and the momentum balance are determined mainly by the buffer gas (while HCl controls the number density). This makes the mixture technique suitable for the determination of the attachment cross section.

In the present analysis we have attempted to determine only the attachment cross section from our experimental data. As expected, the calculated attachment rate constants using the cross section of Penetrante and Bardsley[51] are much larger than our results (see Fig. 7). Scaling their cross section by 0.6 gives results in excellent agreement with the data in pure Ar and in N_2 below 4 Td. However, the disagreement with the data in N_2 above 4 Td exceeded the experimental uncertainty. Scaling by 0.67 improved the agreement at higher E/N in N_2, but the agreement below 4 Td in Ar was not as good. Nevertheless, it can be concluded that

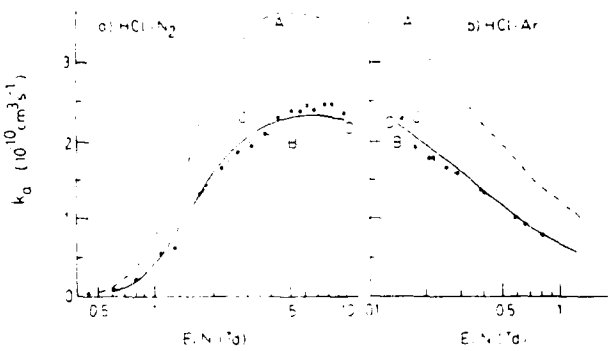

FIG. 7. Comparison between the experimental data and the calculated values using cross sections of Curve A, Penetrante and Bardsley (PB, Ref. 51), Curve B, PB scaled by 0.6; Curve C, PB scaled by 0.67; Curve D, smoothed present result that fits with the cross section shown in Fig. 8. The present experimental data of HCl in N_2 [circles in (a)] and HCl in Ar [circles in (b)] are shown for comparison.

the cross section of Penetrante and Bardsley[51] if reduced by a factor of 0.6–0.7 is consistent with our experimental data. Numerous attempts were made to produce a cross section that would fit the experimental data even better. Both direct modifications of the initial cross section and the "automatic" unfolding procedure of Christophorou, McCorkle, and Anderson[22] were applied. The best fit (see Fig. 7) was obtained by the cross section shown in Fig. 8, where the cross section peaks between 0.88 and 0.9 eV.

The *maximum* attachment cross section is 0.126×10^{-16} cm^2, which is in good agreement with the theoretical calculations of Bardsley and Wadehra[22] (0.12) and the beam data of Azria *et al.*[24] (0.089). However, our value is significantly lower than the results of Orient and Srivastava[21] (0.26) and Christophorou, Compton, and

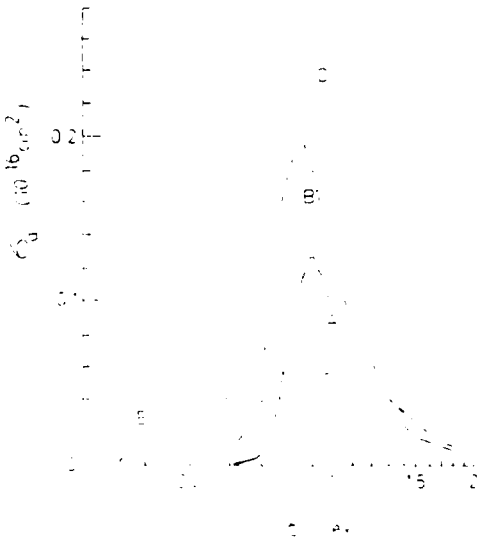

FIG. 8. Low-energy electron attachment cross sections of HCl. Curve A, present result obtained from unfolding of the measured electron-attachment rate constants; Curve B, Penetrante and Bardsley (Ref. 51); Curve C, Bardsley and Wadehra (Ref. 22); Curve D, Orient and Srivastava (Ref. 21); Curve E, Buchel'nikova (Ref. 9).

Dickson[10] (0.20), but it is higher than the results of Buchel'nikova[9] (0.04). Structures (steps) predicted by theory[22,23] could not be clearly resolved by swarm measurements. At low mean electron energies (measured in N_2), the experimental data are systematically higher than calculated values. The discrepancy was resolved by adding a "foot" of 0.01×10^{-16} cm^2 to the cross section starting at 0.45 eV. Nevertheless, even in the case that the attachment at the low E/N is totally attributed to the excited molecules, the influence on the attachment rate at the higher E/N should be negligible.

D. Influence of HCl on EEDF in buffer gases

Measurements of attachment rate constants were performed for several abundances of HCl in order to be able to extrapolate to zero HCl pressure (see Fig. 3) and consequently use the EEDF of pure buffer gases in the analysis. Especially, results in argon are affected by the addition of small quantities of molecular impurities. Helium, which was used to premix HCl (ratio 80% He–20% HCl), could not affect the EEDF in pure Ar at the abundances used (10^{-4}). As shown in Fig. 3, addition of HCl can lead to a decrease of k_a if $\langle\epsilon\rangle$ is below the energy corresponding to the peak cross section and an increase of k_a if $\langle\epsilon\rangle$ is larger than the peak value. If $\langle\epsilon\rangle$ is near the value corresponding to the peak cross section, k_a could be relatively independent of [HCl]. Theoretical calculations were performed to compare with experimental observations.

In argon, HCl has a large effect on the EEDF in a wide range of E/N. Theoretical calculations of the attachment rate constants and the mean electron energies as a function of E/N at varied [HCl]/[Ar] are shown in Figs. 9(a) and 9(b), respectively. The cross sections for HCl of Penetrante and Bardsley[51] were used, but the calculated EEDF was convoluted with the cross section obtained here to calculate k_a. Below 0.2 Td, the k_a values decrease monotonically with the addition of HCl, and above 0.4 Td, they increase monotonically. Relatively small changes of k_a can be expected between 0.2 and 0.4 Td, showing a maximum for a certain abundance of HCl corresponding to $\langle\epsilon\rangle$ being approximately equal to the energy for the peak cross section. Some examples of the calculated k_a values at fixed E/N and varied [HCl]/[Ar] are shown in Fig. 10(a). Calculations predict change of the sign of the slope at $E/N = 0.29$ Td. This calculated result is in excellent agreement with experimental observation as shown in Fig. 3. This calculation supports that the linear extrapolation method is valid even in the case of low E/N where k_a is very sensitive to the addition of HCl. Linear extrapolation will not lead to errors larger than the claimed experimental error bounds. At a fixed E/N, the mean electron energy will decrease monotonically with increasing [HCl]/[Ar] as shown in Fig. 10(b).

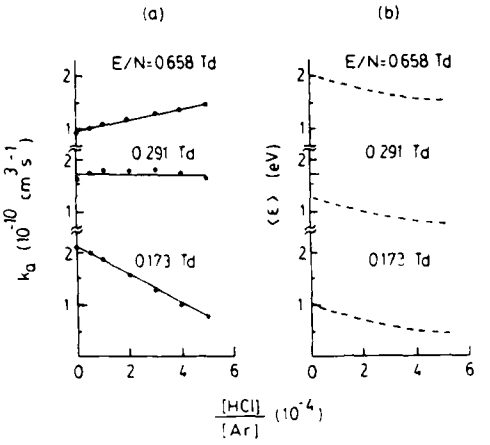

FIG. 10. Calculated influence of the addition of HCl to Ar on (a) the attachment rate constants and (b) the mean energy of electrons as a function of the fraction of [HCl]/[Ar] at varied E/N.

The influence of HCl in N_2 is smaller than that in Ar, though it is observable at lower values of E/N for abundances of the order of 10^{-4} as has been already shown by Penetrante and Bardsley.[51] This is so because even though N_2 is a molecular gas and has a large vibrational excitation cross section, HCl (as a moderately polar molecule) has much large cross sections both for momentum transfer and rotational and vibrational excitation, which could be especially important for energies below the onset of resonant vibrational excitation of N_2.[43] Nevertheless, the influence is small enough to justify linear extrapolation.

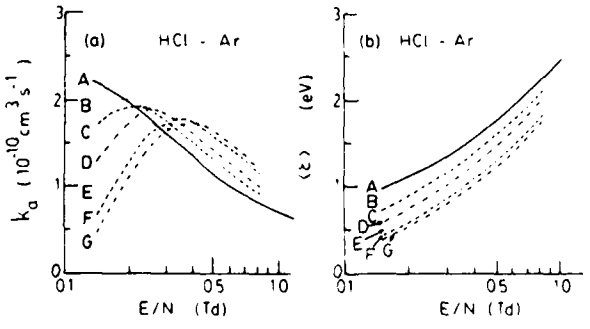

FIG. 9. Calculated influence of the addition of HCl to Ar. (a) electron-attachment rate constants and (b) mean electron energy as a function of E/N. Curve A, [HCl]/[Ar] = 0; Curve B, 0.5×10^{-4}; Curve C, 1×10^{-4}; Curve D, 2×10^{-4}; Curve E, 3×10^{-4}; Curve F, 4×10^{-4}; Curve G, 5×10^{-4}.

V. CONCLUSION

Experimental data for the electron dissociative attachment rate constant of HCl are presented in this paper. Measurements were perfomed with dilute mixtures of varied [HCl] in Ar and N_2. The attachment rate constants obtained by linear extrapolation of the measured values to the zero HCl abundance were converted to electron-attachment cross sections using the electron-energy distribution functions in pure Ar and N_2. The peak value of the cross section is 0.126×10^{-16} cm^2 at the mean electron energy around 0.9 eV. The absolute value is in agreement with one set of beam data[53] and some theoretical predictions[22] but in disagreement with other sets of data. No evidence of significant attachment at low values of E/N was found.

Further work is required before a full set of electron-scattering cross sections can be obtained. These should in-

clude measurements of ionization rates and drift velocities in mixtures with Ar. Such data should provide additional constraints on the cross sections. Nevertheless, the present attachment rate coefficients give absolute values of attachment cross sections independent of the measurements in pure HCl. The data derived in this work can be used directly in studies of electron and ion kinetics of discharges containing small amounts of HCl.

ACKNOWLEDGMENT

This work is supported by the Air Force Office of Scientific Research under Grant No. AFOSR-86-0205.

[1]W. L. Nighan and R. T. Brown, Appl. Phys. Lett. **36**, 498 (1980).
[2]L. F. Champagne, Appl. Phys. Lett. **33**, 523 (1978).
[3]J. S. Logan, N. M. Mazza, and P. D. Davidse, J. Vac. Sci. Technol. **6**, 120 (1968).
[4]A. D. Richards, B. E. Thompson, K. D. Allen, and H. H. Sawin, J. Appl. Phys. **62**, 792 (1987); G. L. Rogoff, J. M. Kramer, and R. B. Piejak, IEEE Trans. Plasma Sci. **PS-14**, 103 (1986).
[5]L. G. Christophorou, S. R. Hunter, J. G. Carter, and R. A. Mathis, Appl. Phys. Lett. **41**, 147 (1982); G. Schaefer and K. H. Schoenbach, IEEE Trans. Plasma Sci. **PS-14**, 561 (1986).
[6]G. Schaefer, P. F. Williams, K. H. Schoenbach, and J. T. Moseley, IEEE Trans. Plasma Sci. **PS-11**, 263 (1983); W. C. Wang and L. C. Lee, *ibid.* **PS-15**, 460 (1987).
[7]J. W. Gallagher, E. C. Beaty, J. Dutton, and L. C. Pitchford, Joint Institute for Laboratory Astrophysics (JILA) Information Center Report No. 22 (1982).
[8]J. W. Gallagher, E. C. Beaty, J. Dutton, and L. C. Pitchford, J. Phys. Chem. Ref. Data **12**, 109 (1983).
[9]I. S. Buchel'nikova, Sov. Phys.—JETP **35**, 783 (1959).
[10]L. G. Christophorou, R. N. Compton, and H. W. Dickson, J. Chem. Phys. **48**, 1949 (1968).
[11]L. G. Christophorou, *Atomic and Molecular Radiation Physics* (Wiley-Interscience, London, 1971).
[12]D. Kligler, Z. Rozenberg, and M. Rokni, Appl. Phys. Lett. **39**, 319 (1981).
[13]R. C. Sze, A. E. Greene, and C. A. Brau, J. Appl. Phys. **53**, 1312 (1982).
[14]D. K. Davies, Bull. Am. Phys. Soc. **26**, 726 (1981); **27**, 110 (1982); and see Ref. 7.
[15]W. J. Miller and R. K. Gould, J. Chem. Phys. **68**, 3542 (1978).
[16]A. A. Christodoulides, R. Schumacher, and R. N. Schindler, J. Phys. Chem. **79**, 1904 (1975).
[17]C. J. Howard, F. C. Fehsenfeld, and M. McFarland, J. Chem. Phys. **60**, 5086 (1974).
[18]N. A. Burdett and A. N. Hayhurst, Nature **245**, 77 (1973).
[19]J. P. Ziesel, I. Nenner, and G. J. Schulz, J. Chem. Phys. **63**, 1943 (1975).
[20]R. Azria, Y. Le Coat, D. Simon, and M. Tronc, J. Phys. B **13**, 1909 (1980).
[21]O. J. Orient and S. K. Srivastava, Phys. Rev. A **32**, 2678 (1985).
[22]J. N. Bardsley and J. M.Wadehra, J. Chem. Phys. **78**, 7227 (1983).
[23]W. Domcke and C. Mundel, J. Phys. B **18**, 4491 (1985).
[24]L. C. Lee and F. Li, J. Appl. Phys. **56**, 3169 (1984).
[25]W. C. Wang and L. C. Lee, J. Appl. Phys. **57**, 4360 (1985).
[26]W. C. Wang and L. C. Lee, J. Chem. Phys. **84**, 2675 (1986).
[27]W. C. Wang and L. C. Lee, J. Chem. Phys. **85**, 6470 (1986).
[28]H. Raether, *Electron Avalanches and Breakdown in Gases* (Butterworths, Washington, 1964).
[29]L. G. H. Huxley and R. W. Crompton, *The Diffusion and Drift of Electrons in Gases* (Wiley Interscience, New York, 1974).
[30]S. R. Hunter and L. G. Christophorou, in *Electron-Molecule Interactions and Their Applications*, edited by L. G. Christophorou (Academic, Orlando, 1984), Vol. 2.
[31]J. H. Whealton, D. S. Burch, and A. V. Phelps, Phys. Rev. A **15**, 1685 (1977).
[32]S. R. Hunter and L. C. Christophorou, J. Chem. Phys. **80**, 6150 (1984).
[33]A. G. Robertson, Aust. J. Phys. **30**, 39 (1977).
[34]G. N. Haddad and T. F. O'Malley, Aust. J. Phys. **35**, 35 (1982).
[35]W. H. Long, Jr., W. F. Bailey, and A. Garscadden, Phys. Rev. A **13**, 471 (1976).
[36]Z. Lj. Petrović, R. W. Crompton, and G. N. Haddad, Aust. J. Phys. **37**, 23 (1984).
[37]J. J. Lowke, Aust. J. Phys. **16**, 115 (1963).
[38]N. E. Levine and M. A. Uman, J. Appl. Phys. **35**, 2618 (1964).
[39]R. A. Nielson, Phys. Rev. **50**, 950 (1936).
[40]W. C. Wang and L. C. Lee, J. Appl. Phys. **63**, 4905 (1988).
[41]M. Allan and S. F. Wong, J. Chem. Phys. **74**, 1687 (1981).
[42]D. K. Gibson, Aust. J. Phys. **23**, 683 (1970).
[43]G. N. Haddad, Aust. J. Phys. **37**, 487 (1984); L. C. Pitchford and A. V. Phelps, Phys. Rev. A **25**, 540 (1982).
[44]H. B. Milloy, R. W. Crompton, J. A. Rees, and A. G. Robertson, Aust. J. Phys. **30**, 61 (1977); A. V. Phelps (personal communication).
[45]H. B. Milloy, J. Phys. B **8**, L414 (1975).
[46]A. V. Phelps and L. C. Pitchford, Phys. Rev. A **31**, 2932 (1985).
[47]H. B. Milloy and R. O. Watts, Aust. J. Phys. **30**, 73 (1977); S. L. Lin, R. E. Robson, and E. A. Mason, J. Chem. Phys. **71**, 3483 (1979).
[48]N. Ikuta, H. Itoh, and K. Toyota, Jpn. J. Appl. Phys. **22**, 117 (1983); T. Makabe and T. Mori, J. Phys. D **17**, 699 (1984).
[49]G. L. Braglia and M. Diligenti, Contrib. Plasma Phys. **26**, 453 (1986).
[50]M. A. Morrison, R. W. Crompton, B. C. Saha, and Z. Lj. Petrović, Aust. J. Phys. **40**, 239 (1987).
[51]B. M. Penetrante and J. N. Bardsley, J. Appl. Phys. **54**, 6150 (1983).
[52]L. G. Christophorou, D. L. McCorkle, and V. E. Anderson, J. Phys. B **4**, 1163 (1971).
[53]R. Azria, L. Roussier, R. Paineau, and M. Tronc, Rev. Phys. Appl. (Paris) **9**, 469 (1974).

Electron attachment rate constants of $SOCl_2$ in Ar, N_2, and CH_4

W. C. Wang and L. C. Lee[a)]
Department of Electrical and Computer Engineering, San Diego State University, San Diego, California 92182

(Received 10 April 1986; accepted 26 August 1986)

The electron attachment rate constants of $SOCl_2$ in the buffer gases of Ar, N_2, and CH_4 (150 to 500 Torr) at various E/N (1–15 Td) were measured by a parallel-plate drift-tube electron-swarm technique. Electrons were produced by irradiating the cathode with KrF laser photons. For the $SOCl_2$–Ar mixture, the electron attachment rate constant has a maximum value of 6.2×10^{-10} cm^3/s at $E/N = 4$ Td. For $SOCl_2$ in N_2, the electron attachment rate constant is 1.25×10^{-9} cm^3/s at $E/N = 1.3$ Td, and decreases with increasing E/N. For $SOCl_2$ in CH_4, the electron attachment rate constant is 4.8×10^{-9} cm^3/s at $E/N = 1$ Td, and decreases with increasing E/N. For every gas mixture studied, the electron attachment rate constant is independent of buffer gas pressure, indicating that the electron attachment to $SOCl_2$ is due to a dissociative process. The electron attachment processes in the studied gas mixtures are discussed.

I. INTRODUCTION

Recently, we have observed that the conduction current in a glow discharge of $SOCl_2$–N_2 mixture can be reduced when the gas medium is irradiated by ArF laser photons. The current reduction may be caused by enhancement of the electron attachment rate due to the Cl and SO radicals, which are produced from photodissociation of $SOCl_2$ by ArF laser photons. This result indicates that $SOCl_2$ may be useful for the development of laser-controlled opening switches. The electron attachment rates for $SOCl_2$ in various buffer gases provide the basic information needed for such application, and motivate us to perform this investigation.

A parallel-plate drift-tube electron-swarm technique has been used in our laboratory to measure the electron attachment rate constants of several molecules.[1–4] The electron attachment rate constants of $SOCl_2$ in Ar, N_2, and CH_4 at varied E/N are reported in this paper. These data are not yet available in the literature. The electron attachment processes of $SOCl_2$ in various buffer gases are discussed based on the experimental data measured.

II. EXPERIMENT

The experimental setup has been described in previous papers.[1–4] In brief, the gas cell was 6 in. six-way aluminum cross. The electrodes were two parallel uncoated stainless steel plates 5 cm in diameter and 3 cm apart. The electron swarm was produced by irradiation of the cathode with a KrF (Lumonics model 861S) laser beam of wavelength 248 nm (5.0 eV). The laser pulse duration was about 10 ns. These photons are energetically capable of dissociating $SOCl_2$.[5,6] The size of the laser beam was reduced to 0.3 cm radius such that only a small fraction of $SOCl_2$ near the cathode was irradiated by laser photons. This small beam size confines the laser-produced photofragments (such as SO, Cl, and Cl_2) to a small region around the cathode. The electron motion near the cathode was excluded from the data analysis, so the measured electron attachment rate is due to $SOCl_2$ only.

A negative high voltage was applied to the cathode to maintain an electric field between the electrodes. The conduction current induced by the electron motion between the electrodes was measured as a transient voltage pulse across a resistor (33–2000 Ω) connecting the anode to ground. Each transient pulse was monitored by a 150 MHz digital storage oscilloscope (Tektronix 2430) and was subsequently stored in an IBM-XT microcomputer. The data were analyzed by the computer.

Pressure in the gas cell was kept constant (monitored by an MKS-Baratron manometer), while a slow flow of gas, ~20 cm^3/min, was maintained. All measurements were performed at room temperature, 23 °C. All gases were supplied by MG Scientific and were used as received; purities of the Ar, N_2, and CH_4 were better than 99.998%, 99.998%, and 99.99%, respectively. Thionyl chloride (99% purity) was supplied by Fisher Scientific.

The thionyl chloride liquid was stored in a glass bottle inside a stainless steel container. The thionyl chloride vapor was carried into the gas cell by a buffer gas, Ar, N_2, or CH_4. The concentration of $SOCl_2$ was determined from the ratio of $SOCl_2$ vapor pressure (110 Torr at 23 °C) to the carrier gas pressure (2 atm). Measurements were also made by premixed $SOCl_2$ in various buffer gasses. These mixtures had well-defined concentrations of $SOCl_2$. Results obtained from different methods of mixing gases do not show a difference. The major dissolved impurity in $SOCl_2$ has been reported to be SO_2[7]; however, the attachment rate constant for SO_2 is much smaller than that for $SOCl_2$,[4] so the effect of possible SO_2 impurity on these measurements should be negligible.

III. RESULTS

A. $SOCl_2$–Ar mixture

The electron transient waveforms for the $SOCl_2$–Ar mixture at $E/N = 0.26$ Td (1 Td = 10^{-17} V cm^2) are shown

[a)] Also, Department of Chemistry, San Diego State University.

 0021-9606/86/236470-05$02.10

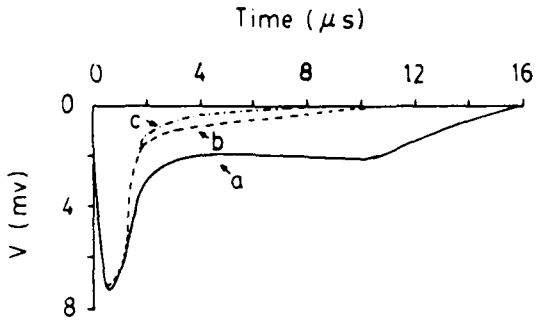

FIG. 1. The waveforms of transient voltage pulses produced from electron motion in 390 Torr of Ar with $SOCl_2$ (a) 0, (b) 23 mTorr, and (c) 50 mTorr. Electrons were produced from irradiation of the cathode by KrF laser photons. The E/N was fixed at 0.26 Td. The electrode spacing was 3 cm, and the external resistor was 1 K Ω.

shown in Fig. 1, where the pressure of Ar was 390 Torr, and the pressures of $SOCl_2$ were (a) 0, (b) 23, and (c) 50 mTorr. Each waveform is the average of 64 pulses which were captured by the digital storage oscilloscope. As can be seen from Fig. 1(a) (with only Ar in the gas cell), voltage decreased rapidly after the first peak. This is probably due to the loss of electrons by back diffusion to the cathode.[8] After the peak, the voltage approached a nearly constant value until the electrons arrived at the anode, where the voltage dropped to zero. The voltage shows a slight increase before it drops. This may be caused by the effect of electron diffusion to absorbing anode; namely, the distribution of electron number density and the mean electron energy in the vicinity of the anode will be distorted by the presence of anode.[9] Since this increase of voltage (near the anode) occurs both in the gas systems with and without electron attacher, it should not affect our data analysis. In fact, when we take the ratio of transient voltages with (V) and without (V_0) $SOCl_2$ as a function of time, a linear dependence of $\ln(V/V_0)$ on time can extend to the region where the second bump occurs. Nevertheless, for most of our data analysis, only the flat portion of the transient voltage is considered.

When small amounts of $SOCl_2$ were added to the gas cell, both pulse duration and amplitude decreased as shown in Figs. 1(b) and 1(c). The shortening of pulse duration is due to the increase of electron drift velocity, and the decrease of amplitude is caused by the electron attachment to $SOCl_2$. This interpretation has been extensively discussed in previous papers.[1-4]

The electron attachment rate, ν_a, at a fixed $SOCl_2$ concentration is obtained from the slope of $\ln(V/V_0)$ vs time which has been previously described in detail.[1,2] Only the flat portion of the trace was used for the data analysis (the first peak and the tail were avoided). For example, ratios for the voltages in Fig. 1 were considered only from $t = 4$ to $8\,\mu$s. At this time interval, the conduction electrons are far away from the region irradiated by laser, so the possible interference by Cl and SO radicals (which may be produced by photodissociation of KrF laser photons) is avoided. Thus, the measured electron attachment rates are caused by $SOCl_2$ only.

The electron attachment rate was found to be directly

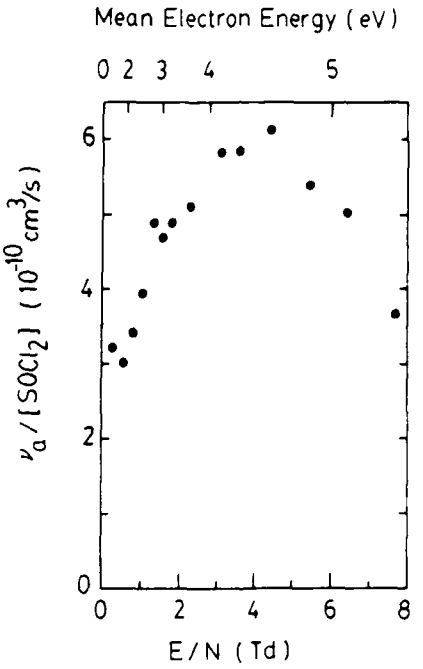

FIG. 2. Electron attachment rate constant as a function of E/N (bottom axis) and mean electron energy (top axis) for $SOCl_2$ in Ar. The Ar pressure was 390 Torr.

proportional to the partial pressure of $SOCl_2$ but independent of the total pressure. This shows that the electron attachment is a two-body dissociative process. The electron attachment rate constant, k_a, of the two-body process is determined by $\nu_a/[SOCl_2]$, when $[SOCl_2] \to 0$. It had been shown[2-4,10,11] that a small fraction of impurity added to Ar gas may affect the electron energy distribution function and hence the electron drift velocity. The increase of electron drift velocity caused by adding $SOCl_2$ to Ar was observed in this experiment. The measured k_a values also decrease with increasing $[SOCl_2]/[Ar]$ because of the effect of $SOCl_2$ on the electron energy distribution. Nevertheless, the $SOCl_2$ partial pressure we used was limited to a small value (0–50 mTorr), thus, the variation of k_a with $[SOCl_2]/[Ar]$ is within the experimental uncertainty estimated to be $\pm$ 20% of each given value.

The k_a values measured at various E/N at $[SOCl_2]/[Ar] \to 0$ are shown in Fig. 2 for an Ar pressure of 390 Torr. The scale of the mean electron energy, $\langle\epsilon\rangle$, is also shown on the top axis of Fig. 2. The mean electron energies used here were calculated by Christophorou and Hunter[11,12] who used a numerical method to calculate the electron energy distribution function $f(\epsilon, E/N)$ in Ar (and N_2). The electron attachment rate constant reaches a maximum value of 6.2×10^{-10} cm^3/s at $E/N = 4$ Td ($\langle\epsilon\rangle = 4.5$ eV). The electron attachment rate constants were also measured at different Ar pressures, and the results are similar to those shown in Fig. 2.

B. $SOCl_2$–N_2 mixture

The measured electron attachment rate is proportional to the partial pressure of $SOCl_2$ but does not depend on the N_2 pressures from 150–500 Torr. This shows that the elec-

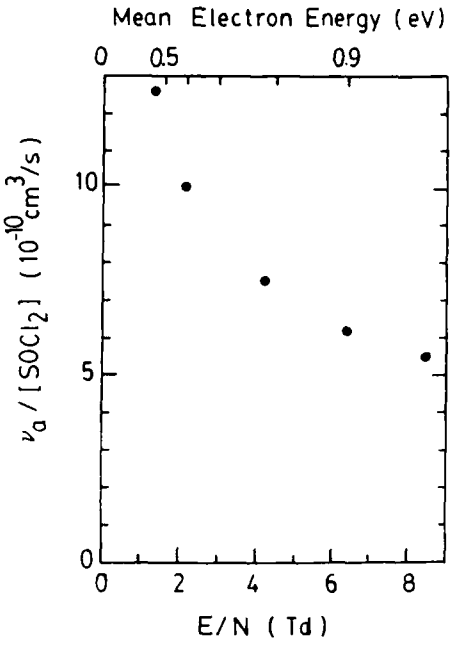

FIG. 3. Electron attachment rate constant as a function of E/N (bottom axis) and mean electron energy (top axis) for $SOCl_2$ in N_2. The N_2 pressure was 475 Torr.

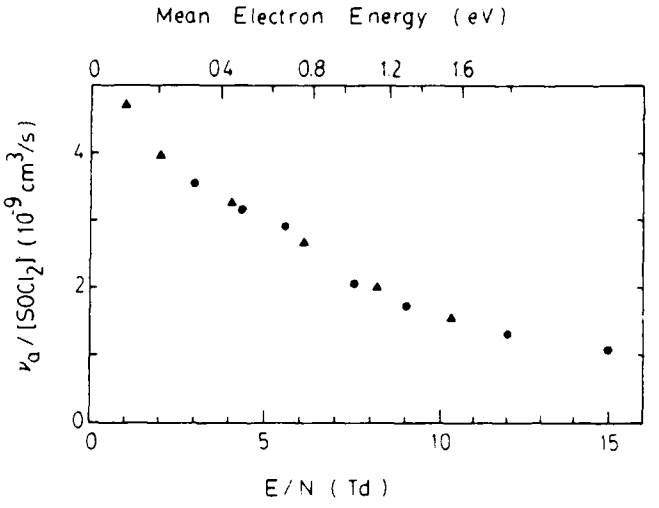

FIG. 4. Electron attachment rate constant as a function of E/N (bottom axis) and mean electron energy (top axis) for $SOCl_2$ in CH_4. The CH_4 pressures were 340 Torr (●) and 490 Torr (▲).

tron attachment is a two-body dissociative process. The measured k_a values for the $SOCl_2$–N_2 mixture are shown in Fig. 3, where the N_2 pressure is about 475 Torr and the E/N is in the range of 1–8 Td. The mean electron energy in N_2 is also shown on the top axis of Fig. 3. Again, the mean electron energies used here were given by Christophorou and Hunter[11,12] who used the calculated $f(\epsilon, E/N)$ in N_2 to obtain $\langle\epsilon\rangle$ at various E/N. The attachment rate constant is about 1.25×10^{-9} cm^3/s at $E/N = 1.3$ Td ($\langle\epsilon\rangle = 0.4$ eV), and decreases with increasing E/N.

C. $SOCl_2$–CH_4 mixture

Similar to the results obtained in the Ar and N_2 buffer gases, the electron attachment rate is proportional to the partial pressure of $SOCl_2$ but does not depend on the CH_4 buffer pressure (varied from 150–500 Torr), indicating that the electron attachment is a two-body dissociative process. The electron attachment rate constants for the $SOCl_2$–CH_4 mixture are shown in Fig. 4 for E/N from 1 to 15 Td and for two different pressures of CH_4. The mean electron energies in CH_4 are shown on the top axis of Fig. 4. (The mean electron energy in CH_4 for E/N higher than 12 Td is not available.) It should be noted that the mean electron energy in CH_4 is calculated from $\langle\epsilon\rangle = 3(eD_L/\mu)/2$ by the assumption that the electron energy distribution is a Maxwell function where D_L/μ is the ratio of lateral electron diffusion coefficient to electron mobility.[12] As shown in Fig. 4, the attachment rate constant is about 4.8×10^{-9} cm^3/s at $E/N = 1$ Td, and it then decreases with increasing E/N.

IV. DISCUSSION

Since the electron energy distributions in Ar and N_2 are similar,[11–13] it may be appropriate to characterize the electron attachment rate constants in both $SOCl_2$–Ar and $SOCl_2$–N_2 mixtures as a function of the $\langle\epsilon\rangle$ parameter. As shown in Fig. 5, the k_a values of $SOCl_2$ in N_2 buffer gas match with the k_a values of $SOCl_2$ in Ar buffer gas. A similar case was observed in C_3F_8[3,11] whose electron attachment rate constants, measured in N_2 and Ar buffer gases, are well matched. For the CH_4 buffer gas, however, the real mean electron energies at various E/N are not calculated yet. The electron energy distribution of the Maxwell function in the mean electron energy calculation is quite different from that of N_2 or Ar. So, it is not appropriate to compare the data derived from the $SOCl_2$–CH_4 mixture with that of the $SOCl_2$–N_2 or $SOCl_2$–Ar mixture. The data obtained from the $SOCl_2$–CH_4 mixture are thus not included in Fig. 5.

The electron attachment rate constant of $SOCl_2$ vs the

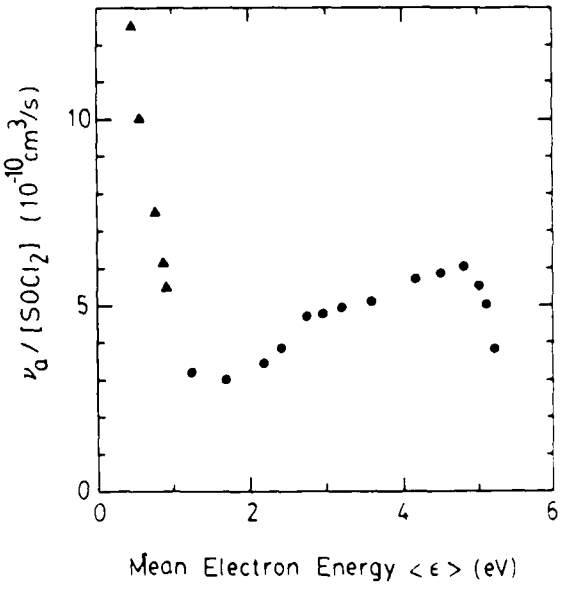

FIG. 5. Electron attachment rate constant as a function of mean electron energy for the $SOCl_2$–N_2 (▲) and $SOCl_2$–Ar (●) mixtures.

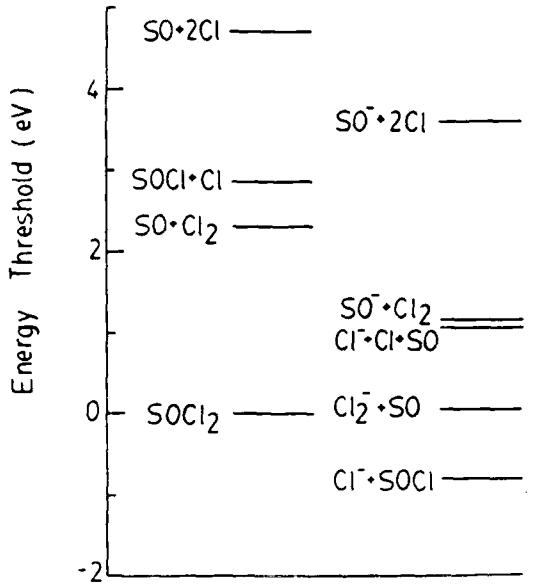

FIG. 6. Energy thresholds for the dissociation processes (left) and the electron dissociative attachment processes (right) of $SOCl_2$.

mean electron energy (shown in Fig. 5) has a peak at the thermal energy and a broad band with a maximum at 4.8 eV. This result indicates that the electron attachment is due to at least two different dissociative attachment processes. (Note that the attachment is attributed to a dissociative attachment process because the electron attachment rate constant is independent of the buffer gas pressure.) The attachment rate constant for the thermal energy electron is higher than the higher energy one. The electron attachment process is discussed below.

When $SOCl_2$ is excited by photons or electrons, it may be dissociated into the following products:

$$SOCl_2 \rightarrow Cl_2 + SO \quad (1)$$

$$\rightarrow Cl + SOCl \quad (2)$$

$$\rightarrow 2Cl + SO. \quad (3)$$

The thresholds for these processes can be determined from their dissociation energies. The dissociation energy for D(Cl–SOCl) was calculated by Sanderson[14] to be 2.86 eV. The dissociation energy for D(SO–2Cl) is 4.70 eV.[15] Using D(Cl–Cl) = 2.52 eV,[15] the dissociation energy for D(SO–Cl_2) is 2.18 eV.

The thermochemical energies for the electron dissociative attachment processes of $SOCl_2$ can be calculated from the dissociation energies as follows:

$$SOCl_2 + e \rightarrow SO^- + 2Cl - 3.6eV \quad (4)$$

$$\rightarrow SO^- + Cl_2 - 1.1 \quad (5)$$

$$\rightarrow Cl^- + Cl + SO - 1.0 \quad (6)$$

$$\rightarrow Cl_2^- + SO + 0.0 \quad (7)$$

$$\rightarrow Cl^- + SOCl + 0.8. \quad (8)$$

The electron affinities[12] of Cl, SO, and Cl_2 used in the calculation are 3.67, 1.1, and 2.2 eV, respectively. The calculated energy thresholds for all these possible dissociation processes and dissociative attachment processes of $SOCl_2$ are shown in Fig. 6.

The energy threshold of $SOCl + Cl^-$ is about 0.8 eV below the ground state energy of $SOCl_2$, indicating that the electron dissociative attachment could occur at thermal energy. This explains our observation that the electron attachment at low electron energy is a two-body dissociative process with a high attachment rate constant. The $Cl_2^- + SO$ process also requires no electron energy to occur, except for the possible potential barrier. Since process (8) has high exothermic energy and the electron energy in the buffer gas of CH_4 or N_2 is low, process (8) is probably the main electron attachment process occurring in the $SOCl_2$–CH_4 and $SOCl_2$–N_2 mixtures. A similar case was observed in the Cl_2–N_2 mixture by McCorkle *et al.*,[16] where the electron dissociative attachment rate constant has a maximum of about 0.07 eV and decreases with increasing mean electron energy.

The electron attachment rate constants of $SOCl_2$ increase when $\langle\epsilon\rangle > 1$ eV as shown in Fig. 5. This increase is probably caused by the dissociative attachment processes (4)–(6). Processes (7) and (8) are responsible for the attachment at the thermal energy and they will be less important at the high electron energy. This is evidenced by the fact that the thermal electron peak rapidly decreases with increasing electron energy. Because the energy thresholds for processes (5) and (6) are about 1 eV above the ground state of $SOCl_2$, these processes are likely responsible for the electron attachment at electron energy higher than 1 eV. For electron energy higher than 3.6 eV, process (4) will provide an additional attachment channel to enhance the attachment rate. For electron energy higher than 4.8 eV, the attachment rate constant starts to decrease; this may be caused by the electron energy moving away from the energy range where the attachment processes are available. The next high energy process is $Cl_2^- + S + O$ whose energy threshold is 5.3 eV, where D(S–O) = 5.34 eV[15] is used to determine the threshold. This high energy process may have a small electron attachment rate, because the attachment rate constant at the energy higher than 5.3 eV is small.

V. CONCLUSION

Electron attachment rate constants of $SOCl_2$ in Ar, N_2, and CH_4 were measured at various E/N (or mean electron energy). The electron attachment rate constant has a maximum at the thermal energy and a second maximum peak around 4.5 eV. The dissociative attachment processes of $Cl^- + SOCl$ and $Cl_2^- + SO$ are likely to be the dominant processes for low energy electrons. For high energy electrons, the dissociative attachment processes of $Cl^- + Cl + SO$, $SO^- + Cl_2$, and $2Cl + SO^-$ become important.

ACKNOWLEDGMENTS

The authors wish to thank Dr. E. R. Manzanares, Dr. M. J. Mitchell, Dr. J. B. Nee, Dr. M. Suto, and Dr. X. Y. Wang in our laboratory for useful discussion and suggestions. This work is supported by the Air Force Office of Scientific Research under Grant No. AFOSR-82-0314.

[1]L. C. Lee and F. Li, J. Appl. Phys. **56**, 3169 (1984).
[2]W. C. Wang and L. C. Lee, J. Appl. Phys. **57**, 4360 (1985).
[3]W. C. Wang and L. C. Lee, J. Appl. Phys. **58**, 184 (1985).
[4]W. C. Wang and L. C. Lee, J. Chem. Phys. **84**, 2675 (1986).
[5]R. J. Donovan, D. Husain, and P. T. Jackson, Trans. Faraday Soc. **65**, 2930 (1969).
[6]M. Kawasaki, K. Kasatani, H. Sato, H. Shinohara, N. Nishi, H. Ohtoshi, and I. Tanaka, Chem. Phys. **91**, 285 (1984).
[7]A. P. Uthman, P. J. Demlein, T. D. Allston, M. C. Withiam, M. J. McClements, and G. A. Takacs, J. Phys. Chem. **82**, 2252 (1978).
[8]L. G. H. Huxley and R. W. Crompton, *The Diffusion and Drift of Electrons in Gases* (Wiley, New York, 1974), pp. 298–303.
[9]G. L. Braglia and J. J. Lowke, J. Phys. D **12**, 1831 (1979).
[10]A. G. Robertson, Aust. J. Phys. **30**, 39 (1977); J. C. Bowe, Phys. Rev. **117**, 1411 (1960).
[11]S. R. Hunter and L. G. Christophorou, J. Chem. Phys. **80**, 6150 (1984).
[12]L. G. Christophorou, and S. R. Hunter, in *Electron–Molecule Interactions and their Applications. Vol. II*, edited by L. G. Christophorou (Academic, Orlando, 1984).
[13]L. G. Christophorou, *Atomic and Molecular Radiation Physics* (Wiley–Interscience, New York, 1971).
[14]R. T. Sanderson, *Chemical Bonds and Bond Energies* (Academic, New York, 1971).
[15]H. Okabe, *Photochemistry of Small Molecules* (Wiley, New York, 1978), p. 292.
[16]D. L. McCorkle, A. A. Christodoulides, and L. G. Christophorou, Chem. Phys. Lett. **109**, 276 (1984).

Dissociative electron attachment to some chlorine-containing molecules

Z. Lj. Petrović,[a] W. C. Wang, and L. C. Lee
Molecular Engineering Laboratory, Department of Electrical and Computer Engineering, San Diego State University, San Diego, California 92182-0190

(Received 9 September 1988; accepted 7 December 1988)

The electron-attachment rate constants of CH_3Cl, C_2H_5Cl, and C_2H_3Cl in N_2 and Ar were measured as a function of reduced electric field (E/N). These data and the previous data of $SOCl_2$ and CCl_2F_2 were converted to the electron-attachment cross sections as a function of electron energy. The present results are compared with existing fragmentary data. The dissociative electron-attachment processes of the studied molecules are discussed.

I. INTRODUCTION

Dissociative electron attachment to chlorine-containing molecules in gas discharges is of importance for many applications, such as excimer (XeCl) lasers,[1] plasma etching,[2] ionospheric chemistry,[3] gaseous dielectrics,[4] and optically controlled diffuse discharge switches.[5,6] Modeling of discharges requires a large number of parameters, and data for the most important processes are lacking. Electron attachment data are needed for the study of dissociation processes, space charge, and field distribution as well as electron kinetics leading to gas breakdown and discharge formation.[7]

The experimental data for the electron attachment rate constants of CH_3Cl (methylchloride), C_2H_5Cl (ethylchloride), and C_2H_3Cl (vinylchloride) diluted in argon and/or nitrogen are presented in this paper. These data and previously published data of $SOCl_2$ (Ref. 8) and CCl_2F_2 (Ref. 9) are converted to the absolute values of low-energy-electron-attachment cross sections. The electron attachment data of chlorine-containing molecules are scarce, and data that are available are in serious disagreement.[10]

In the case of bromine containing molecules,[11,12] the measured electron attachment rate constants of CH_3Cl and C_2H_5Cl are scattered over several orders of magnitude.[13,14] The most detailed study was performed by Schultes *et al.*[13,14] using an electron cyclotron resonance technique to determine the thermal-electron-attachment rate constants. They measured the rate constant for C_2H_3Cl, but only gave the upper limit values for CH_3Cl and C_2H_5Cl. Rossi *et al.*[15] measured the electron-attachment rate constants of C_2H_3Cl diluted in He. The electron-attachment rate increases dramatically, when C_2H_3Cl is photodissociated by excimer laser photons to produce the highly excited HCl molecule.[15] This phenomenon was applied to develop a fast diffuse discharge opening switch by Kobayashi *et al.*[6] Chantry and Chen[16] measured the electron attachment cross section of this molecule as a function of temperature by a beam technique. The cross section increases dramatically at low electron energy when the temperature is increased.[16]

A large number of data exists for electron attachment to CCl_2F_2. McCorkle *et al.*[17] determined the cross section from unfolding the attachment rate constants of CCl_2F_2 in N_2 up to 1 eV. Pejcev *et al.*[18] measured both ionization and attachment cross sections in an electron beam experiment. They found a nonzero cross section at zero energy. This disagrees with the findings of Illenberger *et al.*[19] and Novak and Frechette[20,21] who analyzed the electron transport coefficients in pure CCl_2F_2 and in mixtures. A similar analysis was performed by Okabe and Kuono,[22,23] who found that the electron attachment cross section of Pejcev *et al.*[18] was consistent with their experimental results, even though the ionization cross sections measured by the same apparatus was too large by a factor of 10. It may be concluded that the order of magnitude for the cross section of CCl_2F_2 has been established, but a serious discrepancy exists for the energy dependence. The electron attachment rate constants for CCl_2F_2 in Ar and N_2 were measured by Wang and Lee,[9] and their data are converted into cross sections here.

It has been suggested that discharge switching can be achieved in CCl_2F_2 and CH_3Cl (Ref. 9) as well as in $SOCl_2$ (Ref. 24) by photodetachment of electrons from Cl^- ions induced by excimer laser photons. The published electron-attachment rate constants[8] for $SOCl_2$ in Ar and N_2 are converted to electron attachment cross sections in the present analysis. No other data are available for comparison.

II. EXPERIMENTAL

The experimental setup has been described in previous papers.[8,11,25,26] Two parallel, flat, stainless steel electrodes (5 cm in diameter) were placed 2.5 cm apart inside a 15 cm i.d. vacuum chamber (a six-way black anodized aluminum cross). The initial electrons were produced by irradiating the uncoated cathode surface with a KrF excimer laser beam at 248 nm (5 eV). The beam diameter was reduced by a 3 mm aperture to make sure that the electron swarm did not extend outside the region of the homogeneous field. The laser pulse duration was about 10 ns, which was significantly shorter than the transit time of the electrons. The laser was operated at 5 Hz.

This experiment belongs to the class of pulsed Townsend experiments.[27] The cathode is connected to a high negative voltage, while the anode is connected to ground through a resistor. A low value resistor (1000 Ω) is selected so that resistance–capacitance (RC) will be lower than the transit time and $V(t)$ will be proportional to the displacement current between the electrodes. Transient voltage waveforms were monitored by a 150 MHz digital storage oscilloscope (Tektronix 2430). An average waveform of at least 100

[a] Permanent address: Institute of Physics, University of Belgrade, P.O. Box 57, 11001 Belgrade, Yugoslavia.

 0021-9606/89/063145-08$02.10

pulses was acquisitioned by a microcomputer for subsequent analysis.

The purities of buffer gases N_2 and Ar (MG Scientific) were better than 99.999% and 99.998%, respectively. Attaching gases (research grade) were purchased from Matheson and diluted by premixing (5000 ppm C_2H_3Cl in Ar) or by mixing through the calibrated flow meters. The gasses were used as delivered. Uncertainty of the mixture composition was anticipated to be less than 3%. Gas pressure was determined by a calibrated capacitance manometer (MKS Baratron), and the uncertainty of the gas number density is believed not to exceed $\pm$ 0.5%. All measurements were performed at room temperature (295 $\pm$ 2 K).

Typical voltage waveforms are shown in Fig. 1 of Ref. 8, and therefore further explanations will not be given. Our method of measuring attachment rate constants is to compare the voltage waveforms (obtained under identical conditions) in pure buffer gas and in buffer gas mixed with a small amount of attaching gas.[25,26,28] The procedure for data acquisition and analysis has been described in previous papers.[25,26] In order to avoid the errors that could be caused by the influence of the added attaching gas on drift velocity,[29] the attachment rate is determined from the ratio of electron densities at the same position between the electrodes (i.e., normalized by the electron transit time).[26]

III. EXPERIMENTAL RESULTS

To ensure that reliable data were obtained, all the precautions as explained in our previous papers were performed (i.e., comparison of drift velocities in pure buffer gases, etc.). When the attaching gas was added to the buffer gas, voltage waveforms changed (see example in Fig. 1 of Ref. 8, curves b and c). A comparison of the waveforms gives the attachment rate constant k_a, which is the electron attachment rate normalized by the partial pressure of the attacher. In order to check whether or not the electron-energy distribution function (EEDF) is affected by the added attaching gas, measurements were performed at several partial pressures.

For gases with high attachment rate constants, small concentrations were used; therefore, the attaching gas did not significantly influence the measured rate constants as shown in Fig. 1 for the C_2H_3Cl in N_2 and Ar. However, for CH_3Cl and C_2H_5Cl the attachment rate constants are small and the abundance of additional gasses are large; therefore, a pronounced and nonlinear dependence of the measured rate constant on the abundances of attaching gas was observed. As an example, the attachment rate constants of C_2H_5Cl in N_2 at varied concentrations and E/N are shown in Fig. 2. In those cases, the measurements were extended to as low abundances as possible before performing extrapolation to zero concentration. The error bounds of the rate constants are estimated to be $\pm$ 30% at the lowest E/N data in N_2, while the uncertainty of other data is normally not greater than $\pm$ 10% for the high E/N data in N_2 and for the data in argon.

With the abundances used for the measurements of CH_3Cl and C_2H_5Cl in Ar and even in N_2, the influence of attaching gas on EEDF was large. These two molecules are

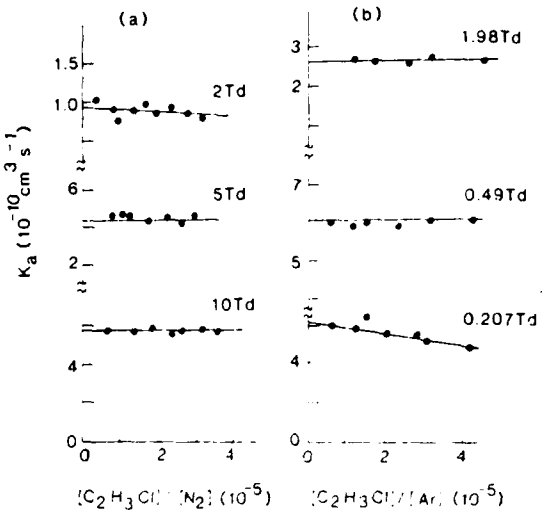

FIG. 1. Dependence of electron-attachment rate constant of C_2H_3Cl on its abundance in (a) N_2 and (b) Ar.

moderately polar, their dipole moments are of the same order as that of H_2O. Therefore, they can affect the momentum and energy transfer even at the level of 1 °C[12,30] because their cross sections for momentum transfer and rotational excitation increase rapidly towards zero energy.[31] Their influence, however, diminishes rapidly at the higher energies, because the inelastic cross sections for N_2 become sufficiently large to account for the majority of energy loss (and the same is true for momentum balance). In accord with this, the uncertainty becomes high for the data at the lower E/N values. When the abundance of an attaching gas was sufficiently high, the attachment rate was saturated at the lower E/N values, indicating that the mean electron energy became thermal. Due to uncertainties inherent in the extrapolation

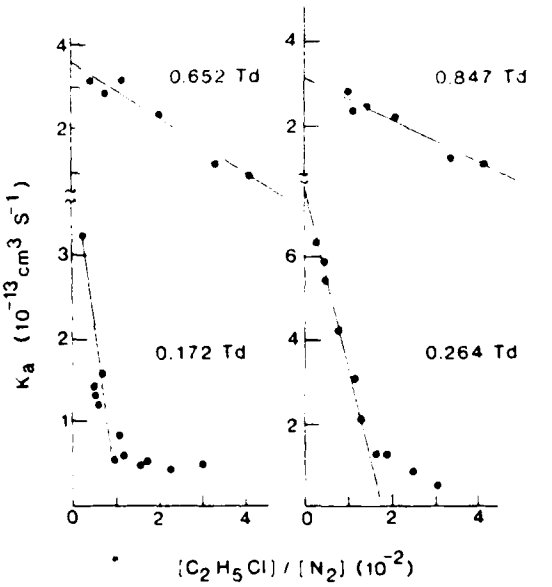

FIG. 2. Dependence of attachment rate constant of C_2H_5Cl on its abundance in N_2.

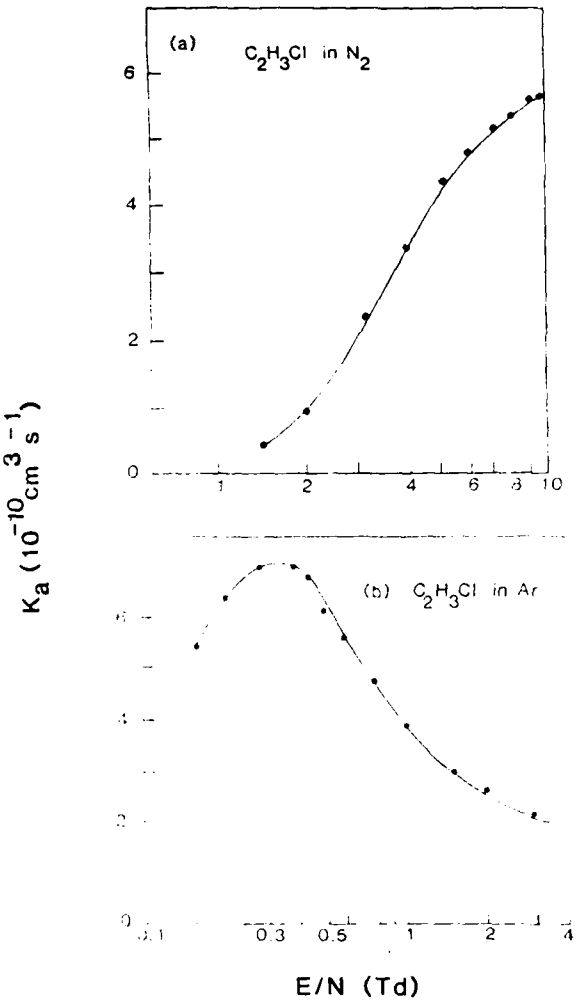

FIG. 3. Electron attachment rate constants of C_2H_3Cl as a function of the reduced field strength (E/N). Measured in (a) N_2 and (b) Ar.

procedure, relatively large errors were assigned to the measured rates of CH_3Cl and C_2H_5Cl. The measurements of these two molecules are on the limit of the present technique.

Attachment rate constants for C_2H_5Cl in N_2 and Ar at the extrapolated zero abundance of attaching gas are shown in Fig. 3 as a function of E/N. The results for CH_3Cl and C_2H_5Cl obtained in N_2 are shown in Fig. 4.

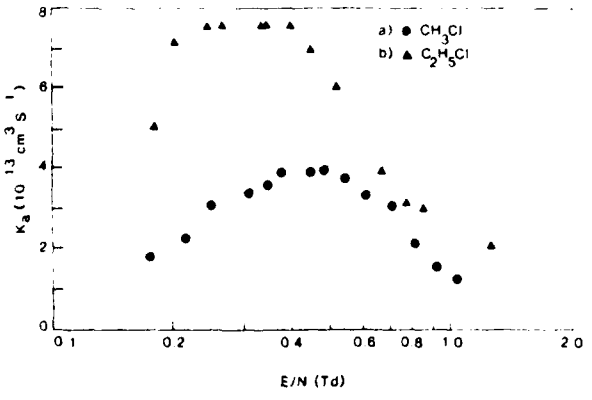

FIG. 4. Electron-attachment rate constants measured in N_2 for (a) CH_3Cl and (b) C_2H_5Cl as a function of reduced electric field.

IV. UNFOLDING OF ATTACHMENT CROSS SECTIONS

Electron-energy distribution functions were calculated from the Boltzmann equation using a standard two term computer code that takes into account the superelastic collisions.[12] The procedure has been described in detail in our paper on electron attachment to HCl.[26] Calculations were performed in pure buffer gases to verify that the compiled cross sections produce the correct values of transport coefficients and especially reproduce the values of electron-attachment rate constants.[13,14] Our measurements did not extend to the E/N region, where errors could be introduced by the breakdown of the two term approximation and/or the inadequacy of the definition of transport coefficients.[15]

The EEDF values were first calculated for given values of E/N. As mentioned above, calculated values for the transport coefficients and mean electron energies were compared with the available data. It was assumed that the EEDF corresponding to the extrapolated (zero abundance) rate constants was the same as for the pure buffer gas. The EEDF values were stored in a separate file which was used by a program for automatic cross section fitting as proposed by Christophorou *et al.*[16]

A trial cross section was used to calculate the attachment rate constant using the stored EEDF [$f_j(E/N,\epsilon)$] calculated for the E/N values used in the experiment. All subsequent modifications of the cross section were obtained as

$$\sigma_{a_i}(\epsilon) = \sigma_{a_{i-1}}(\epsilon)\left[\frac{\Sigma_j w_j(E/N) f_j(E/N,\epsilon) g_j(E/N)}{\Sigma_j f_j(E/N,\epsilon) g_j(E/N)}\right]^m, \quad (1)$$

where $w_j(E/N)$ is the ratio of the experimental and calculated values of the attachment rate constant at a given E/N, $g_j(E/N)$ is a statistical weight that might be given to experimental data at the E/N, and the EEDF is normalized by

$$\int f_j(E/N,\epsilon)\,d\epsilon = 1. \quad (2)$$

The exponent m is used to speed up the convergence. Iteration with m larger than one should be followed by several iterations with $m = 1$ to prevent possible divergence of the procedure, as mentioned by Christophorou and coworkers.[14,16] One should be careful when applying this procedure to correctly select the energy range. If the range is too large, then a small mismatch between experimental and calculated data at either end of the E/N range could lead to the generation of artificial cross sections at appropriate ends of the energy range. If the range is too small, then the cross section will be deformed in an attempt to compensate for the missing part. However, this method does not suffer from the difficulties that were encountered by attempts to devise an "automatic" cross-section fitting routine for pure gases,[17] because here the EEDF remains invariant. Also, the cross sections for the buffer gases are well established, and only one cross section is determined from a single set of experimental data, thus, the results are unique.[18] There is only one possible cause for the nonuniqueness of the results (which is

universal to all swarm techniques), that is, the features of the cross section (either a sharp peak or minimum) are much narrower than the EEDF for a corresponding E/N range. If that is the case, correspondingly reducing the width and increasing the height does not make a difference in the calculated attachment rates.

The whole procedure for unfolding the cross sections is applicable only when the measured attachment rate coefficients are properly extrapolated to the values corresponding to pure buffer gases. This was the case in our experiments. Thus, it is possible to obtain unique values of attachment cross sections from the data of gas mixtures. That is, the mixture technique is suitable for the determination of attachment cross sections. The unfolded cross sections for C_2H_3Cl, CH_3Cl, C_2H_5Cl, $SOCl_2$, and CCl_2F_2 are presented below.

V. DISCUSSION

A. C_2H_3Cl

Electron attachment to C_2H_3Cl is dissociative, and the channel at the lowest energy is

$$C_2H_3Cl + e \rightarrow C_2H_3 + Cl^- \quad (3)$$

with a threshold at approximately 0.36 eV. This value is determined from the dissociation energy of 4.03 eV [as calculated from the heats of formation for C_2H_3Cl, C_2H_3, and Cl (5.0, 69 $\pm$ 2, and 28.992 kcal/mol)[39,40]] and the electron affinity of Cl that is 3.67 eV.[41]

Figure 5(a) shows the attachment rate constants for this molecule plotted as a function of mean electron energy. Also shown are the values calculated using the cross section of Chantry and Chen[16] as well as the values calculated from the cross section which is unfolded from the experimental data using the procedure described above. The data of Rossi *et al.*[15] are also shown in Fig. 5(a). Their data were measured in He buffer gas, and therefore the EEDF is different from that in Ar or N_2. Nevertheless, the data agree reasonably well.

The unfolded cross section is shown in Fig. 5(b), in which the data of Chantry and Chen[16] are also shown for comparison. The present peak value is smaller by about 20% than the values of Chantry and Chen[16] and Strickett *et al.*[42] The half-width of the current-cross section curve is 0.69 eV, which is larger than the value of 0.59 eV measured by various electron beam experiments.[16,42-46] The energy of the present unfolded peak (1.48 eV) is higher than the values measured by the beam experiments that are in the range of 1.2–1.35 eV.[16,42-46] In spite of these differences, the agreement between the current swarm and the beam experiments is regarded as reasonably good. These measurements were taken under different experimental conditions, but the differences are within experimental uncertainties.

B. CH_3Cl

Low-energy electrons can induce dissociative attachment to CH_3Cl. The energy threshold for the process

$$CH_3Cl + e \rightarrow CH_3 + Cl^- \quad (4)$$

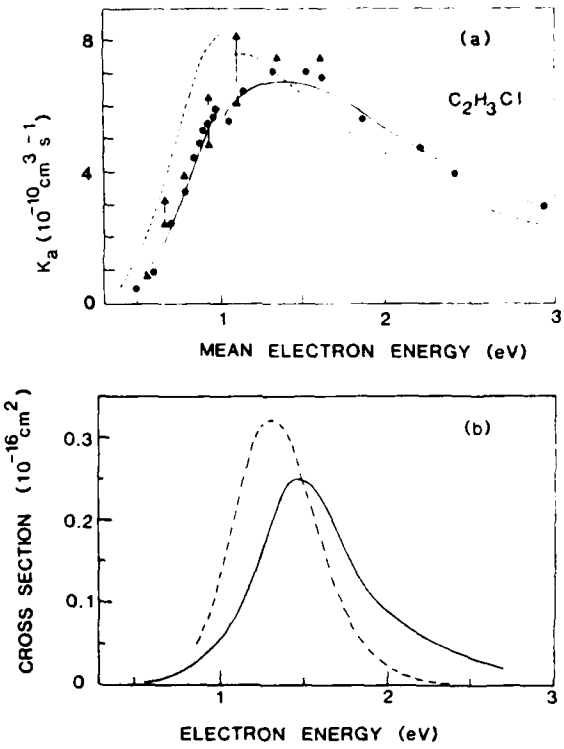

FIG. 5. (a) Electron-attachment rate constant of C_2H_3Cl as a function of mean electron energy. Present experimental results are shown as solid circles, and the data of Rossi, Helm and Lorents (Ref. 15) as triangles. The solid line shows the best fit with the cross section shown in (b), and the dashed line shows the values calculated using the cross section measured by Chantry and Chen (Ref. 16). (b) Cross section for dissociative electron attachment to C_2H_3Cl as a function of electron energy unfolded from the data in (a). The data of Chantry and Chen are plotted as the dashed line.

is -0.03 eV. This threshold is determined from the electron affinity of Cl and the dissociation energy of $D(CH_3-Cl) = 3.637$ eV as calculated from the heats of formation[40] of CH_3Cl, CH_3, and Cl (-83.68, 145.687, and 121.302 kJ/mol).

The maximum attachment rate constant of CH_3Cl occurs at the mean electron energy of 0.17 eV as shown in Fig. 6(a). As in the case of C_2H_3Cl where the present peak energy is higher than those of the beam experiments, the unfolded peak energy for CH_3Cl may be on the high energy side. Nevertheless, the peak at nonzero energy is true. The electron-attachment rate constant decreases when an abundance of CH_3Cl is added to N_2. This indicates that the attachment rate constant at thermal electron energy is smaller than the peak. The observed peak energy is much smaller than the potential barrier of 0.6 eV determined from the potential curves given by Wentworth *et al.*[47] The attachment rate constant is in the order of 10^{-13} cm^3/s which corresponds to a cross section smaller than 10^{-19} cm^2 as shown in Fig. 6(b). Our data are in the same order of magnitude as the data of Chu *et al.*[48] However, the energy dependence of our data is not consistent in shape with the results calculated from the cross sections measured by Chu *et al.*[48] and the predictions of Schultes *et al.*[13] Both groups obtained maximum at zero energy, but the magnitude is different by 1 order of magnitude.

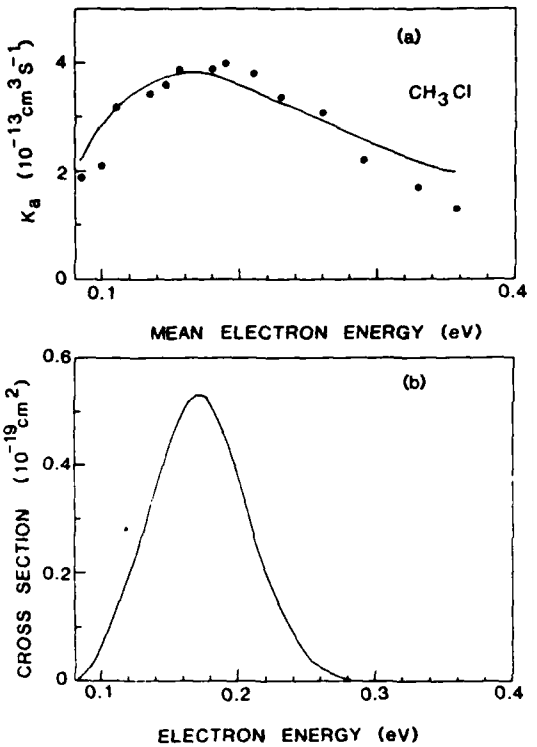

FIG. 6. (a) Electron-attachment rate constant of CH_3Cl, k_a, as a function of mean electron energy. Experimental data are shown as solid circles, and the best fit with the unfolded cross section in (b) is shown as the line. (b) Unfolded cross section for electron attachment to CH_3Cl as a function of electron energy.

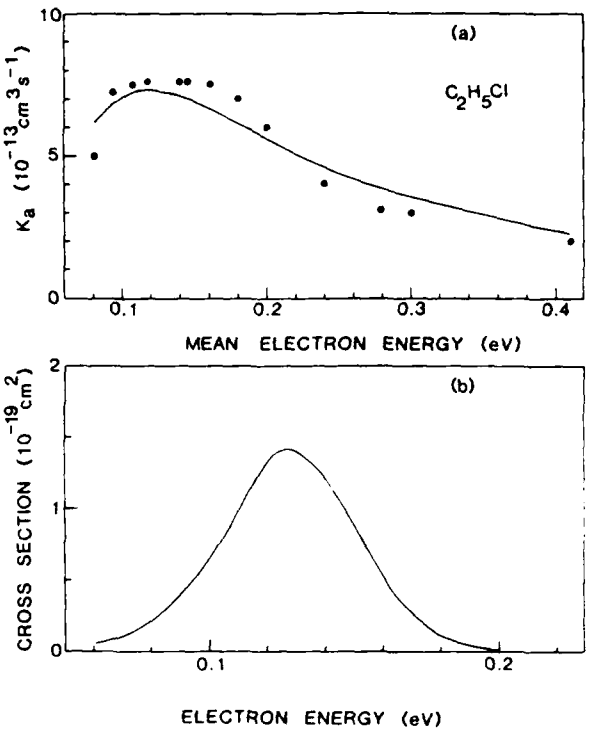

FIG. 7. Same as Fig. 6, but for C_2H_5Cl.

On the other hand, the upper limit for the electron-attachment rate constant at thermal electron energy was determined[49] to be 1.9×10^{-15} cm^3/s. The low attachment rate constants are close to the limits that can be observed by all techniques; thus, it is difficult to measure them accurately.

The zero energy peak and its varied magnitude in different measurements can be explained by the presence of a small amount of CCl_4, which is likely an impurity in CH_3Cl. CCl_4 has a peak at zero energy with a cross section almost 6 order of magnitude larger than the observed peaks in CH_3Cl. We analyzed the CH_3Cl sample, and no trace of CCl_4 was found. The sensitivity for checking trace impurity was better than one part in 10^5.

The energy band width for the electron-attachment cross section of CH_3Cl is smaller than 0.1 eV as shown in Fig. 6(b). This may indicate that the repulsive potential curve leading to the $CH_3 + Cl^-$ products is quite flat in the Franck–Condon region. The residence time of CH_3Cl^- in the potential well of CH_3Cl may be sufficiently long so that CH_3Cl^- is autoionized to CH_3Cl. This explains[50] the present observation that the electron-attachment cross section is quite small.

C. C_2H_5Cl

The thermochemical energy threshold for the dissociative electron attachment process

$$C_2H_5Cl + e \rightarrow C_2H_5 + Cl \qquad (5)$$

is 0.12 eV. This value is obtained from the electron affinity of Cl and the dissociation energy of $D(C_2H_5\text{–}Cl) = 3.789$ eV as calculated from the heats of formation[40] of C_2H_5Cl, C_2H_5, and Cl (-136.52, 107.5, and 121.302 kJ/mol).

Schultes *et al.*[13] reported that C_2H_5Cl has an almost identical zero energy peak as that of CH_3Cl. This is different from the present data that the attachment peak occurs at about 0.12 eV as shown in Fig. 7(a). Although our data are subject to large errors due to extrapolation, the observed energy peak is consistent with the thermochemical threshold. The dependence of the attachment rate constant on the abundance of C_2H_5Cl (Fig. 2) indicates that the rate constant decreases rapidly towards the thermal energy. The upper limit for the electron-attachment rate constant at thermal electron energy was determined[49] to be 1.6×10^{-15} cm^3/s. The electron attachment rate constants shown in Fig. 7(a) are unfolded to cross sections as shown in Fig 7(b).

Christophorou *et al.*[51] have measured the electron-attachment rate constants of C_2H_5Cl diluted in C_2H_2 and N_2. Their results in nitrogen are in the same order of magnitude as our data, but the E/N dependence is different. Nevertheless, they observed a narrow resonance peak at 0.4 eV in their electron beam data which is consistent with our observation of a resonance peak at low energy. A more efficient channel for dissociative attachment is expected at energies higher than 7 and 10 eV.[51,52]

A mass analysis was carried out to check whether or not our gas sample was contaminated by impurities. No trace of CCl_4 was found. All the ions detected were from the parent molecule or its fragments.

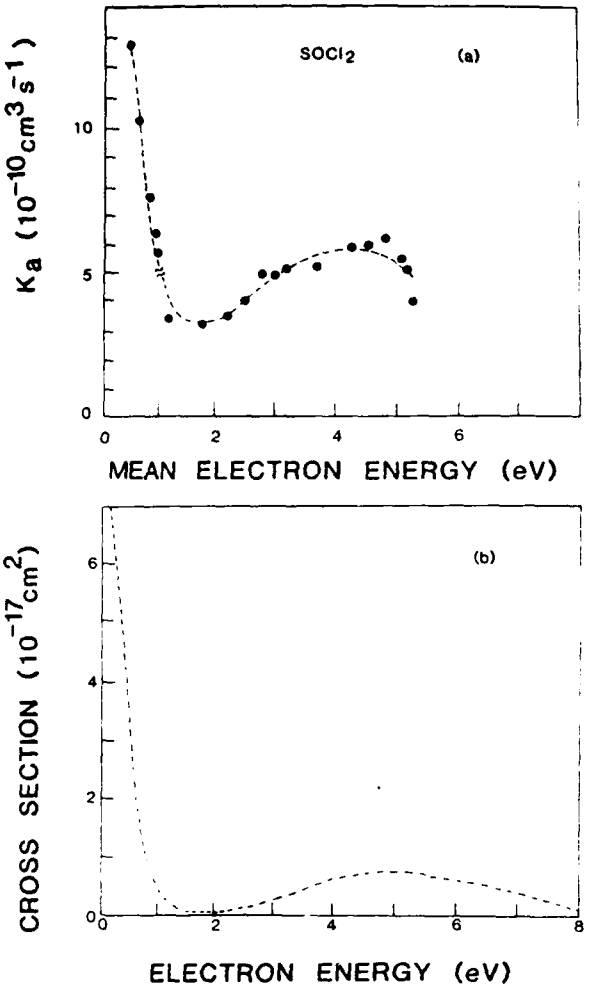

FIG. 8. Same as Fig. 6, but for $SOCl_2$. The k_a values are from Ref. 8.

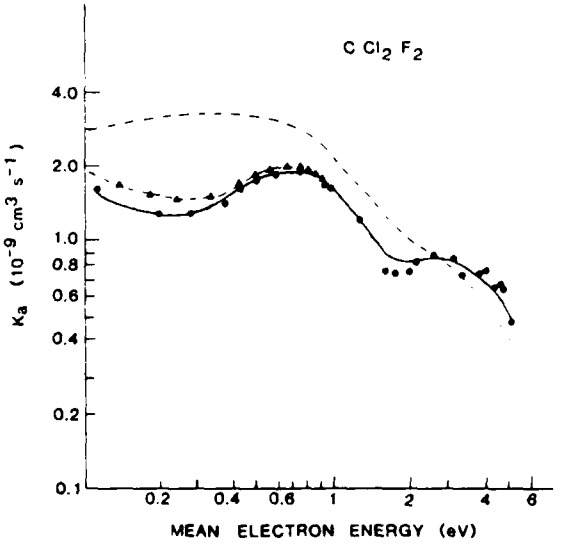

FIG. 9. Electron-attachment rate constant of CCl_2F_2 as a function of mean electron energy. Experimental data from Ref. 9 are shown as solid circles and from Ref. 17 as triangles. Solid line (—) is the best fit curve of the data of Wang and Lee (Ref. 9) based on the cross section shown in Fig 10; the dotted-dashed line (· · · -) is the cross section of McConkle *et al.* (Ref. 12); dotted-dashed line (- · · -) is the cross section of Pejcev, Kurepa and Cadez (Ref. 18), and the dotted line (· · ·) is the cross section of Illenberger *et al.* (Ref. 19) as normalized by Novak and Fréchette (Ref. 20).

D. $SOCl_2$

The dissociative electron-attachment processes were discussed in Ref. 8. The thermochemical threshold for the process

$$SOCl_2 + e \rightarrow SOCl + Cl^- \qquad (6)$$

is -0.8 eV. Several dissociative attachment channels occur at the higher energies.[8] The electron-attachment rate constants measured in nitrogen and argon indicate that there are two major processes below 5 eV, one starting at zero energy and the other starting at about 2 eV with a peak at 5 eV. The attachment rate constants and the unfolded cross section are shown in Figs. 8(a) and 8(b), respectively.

The shape of the unfolded cross section is consistent with the thermochemical data. It is likely that Cl^- is the major ion for the dissociative attachment processes that lead to both peaks.[8] A possibility that other ions (or excited chlorine ions) may be present is indicated in the photodetachment experiment.[24] There are no published data for comparison with the unfolded electron-attachment cross section.

E. CCl_2F_2

Possible dissociative electron-attachment processes for CCl_2F_2 were discussed (and the sources of thermochemical data given) in Ref. 9. The threshold for the process

$$CCl_2F_2 + e \rightarrow CClF_2 + Cl^-$$

is -0.17 eV.

The electron attachment rate constants of CCl_2F_2 as a function of mean electron energy measured by Wang and Lee[9] and McCorkle *et al.*[17] are shown in Fig. 9. Both data are in good agreement in the overlap electron energy range. Even around the mean electron energy of 0.2 eV, the results are within the combined error bounds. Therefore, it is assumed that the cross section of McCorkle *et al.*[17] would fit our data to within the acceptable error bounds in the overlap range. When initiated either from a constant cross section or from an arbitrary cross section with an energy dependence similar to that of the attachment rate constant, or from the cross section of Pejcev *et al.*,[18] the achieved final forms are the shapes shown in Fig. 10. Starting from the cross section of McCorkle *et al.*,[17] an improved fit is obtained after several iterations while preserving the shape of three peaks. However, after a large number of iterations, the second peak as shown in the results of McCorkle *et al.*,[17] is diminishing. Both cross sections of the two and three peaks fit the electron-attachment rate constants within the experimental uncertainties. Since there is no clear indication of three processes in the 0–2 eV range, we have selected the cross section given in Fig. 10 as the best fit to our data. The electron beam of Pejcev *et al.*[18] had a resolution of 0.2 eV, the first narrow minimum in the cross section was thus not resolved. Therefore, our unfolded cross section is roughly consistent with their results in shape, but not in magnitude. These authors[18] have quoted the unpublished results of Chen and Chantry who have managed to resolve the cross section below 1 eV and have observed two maxima in agreement with the shape of our cross section.

Our results disagree with the data of Illenberger *et al.*[19]

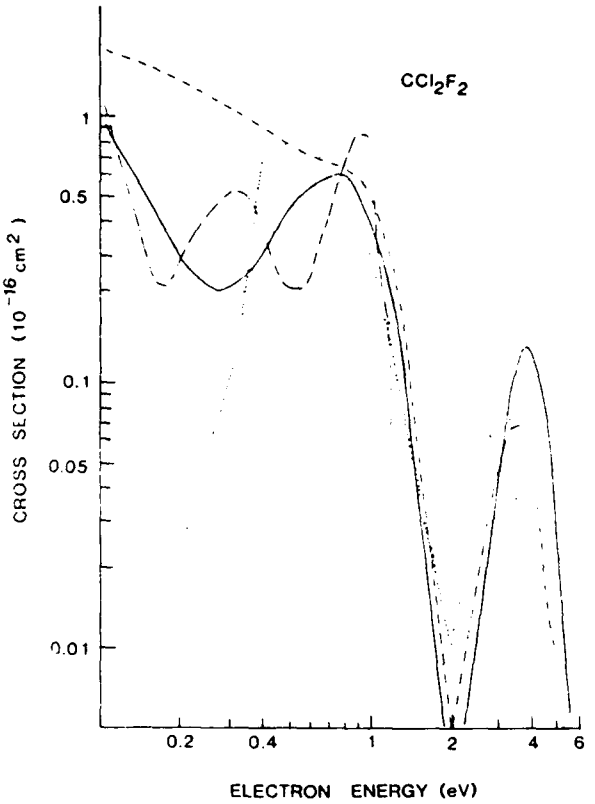

FIG. 10. Cross sections for electron attachment to CCl_2F_2 as a function of electron energy. The best fit to the data of Ref. 9 is shown as the solid curve. Other curves follow the notation of Fig. 9.

(and normalized by Novak and Frechette[20]) who reported very low values of cross section at low energy as shown in Fig. 10. The measured electron-attachment rate constants at the lowest E/N (mean electron energy of 0.11 eV) is comparable to the thermal attachment rate measured by Smith *et al.*,[53] for which the observed large increase of the attachment rate with temperature is probably caused by the increased population in the rotationally and vibrationally excited states and the strong dependence of the cross section on internal energy. Our electron attachment cross sections are higher than the values compiled by Hayashi.[54]

At energies above 1.5 eV, it was impossible to determine a unique cross section. It is evident that the cross section is larger than that of Pejcev *et al.*[18] or Illenberger *et al.*[19] in order to be consistent with the electron-attachment rate constants measured in pure argon. However, these data were not obtained in a range of E/N wide enough to provide sufficient information for a unique result. Therefore, the unfolded cross section depends on the weight g_i that is given to the experimental data at a minimum of 2 eV and at the range end. Because of a rather large uncertainty in the experimental data, the cross section presented here is only one of the possible solutions that make the calculated attachment rate constants comparable with experimental data. This cross section is a compromise between preserving the general features of the cross sections measured by beam methods and the agreement with the measured attachment rate constants (to within the experimental error bounds).

It is possible to adjust the peak cross section to the same absolute value measured by Pejcev *et al.*,[18] but, if that were the case the cross section for the high energy portion would be significantly extended. Therefore, the unfolded electron-attachment cross section at energies above 1.5 eV should be confirmed by additional information such as data from pure gas and other mixtures as well as new results from beam experiments. It should be noted that the shape of the unfolded cross section at high-energy does not affect that at low energy (and vice versa). Since this molecule has important applications in atmospheric chemistry, gaseous dielectrics, and plasma etching, it is of interest to have more reliable data for transport coefficients (drift velocities and characteristics energies) in pure gas, because, quite often, CCl_2F_2 is used pure or in mixtures of abundances that cannot be regarded as small.

VI. CONCLUDING REMARKS

The electron-attachment rate constants of CH_3Cl, C_2H_5Cl, and C_2H_3Cl were measured as a function of mean electron energy. The cross sections were unfolded from the experimental data of these gases together with CCl_2F_2 and $SOCl_2$. Our data are consistent with some published results for gases that have relatively large attachment rates. Some controversy, such as the large discrepancy for the published attachment cross sections of CCl_2F_2 at low electron energies, may be resolved by the present data. The cross sections for $SOCl_2$ are new results. The C_2H_3Cl results are in good agreement with available swarm data as well as electron beam data. The CH_3Cl and C_2H_5Cl results were obtained at the technique limits so that the uncertainties were high; but since fragmentary data only are available, the current data are of interest. These molecules should be studied further, especially by beam techniques.

ACKNOWLEDGMENTS

The authors are grateful to Dr. P. J. Chantry and Dr. P. D. Burrow for sending us their results prior to publication. The comments received from Dr. P. J. Chantry and Dr. L. G. Christophorou are appreciated. This work is supported by the Air Force Office of Scientific Research under Grant No. AFOSR-86-0205.

W. L. Nighan and R. T. Brown, Appl. Phys. Lett. **36**, 498 (1980); L. F. Champagne, *ibid.* **33**, 523 (1978).

J. S. Logan, N. M. Mazza, and P. D. Davidse, J. Vac. Sci. Technol. **6**, 120 (1968); D. L. Flamm, V. M. Donnely, and D. E. Ibbotson, in *Plasma Processing for VLSI*, edited by N. G. Einspruch (Academic, New York, 1984), p. 190; A. D. Richards, B. E. Thompson, K. D. Allen, and H. H. Sawin, J. Appl. Phys. **62**, 792 (1987); G. L. Rogoff, J. M. Kramer, and R. B. Piejak, IEEE Trans. Plasma Sci. **PS-14**, 103 (1986).

B. J. Finlayson-Pitts and J. N. Pitts Jr., *Atmospheric Chemistry* (Wiley-Interscience, New York, 1986).

R. E. Wootton and M. R. Kegelman, Electric Power Research Institute Report No. EI-2620, 1982; R. J. VanBrunt, J. Appl. Phys. **61**, 1773 (1987).

L. G. Christophorou, S. R. Hunter, J. G. Carter, and R. A. Mathis, Appl. Phys. Lett. **41**, 147 (1982); G. Schaefer and K. H. Schoenbach, IEEE Trans. Plasma Sci. **PS-14**, 561 (1986); G. Schaefer, P. F. Williams, K. H. Schoenbach, and J. T. Moseley, IEEE Trans. Plasma Sci. **PS-11**, 263 (1983).

[6]O. Kobayashi, T. Sasagawa, and M. Obara, Appl. Phys. Lett. **51**, 2103 (1987).
[7]A. C. Breslin and K. G. Emelius, Int. J. Electron. **22**, 429 (1967); P. Bletzinger and C.A. DeJoseph, Jr., IEEE Trans. Plasma Sci. **PS-14**, 124 (1986).
[8]W. C. Wang and L. C. Lee, J. Chem. Phys. **85**, 6470 (1986).
[9]W. C. Wang and L. C. Lee, IEEE Trans. Plasma Sci. **PS-15**, 460 (1987).
[10]J. W. Gallagher, E. C. Beaty, J. Dutton, and L. C. Pitchford, Joint Institute for Laboratory Astrophysics (JILA) Information Center Report No. **22**, 1982; J. Phys. Chem. Ref. Data. **12**, 109 (1983).
[11]W. C. Wang and L. C. Lee, J. Appl. Phys. **63**, 4905 (1988).
[12]Z. Lj. Petrović and R. W. Crompton, J. Phys. B **20**, 5552 (1987).
[13]E. Schultes, A. A. Christodoulides, and R. N. Schindler, Chem. Phys. **8**, 354 (1975).
[14]A. A. Christodoulides, R. Schumacher, and R. N. Schindler, J. Phys. Chem. **79**, 1904 (1975).
[15]M. J. Rossi, H. Helm, and D. C. Lorents, Appl. Phys. Lett. **47**, 576 (1985).
[16]P. J. Chantry and C. L. Chen, Bull. Am. Phys. Soc. **33**, 152 (1988); J. Chem. Phys. (submitted).
[17]D. L. McCorkle, A. A. Christodoulides, L. G. Christophorou, and I. Szamrej, J. Chem. Phys. **72**, 4049 (1980).
[18]V. M. Pejcev, M. V. Kurepa, and I. M. Cadez, Chem. Phys. Lett. **63**, 301 (1979).
[19]E. Illenberger, H. U. Scheunemann, and H. Baumgartel, Ber. Busenges. Phys. Chem. **82**, 2248 (1978).
[20]J. P. Novak and M. F. Fréchette, J. Appl. Phys. **57**, 4368 (1985).
[21]M. F. Fréchette and J. P. Novak, J. Appl. Phys. **60**, 552 (1986); M. F. Fréchette, J. Appl. Phys. **59**, 3684 (1986).
[22]S. Okabe and T. Kuono, Jpn. J. Appl. Phys. **24**, 1335 (1985).
[23]S. Okabe and T. Kuono, Jpn. J. Appl. Phys. **24**, 836 (1985).
[24]W. C. Wang and L. C. Lee, Proceeding of 6th IEEE Pulsed Power Conference, Arlington, 1987, p. 359.
[25]L. C. Lee and F. Li, J. Appl. Phys. **56**, 3169 (1984); W. C. Wang and L. C. Lee, J. Appl. Phys. **57**, 4360 (1985); W. C. Wang and L. C. Lee, J. Chem. Phys. **84**, 2675 (1986).
[26]Z. Lj. Petrović, W. C. Wang, and L. C. Lee, J. Appl. Phys. **64**, 1625 (1988).
[27]H. Raether, *Electron Avalanches and Breakdown in Gases*, (Butterworths, Washington, 1964); L. G. H. Huxley and R. W. Crompton, *The Diffusion and Drift of Electrons in Gases* (Wiley–Interscience, New York, 1974); S. R. Hunter and L. G. Christophorou, in *ElectronMolecule Interactions and Their Applications*, edited by L. G. Christophorou (Academic, Orlando, 1984), Vol. 2.
[28]L. G. Christophorou, *Atomic and Molecular Radiation Physics* (Wiley–Interscience, London, 1971); S. R. Hunter and L. G. Christophorou, J. Chem. Phys. **80**, 6150 (1984).
[29]W. H. Long, Jr., W. F. Bailey, and A. Garscadden, Phys. Rev. A **13**, 471 (1976); Z. Lj. Petrović, R. W. Crompton, and G. N. Haddad, Aust. J. Phys. **37**, 23 (1984).
[30]Z.Lj. Petrovic, Aust. J. Phys. **39**, 249 (1986).
[31]Y. Itikawa, Phys. Rep. **46**, 118 (1978); D. W. Norcross and L. A. Collins, in *Advances in Atomic and Molecular Physics*, edited by D. R. Bates and B. Bedorson (Academic, New York, 1981), p. 341.
[32]D. K. Gibson, Aust. J. Phys. **23**, 683 (1970).
[33]G. N. Haddad, Aust. J. Phys. **37**, 487 (1984); L. C. Pitchford and A. V. Phelps, Phys. Rev. A **25**, 540 (1982); H. B. Milloy, R. W. Crompton, J. A. Rees, and A. G. Robertson, Aust. J. Phys. **30**, 61 (1977); A. V. Phelps (private communication, 1983).
[34]S. R. Hunter and L. G. Christophorou, J. Chem. Phys. **80**, 6150 (1984).
[35]A. V. Phelps and L. C. Pitchford, Phys. Rev. A **31**, 2932 (1985); S. L. Lin, R. E. Robson, and E. A. Mason, J. Chem. Phys. **71**, 3483 (1979); N. Ikuta, H. Itoh, and K. Toyota, Jpn. J. Appl. Phys. **22**, 117 (1983); T. Makabe and T. Mori, J. Phys. D **17**, 699 (1984); G. L. Braglia and M. Diligenti, Contrib. Plasma Phys. **26**, 453 (1986).
[36]L. G. Christophorou, D. L. McCorkle, and V. E. Anderson, J. Phys. B **4**, 1163 (1971).
[37]T. F. O'Malley and R. W. Crompton, J. Phys. B **13**, 3451 (1980); T. Taniguchi, M. Suzuki, K. Kawamura, F. Noto, and H. Tagashira, J. Phys. D **20**, 1085 (1987); P. Segur (private communication, 1987).
[38]M. A. Morrison, R. W. Crompton, B. C. Saha, and Z. Lj. Petrovic, Aust. J. Phys. **40**, 239 (1987).
[39]S. W. Benson, *Thermochemical Kinetics* (Wiley, New York, 1976).
[40]M. W. Chase, Jr., C. A. Davies, J. R. Downey, Jr., D. J. Frurip, R. A. McDonald, and A. N. Syverud, J. Phys. Chem. Ref. Data Suppl. **1**, Parts I and II (1985).
[41]A. A. Christodoulides, D. L. McCorkle, and L. G. Christophorou, *Electron Molecule Interactions and Their Applications*, Ref. 27, Vol. II, p. 478.
[42]K. L. Stricklett, S. C. Chu, and P. D. Burrow, Chem. Phys. Lett. **131**, 279 (1986).
[43]P. D. Burrow, A. Modelli, N. S. Chiu, and K. D. Jordan, Chem. Phys. Lett. **82**, 270 (1981).
[44]R. Kaufel, E. Illenberger, and H. Baumgarter, Chem. Phys. Lett. **106**, 342 (1984).
[45]J. K. Oltoff, J. A. Tossell, and J. H. Moore, J. Chem. Phys. **83**, 5627 (1985).
[46]R. Dressler, M. Allan, and E. Haselbach, CHIMIA **39**, 385 (1985).
[47]W. E. Wentworth, R. George, and H. Keith, J. Chem. Phys. **51**, 1791 (1969).
[48]S. C. Chu, K. L. Stricklett, and P. D. Burrow (private communication, 1987).
[49]K. M. Bansal and R. W. Fessenden, Chem. Phys. Lett. **15**, 21 (1972).
[50]L. G. Christophorou (private communication, 1988).
[51]L. G. Christophorou, R. N. Compton, G. S. Hurst, and P. W. Reinhardt, J. Chem. Phys. **45**, 536 (1966).
[52]S. Srivastava (private communication, 1987).
[53]D. Smith, N. G. Adams, and E. Alge, J. Phys. B **17**, 461 (1984), and references therein.
[54]M. Hayashi, *Proceeding of the Fourth International Swarm Seminar and the Inelastic Electron-Molecule Collisions Symposium*, edited by L. C. Pitchford, B. V. McKoy, A. Chutjian, and S. Trajmar (Springer, New York, 1987).

LOW ENERGY ELECTRON ATTACHMENT TO BCl_3

Z. Lj. Petrović,* W. C. Wang, M. Suto, J. C. Han, and L. C. Lee
Molecular Engineering Laboratory
Department of Electrical and Computer Engineering
San Diego State University
San Diego, CA 92182

Abstract

The rate constants of low-energy-electron attachment to BCl_3 diluted in N_2 are measured as a function of E/N at 1-11 Td, corresponding to mean electron energies at 0.4-1.0 eV. The negative ions produced by hollow-cathode discharges of either pure BCl_3 or mixtures of BCl_3 in N_2 are mass-analyzed to identify the products of electron attachment to BCl_3. Only Cl^- ion is found in the discharge media, although BCl_3^- is observed at the applied voltage significantly lower than the breakdown voltage. The electron attachment processes of BCl_3 are discussed.

* Permanent address: Institute of Physics, University of Belgrade, P. O. Box 57, 11001 Belgrade, Yugoslavia

I. Introduction

Electron attachment to electronegative gases determines the electron kinetics in gas discharges: by reducing the number and changing the energy distribution function of electrons that sustain discharges[1], by affecting the spatial distribution of electric field and inducing double layers under certain conditions[2,3], and by being a major source of radicals through dissociative attachment. BCl_3 is a gas of great importance for plasma technologies in microelectronics fabrication, especially for etching of aluminum.[4,5] Therefore, kinetics in discharges of BCl_3 and its mixtures were studied extensively[2,6-8]. However, apart from some indirect evidence, the identity of negative ions in BCl_3 discharges were not established. The swarm or beam data for electron attachment to BCl_3 are only fragmentary. Stockdale *et al.*[9] measured the thermal electron attachment rate constants of 2.7×10^{-9} cm^3/s by a drift-dwell-drift technique, and observed the excitation function of dissociative electron attachment by a beam experiment that shows a peak at 1.1 eV. On the other hand, Buchel'nikova[10] measured the cross section for the same process with an absolute peak value of 2.8×10^{-17} cm^2 at 0.4 eV. The magnitude of the electron attachment rate could be indirectly estimated from the modeling of the discharge data of Ar-BCl_3 mixtures[7].

It is evident that the availability of the data for BCl_3 is inversely proportional to its importance. The reason for the lack of data is that BCl_3 is highly reactive and consequently difficult to handle for accurate measurements. In this paper, we present the electron attachment rate constants for BCl_3 diluted in N_2. We also present the results for mass spectrometric studies of discharges of BCl_3 in N_2. The negative ions

observed in discharge media provide useful information for the understanding of electron attachment processes of BCl_3.

II. Experimental

An apparatus previously used in our laboratory for electron attachment rate measurements[11] was significantly modified for this experiment. The modified apparatus shown in Fig. 1, is a stainless steel chamber with three sections: the first section (5" OD) that is pumped by a mechanical pump is for discharge, the second section (6" OD) that is pumped by a diffusion pump (Varian, VHS-6) is for differential pumping, and the third section (4" OD), pumped by a turbomolecular pump (Varian Turbo V-450), is for the housing of a quadrupole mass analyzer (Extrel).

The apparatus operated in two modes. In mode one, the first and the second chambers were isolated, and the discharge chamber was filled to a relatively high pressure (100-400 Torr). This experiment is similar to the one described in our previous papers[11]. An excimer laser (Lumonics) was used to produce pulsed electron swarms by irradiation of the cathode. Conduction current induced by electrons moving between electrodes was measured by the voltage drop across a resistor of 1 KΩ. The transient voltage waveforms were recorded by a digital oscilloscope (Tektronix 2430) and stored in a computer. In mode two, the first and second chambers were connected through a skimmer hole of 0.7 mm ID. In order to keep the pressure in the mass analyzer chamber sufficiently low ($< 10^{-7}$ Torr), the discharge chamber could only be filled to 1 Torr. The self-sustained DC discharge was formed between two hollow electrodes of 1 cm OD. (Parallel plate geometry was also used for some test measurements.) The space between the two electrodes was adjustable. Both positive and negative ions produced in discharges were sampled and mass analyzed.

For the measurement of electron attachment rates, gas mixtures of BCl_3 in N_2 were prepared in a separate stainless steel container. The container was filled first with BCl_3, and after the container walls were saturated it was then filled with the buffer gas N_2. The volume of the connection tubing was considerably smaller than the volume of the mixing container. The initial pressure of the gas mixture was 1500 Torr, and a time of 20 hours was allowed for the mixing. (Mixtures were mixed in periods between 16 and 64 hours and no differences were observed.) Commercial gas mixtures were not used, because the manufacturers refused to guarantee the composition of their mixtures.

Measurements were carried out in a flow system of 540 sccm for 200 Torr. At the beginning of the experiment, the pure buffer gas was allowed to flow, and the voltage waveforms induced by laser irradiation of the cathode were recorded (see Ref. 11 for the more detailed description of the experimental procedure). The BCl_3 in N_2 mixture was then added to the flow. Typically, 2-15 sccm of mixture was added that was measured and controlled by a MKS flow controller. Sufficient time was normally allowed to saturate the walls of the tubing and the chamber before the measurements commenced. Following this procedure, mixtures could be made with the abundance of BCl_3 between 0.1% and 0.5%. The experimental results were reproducible if this procedure was followed carefully. The reproducibility of the BCl_3 gas density was the major source of uncertainty. For the mass analysis of the negative ions, both pure BCl_3 and gas mixtures of about 0.5% BCl_3 in N_2 were used for discharges. The ion density was measured as a function of discharge current and gas pressure.

The BCl_3 gas was supplied by Matheson with a stated purity of 99.9% minimum. The gas sample was analyzed by the mass spectrometer in this

experiment. Trace amounts of Cl_2 and $BFCl_2$ were observed in the mass spectrum, but the total impurity concentration was estimated to be smaller than 0.1%.

III. Results and Discussion

A. Electron Attachment Rate Constants

At each E/N, the electron attachment rate constants were measured at several BCl_3 concentrations for the gas mixtures of BCl_3 in N_2. The data extrapolated to the zero BCl_3 abundance are shown in Fig. 2 for the E/N in the range of 1-11 Td (1 Td = 10^{-17} V cm^2), corresponding to mean electron energy in the 0.4-1 eV range. Measurements at E/N lower than 1 Td were difficult because of low signals and the need to use more diluted mixtures which caused poor reproducibility. Nevertheless, it is evident that the trend of increase towards low E/N does not continue below the data points presented in Fig. 2. The experimental uncertainty was estimated to be within 30% of the given value. The uncertainty contains: (1) geometric distribution, E/N determination and pressure measurement, < 2%, (2) waveform determination, < 1%, (3) statistical fluctuations of the measured rates, < 5-7%, extrapolation to zero abundance, < 5-10%, and (4) uncertainty in gas mixture composition, < 10%. We have set the overall uncertainty to be higher than the estimated value, because of the difficulty inherent in handling the BCl_3 gas.

The strong dependence of the attachment rate constant on E/N suggests that the attachment be a three-body process with a peak at low energy. As determined by thermochemical data[12] and the electron affinity[13] of Cl, the threshold for the dissociative attachment process of $e + BCl_3 \rightarrow BCl_2 + Cl^-$ is about 1.0 eV. This threshold is above the electron energy range studied in this experiment. Therefore, BCl_3^- is the only ion possibly produced at

low energy electron attachment. (BCl_3^- was in fact observed in the low pressure experiment described in the next section). This result is consistent with the conclusion of Gottscho and co-worker[6] who attribute BCl_3^- as the *dominant negative ions* observed in the RF discharge of pure BCl_3. Nevertheless, our measured attachment rate constants are not significantly dependent on gas pressures in 100-400 Torr; that is, the attachment is like a two-body process. Our observation is, in fact, consistent with the earlier observation[9] that the thermal electron attachment rate constant was not dependent on the gas pressures at 5-15 Torr. The negative ions in these measurements was not mass-analyzed, because the gas pressures were very high.

We have also performed measurements for the BCl_3 -Ar mixtures. Unfortunately, the results were not as reproducible as the data for N_2. The basic difficulty was that the extrapolation to zero BCl_3 abundances could not be easily performed because the measurements could not be extended to sufficiently low abundances, because the influence of the attaching gas on the electron drift velocity in Ar was large in the most interesting range. However, the crude experimental results indicate that the attachment rate constants increase in the mean electron energy range of 1.5-2.5 eV.

The electron attachment rate constants converted from the cross sections of Buchel'nikova[10] are shown in Fig. 2 for comparison. The calculation method was described in a previous paper by Petrović *et al.*[11]. Our results agree with the calculated values in the order of magnitude, but the E/N dependence is different. The agreement is only accidental because the attachment mechanism is quite different; that is, these results cannot be regarded as in agreement. However, our measurements at low E/N agrees with

the thermal electron attachment rate constant measured by Stockdale *et al.*[9] as shown in Fig. 2.

The measured attachment rate constants are too large to be affected by the possible impurities, such as Cl_2. The impurity level of Cl_2 was determined to be less than 0.1% that will contribute to the electron attachment rate constant at most 2×10^{-12} cm^3/s, in considering that the maximum rate constant of Cl_2 is only 2×10^{-9} cm^3/s at 0.06 eV[14]. The other possible impurity, $BFCl_2$, may have electron attachment rate constant similar to BCl_3 so that the small impurity level does not cause significant effect. Some molecules such as SF_6 and CCl_4 could cause similar attachment coefficient if they present on 1% level. We have carefully scanned the mass spectrum up to the mass number of 190, but such impurities were not detected.

B. Negative Ions in Discharges of BCl_3

The negative ions produced by discharges were observed for the product analysis of electron attachment to BCl_3. Initial studies of negative ions presented in discharges were carried out in a parallel plane geometry with either pure BCl_3 or its mixture with N_2. Later, most measurements were performed with hollow-cathode discharges using diluted mixtures (0.5% BCl_3 in N_2). In all cases, only Cl^- ions were found as shown in Fig. 3(a). In DC discharges, the mean electron energy may be too high to enable the production of BCl_3^-, in contrast to the bulk of RF plasmas[15] where thermal energy electrons exist for the production[6] of BCl_3^-. When the applied voltage was lowered below breakdown voltage (for instance, 120 V) and photoelectrons were produced by irradiation of the cathode with ArF laser photons, BCl_3^- ions were observed in the gas mixture of trace BCl_3 in 0.66 torr N_2. This observation indicates that BCl_3^- can be produced by attachment of low energy electrons to BCl_3 and survive for sufficiently long time

such that it can be detected either by our mass analyzer or to affect the current waveform. One should, however, keep in mind that for such conditions BCl_3^- signal would be very small (as observed by us that is about 10% of Cl^-), because the mean electron energy is so high that it favors the dissociative attachment.

The Cl^- ion intensity was measured as a function of the discharge current and the pressure. The ion intensity has a peak between 2 and 3 mA of discharge current as shown in Fig. 3(b), where the electrode space was fixed at 2 cm, the gas pressure was 0.6 Torr, and the discharge current was varied by adjusting the applied voltage (784 V at the maximum Cl^- intensity). For a fixed discharge current of 2 mA, the ion intensity had a rather sharp maximum at 400 mTorr as shown in Fig. 3(c), where the electron space was 2 cm, and the applied voltage was 784 V.

The observed Cl^- ions are produced by the electron dissociative attachment process that has a sharp peak at the energy of about 1 eV as observed by Stockdale *et al.*[9]. This basic result implies that in our measurements, the mean electron energies are varied along with the changes of discharge current and gas pressure, and the maximum Cl^- ion intensity corresponds to the mean electron energy in a discharge medium of about 1 eV. The phenomena could be described by the electron energy distribution function which is, however, quite complicated for the hollow-cathode discharges. In general, there are two groups of electrons[16] in a discharge medium: one group consists of the initial electrons that are accelerated in inhomogeneous but very high electric field and practically have a beam-like behavior[17], and the second group consists of inelastically scattered and secondary electrons which have low energies. Relative magnitudes of the two groups are strongly dependent on the discharge conditions. Monte Carlo simulations[16,18-20]

indicate that at these pressures the initial electrons are the dominant group. A sharp peak in the pressure dependence probably indicates the shape of the dissociative cross section, although the correspondence between the mean electron energy and the E/N value (or the available energy for run-away electrons) in the discharge could be very nonlinear. Current dependence of the ion intensity is less sharp; but since the current-voltage dependence is not linear, it is not inconsistent with the proposed picture. However, the low ion signals at high currents may also be possibly due to the influence of space charge force among electrons, negative and positive ions in the bulk of discharge.

In order to establish that negative ions are originated from the discharge, but not by electron impact on BCl_3 in the transition region to the mass analyzer, we have performed the following experiment[21]. Excimer laser light was used to irradiate the region between the electrodes. As a consequence, negative ion signal was significantly reduced. The delay between the laser light pulse and the reduction of the negative ion signal was of the order of tens of microseconds. The effect depends on the laser beam position between the electrodes. The detailed results will be presented in a later publication. The decrease of negative ions following laser irradiation demonstrates that the observed negative ions were produced in the discharge media, but not in the transition region, because the ion signal did not increase by the laser photoelectrons.

IV. Concluding Remarks

The electron attachment rate constants increase toward the low E/N, indicating that the attachment is due to a three-body process. This is consistent with the observations of photodetachment thresholds that BCl_3^- is the dominant negative ion in RF discharges[6]. However, the measured attach-

ment rate constant is not significantly dependent on the buffer gas pressure, suggesting that the attachment is apparently like a two-body process. This observation is in agreement with a previous observation[9] that the thermal electron attachment rate constant is not dependent on total gas pressure. At high pressures, it is possible that the mean time between collisions is sufficiently shorter than the autodetachment time, thus practically every excited negative ion is stabilized in the first step of attachment. At much lower pressures this might not be the case, and even more so in the low pressure region of the mass analyzer; for these cases, the BCl_3^- ions could be lost due to autodetachment. However, the BCl_3^- ion was observed by attachment of low energy electrons to BCl_3, although the BCl_3^- signal was much smaller than Cl^-.

It is worth noting that Stockdale and co-workers[9] observed a peak attachment for the two-body process of $e + BCl_3 \rightarrow BCl_2 + Cl^-$ at 1.1 eV, while at the same time they observed a relatively high thermal electron attachment rate constant. This observation is consistent with the assertion that the electron attachment is due to the three-body process at low energy, and Cl^- is produced by the two-body process at high electron energy. Our results are also consistent with this assertion that the electron attachment rate constants shown in Fig. 2 are mainly due to the three-body process, and the Cl^- ions observed in discharges are due to the two-body process.

The unpublished results of Dr. J. K. Olthoff[22] confirm the existence of BCl_3^- ions. This author has also observed that attachment for BCl_3 molecules peaks close to zero energy (both in the intensity of negative ion current and through the broadening of the zero energy peak of the electron transmission spectrum[23]). The level of impurities in his experiment is uncertain. From some theoretical considerations and the characteristics of

his apparatus, the lifetime of the metastable BCl_3^- ion was estimated to be 60 μs which is consistent with our data.

Acknowledgement

This paper is based on the work supported by the SDIO/IST managed by ONR under Grant No. N00014-86-K-0558 and partly by the Air Force Office of Scientific Research under Grant No. AFOSR-86-0205.

References

1. J. W. Gallagher, E. C. Beaty, J. Dutton and L. C. Pitchford, J. Phys. Chem. Ref. Data, **12** 109 (1983); L. G. Christophorou, *"Atomic and Molecular Radiation Physics,"* (Wiley Interscience, London 1971).
2. R. A. Gottscho, Phys. Rev., A **36**, 2233 (1987).
3. K. G. Emeleus, Int. J. Electron, **61**, 281 (1986); A. C. Breslin and K. G. Emeleus, Int. J. Electron. **22**, 429 (1967).
4. D. L. Flamm and V. M. Donnelly, Plasma Chem. Plasma Proc. **1**, 317 (1981); also, K. E. Greenberg, G. A. Hebner, and J. T. Verdeyen, Appl. Phys. Lett., **44**, 299 (1984).
5. R. A. Morgan, *"Plasma Etching in Semiconductor Fabrication,"* (Elsevier, Amsterdam 1985); T. Sugano, Ed., *"Application of Plasma Processes to VLSI Technology,"* (Wiley-Interscience, New York, 1985).
6. R. A. Gottscho and C. E. Gaebe, IEEE Trans. Plasma Sci., **PS-14**, 92 (1986).
7. G. R. Scheller, R. A. Gottscho, T. Intrator, and D. B. Graves, J. Appl. Phys., **64**, 4384 (1988); R. A. Gottscho, G. R. Scheller, D. Stoneback, and T. Intrator, J. Appl. Phys. in press (1989).
8. G. R. Scheller, R. A. Gottscho, D. B. Graves, and T. Intrator, J. Appl. Phys., **64**, 598 (1988); R. A. Gottscho, G. R. Scheller, T. Intrator, and D. B. Graves, J. Vac. Sci. Technol., A **6**, 1393 (1988).
9. J. A. Stockdale, D. R. Nelson, F. J. Davis, and R. N. Compton, J. Chem. Phys., **56**, 3336 (1972).
10. I. S. Buchel'nikova, Sov. Phys., JETP **35 (8)**, 783 (1959); also, L. G. Christophorou and J. A. D. Stockdale, J. Chem. Phys., **48**, 1956 (1968).

11. L. C. Lee and F. Li, J. Appl. Phys., **56**, 3169 (1984); W. C. Wang and L. C. Lee, J. Appl. Phys., **57**, 4360 (1985); Z. Lj. Petrović, W. C. Wang, and L. C. Lee, J. Appl. Phys., **64**, 1625 (1988).

12. M. W. Chase, Jr., C. A. Davies, J. R. Downey, Jr., D. J. Frurip, R. A. McDonald, and A. N. Syverud, J. Phys. Chem. Ref. Data, **14**, Suppls 1 and 2 (1985).

13. A. Christodoulides and L. G. Christophorou, *"Electron Molecule Interactions and Their Applications,"* Vol. 2. (Ed. L. G. Christophorou, Academic Press, Orlando, 1984).

14. D. L. McCorkle, A. A. Christodoulides, and L. G. Christophorou, Chem. Phys. Lett. **109**, 276 (1984).

15. C. A. Andersen, W. G. Graham, and M. B. Hopkins, Appl. Phys. Lett., **52**, 783 (1988).

16. S. Hashiguchi and M. Hasikuni, Jpn. J. Appl. Phys., **27**, 1010 (1988).

17. B. M. Jelenković and A. V. Phelps, Phys. Rev., A **36**, 5310 (1987); A. V. Phelps, B. M. Jelenković, and L. C. Pitchford, Phys. Rev. A **36**, 5327 (1987); A. V. Phelps and B. M. Jelenković, Phys. Rev., A **38**, 2975 (1988).

18. D. Bhasavanich and A. B. Parker, Proc. R. Soc. Lond., A **358**, 385 (1977).

19. T. J. Moratz, J. Appl. Phys., **63**, 2558 (1988).

20. R. J. Carman, J. Phys., D: Appl. Phys. **22**, 55 (1989).

21. J. C. Han, M. Suto, and L. C. Lee, unpublished (1989).

22. J. K. Olthoff, Ph.D. Thesis (University of Maryland, 1985-unpublished).

23. J. A. Tossell, J. H. Moore and J. K Olthoff, Int. J. Quantum Chemistry **29**, 1117 (1986).

Figure Captions

Fig. 1. Schematic diagram of the experimental apparatus.

Fig. 2. Electron attachment rate constants of BCl_3 in N_2 as a function of E/N. Present data are shown as dots and are connected by lines for eye-guide. The results calculated from the cross section of Buchel'nikova (Ref. 10) are shown as triangles, and the thermal electron attachment rate constant of Stockdale *et al.* (Ref. 9) is shown as a rectangle.

Fig. 3. Cl^- ions observed in hollow-cathode DC discharges. (a) Mass spectrum of negative ions present in the discharges of gas mixtures of 0.5% BCl_3 in N_2. (b) Dependence of the Cl^- ion intensity on the discharge current at a total pressure of 585 mTorr. (c) Dependence of the Cl^- ion intensity on the total gas pressure at a discharge current of 2 mA.

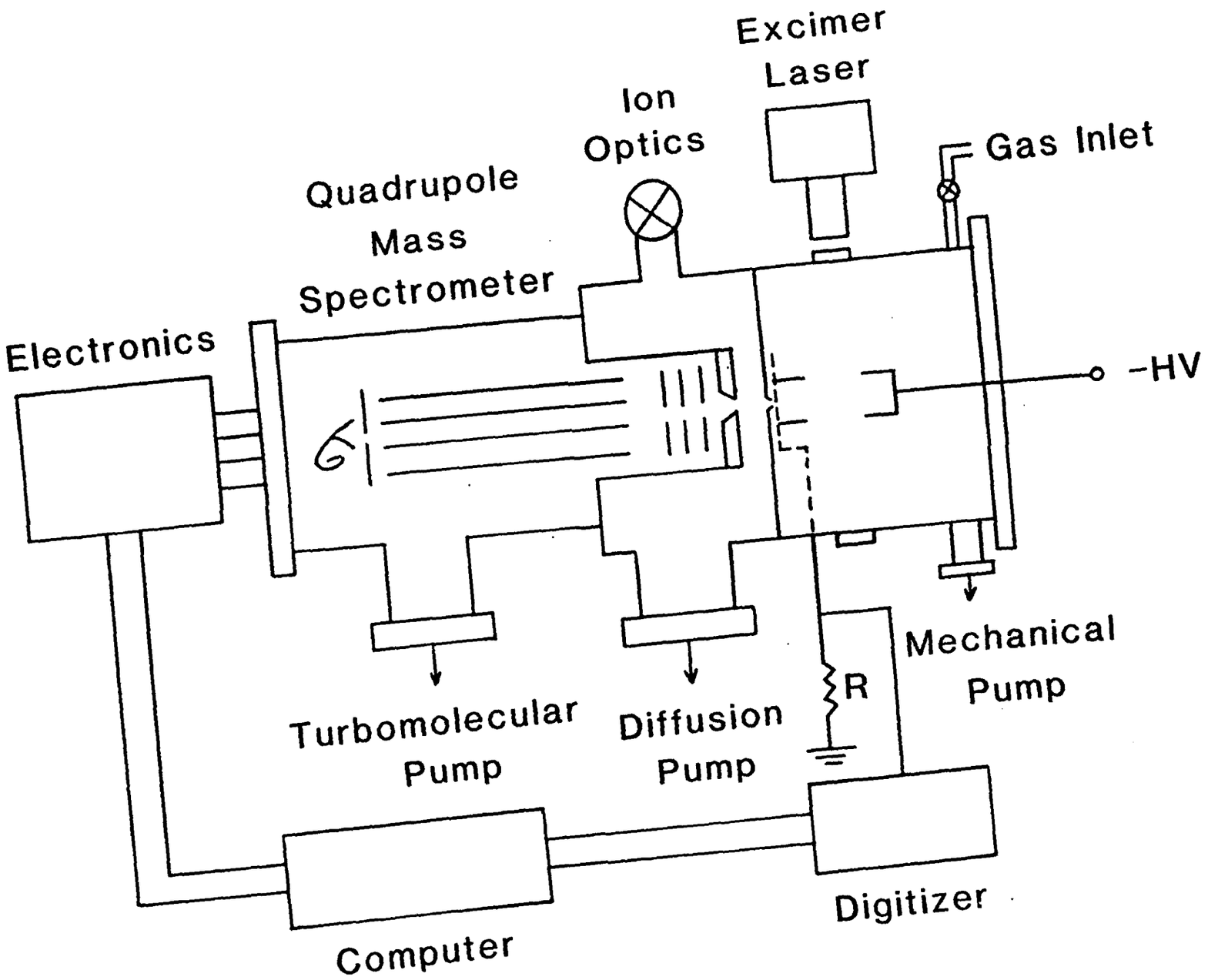
Excimer
Laser
Ion
Optics
Gas Inlet
Quadrupole
Mass
Spectrometer
Electronics
-HV
Mechanical
Pump
R
Turbomolecular
Pump
Diffusion
Pump
Digitizer
Computer

Fig. 1

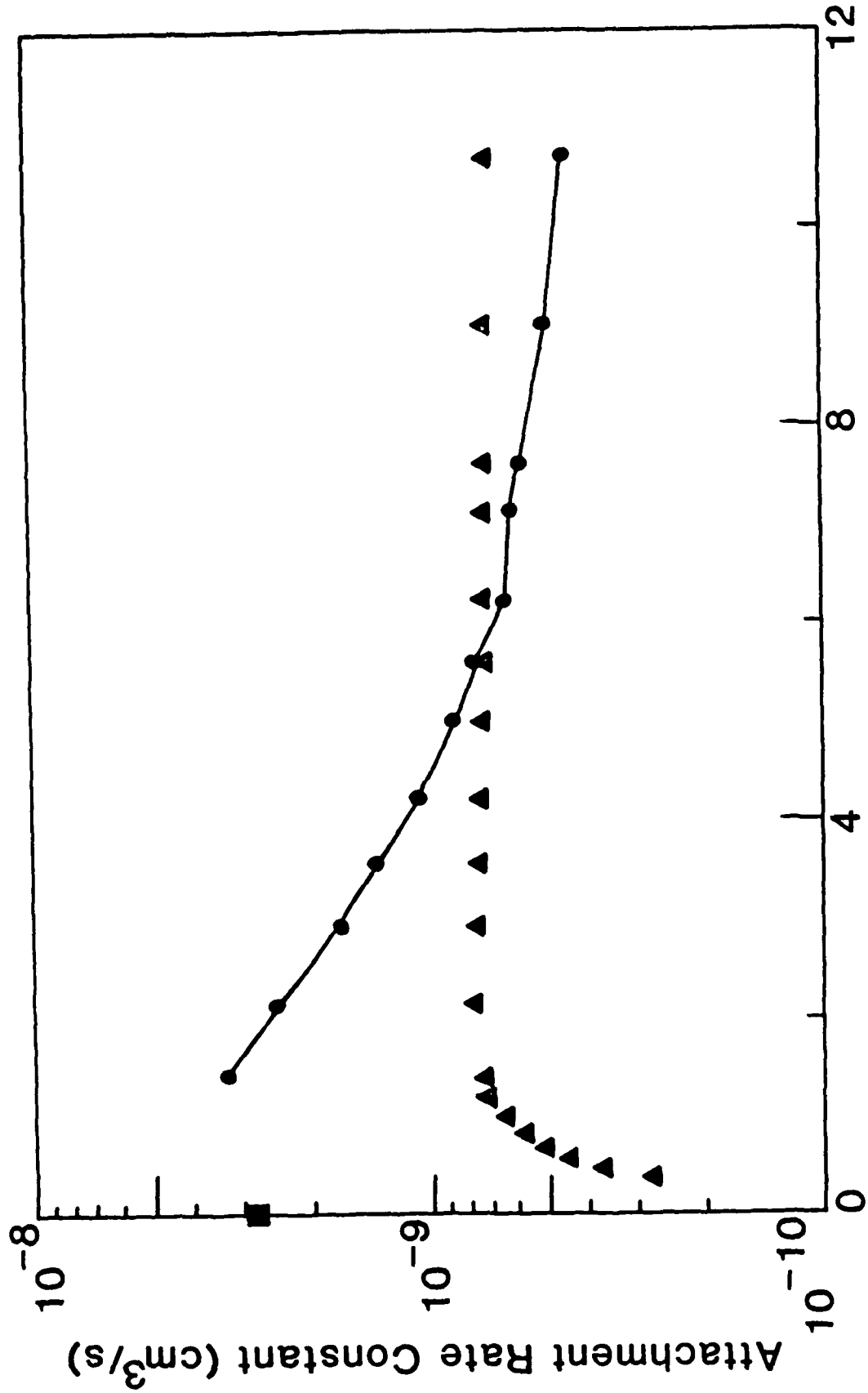

Fig. 2

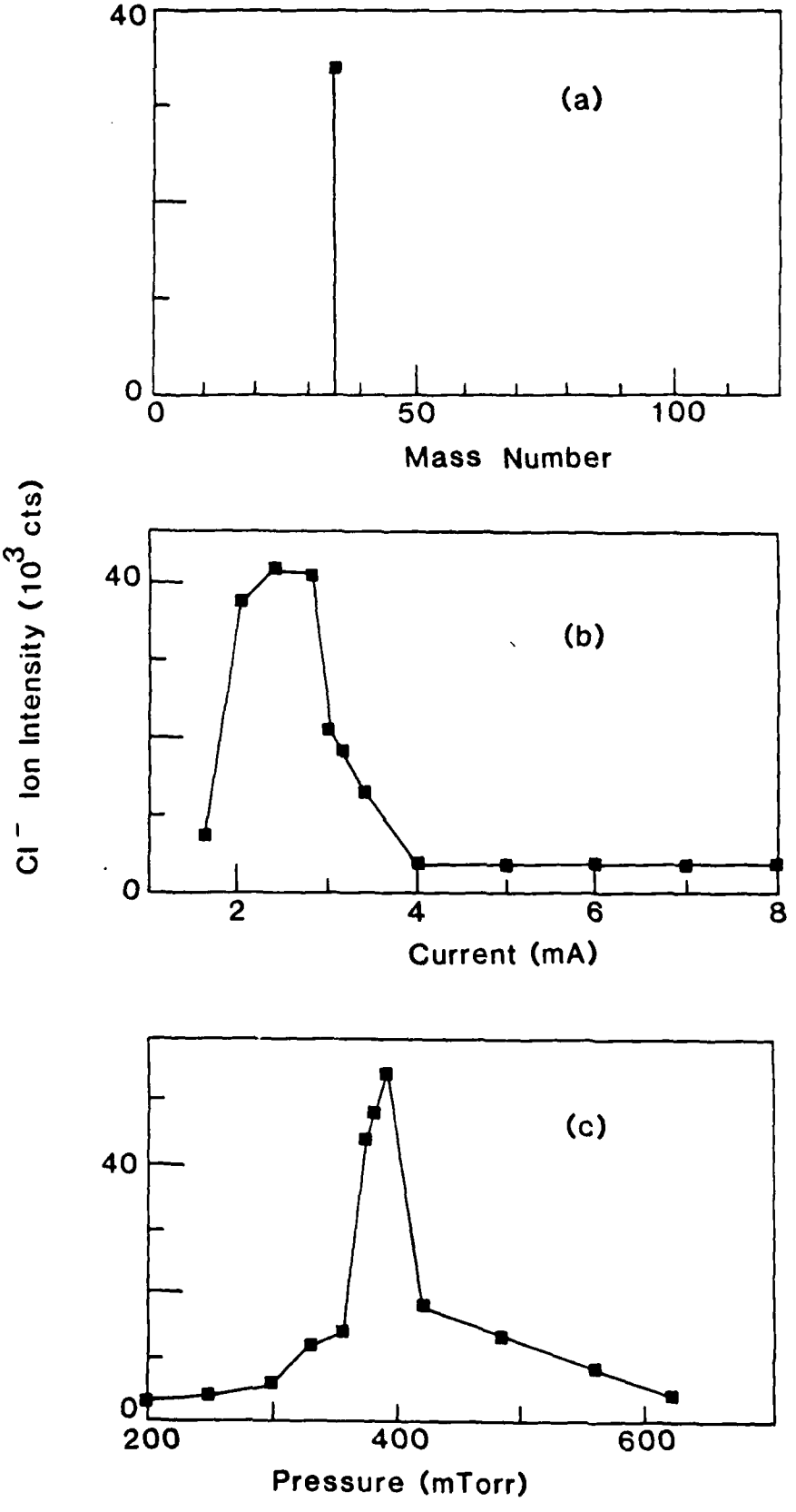
40
0
(a)
0
50
100
Mass Number
Cl⁻ Ion Intensity (10^3 cts)
40
0
(b)
2
4
6
8
Current (mA)
40
0
(c)
200
400
600
Pressure (mTorr)

Fig. 3